



ADDIS ABABA UNIVERSITY

ADDIS ABABA INSTITUTE OF TECHNOLOGY
SCHOOL OF MECHANICAL AND INDUSTRIAL
ENGINEERING

**DESIGN AND PERFORMANCE ANALYSIS OF SMALL-SCALE MILK
CHILLER BY USING PV SYSTEM**

*A thesis submitted to the school of Mechanical and Industrial engineering in
partial fulfillment of the requirement of the Degree of Master of Science in
Mechanical Engineering (Thermal Engineering Stream)*

By:

ESAYAS HABTE

Advisor:

Dr. Ing. Demiss Alemu

October, 2018

ABSTRACT

Photovoltaic powered refrigerators are a new technology for chilling milk in remote areas of developing countries. This thesis project primarily aims at design and analyzing the performance of small-scale milk chiller using PV for cooling 50 liters of milk from 33°C to 4°C within four hours of time.

Preserving perishable goods primarily milk as soon as they are harvested is the main concern for the farmers in the rural areas of Ethiopia due to lack of cold storage facilities and absence of electricity supply. To supply ample facilities in the rural areas of the country this project is aimed to provide cold storage facilities incorporating renewable energy (Solar energy) and batteries; it will give a total off grid solution to the problem of storing perishable goods and ensure food security. The designing system of the cold storage consists of solar Photovoltaic (PV) panels, batteries, charge controller, freezer and a DC compressor. The DC compressor, which is replaced by the AC compressor in the freezer, is the most vital component of the system as it runs the freezer taking DC output from the PV panels. The power supplied from the PV panels simultaneously runs the DC compressor and charges the batteries through the charge controller. The batteries give backup and run the DC compressor at night in nonappearance of the sun.

In doing this, it's used the weather data for estimating the annual performance of the system is average meteorological year data for Semera region. The electrical characteristics, programming algorithm and MAT-LAB code based on the manufacturer's data and hourly converted data has been developed. The optimum tilt angle is calculated for both summer and winter season is used and a MAT-LAB code is used for variation of hourly angle as well as declination angle. The PV system also employs a battery of 24V, 360Ah for two day autonomy and Outback FLEX-max30/40 series (MPPT) charge controller. In general the system has the complete solution for supplying cold storage facilities in off grid areas and gives an environment friendly solution of the storage problem.

ACKNOWLEDGMENT

First and foremost I would like to thank my God and my provider for being with me throughout my life and helping me a lot in every step of doing this thesis. I want to give my deep gratitude for my advisor Dr. Ing. Demiss Alemu for his tireless support by showing me the pillars on how the way to achieve this work and make me self-confident on facing such kind of research in the future and also Dr. Yilma Tadesse for supporting me in getting the necessary documents.

I also thank Samara University and Ministry of Education for granting me such a privilege to empower my level of understanding and make me problem solving person by financially supporting my Msc education, Elias mesfin; alumnus of Adiss Abeba institute of technology from school of Mechanical and Industrial Engineering, the staffs of Addis Ababa University and my beloved friend Fikadu Geremu for his being supportive in giving me his ideas together with PhD candidate Ato Alemayew .

Finally I would like to immensely thank my family for their tireless support, love, care and enthusiastic confer that I received to strengthen me by far and I dedicate this thesis work for them especially my mother Fetlework Sahilemariam.

Table of Contents

<i>Abstract</i>	i
<i>Acknowledgement</i>	ii
<i>Table of content</i>	iii
<i>Lists of Figures</i>	vii
<i>Lists of Tables</i>	ix
<i>Nomenclature</i>	x
CHAPTER-1: INTRODUCTION	1
1.1 Renewable energy.....	1
1.2 Distribution of solar radiation	2
1.3 Solar radiation reaching earth surface	2
1.4 Spectrum of sun	2
1.5 Background of the Study	3
1.6 Statement of Problem	5
1.7 Objectives.....	6
1.7.1 General objective	6
1.7.2 Specific objectives	6
1.8 Scope and Delimitations	6
1.9 Thesis Organization	6
CHAPTER-2: LITERATURE REVIEW	8
2.1 Definitions of PV (photovoltaic) Chiller	8
2.2 Historical Background of PV	8
2.3 PV cell Science.....	8

2.4	Different types of Solar Refrigeration Technologies	10
2.4.1	Solar thermo-electrical cooling	10
2.4.2	Solar thermo-mechanical cooling	11
2.4.3	Solar thermal cooling technologies.....	11
2.4.4	Solar photovoltaic cooling systems	11
2.5	Previous Researches on PV cooling	12
CHAPTER-3: DETAILS OF PHOTOVOLTAIC ARRANGMENT AND MODULE SELECTION		14
3.1	Photovoltaic Arrangement	14
3.1.1	Photovoltaic cells	14
3.1.2	Photovoltaic module	14
3.1.3	Photovoltaic array	14
3.2	Materials used in a cell	15
3.3	PV panel types and Multi-criteria selection	16
3.3.1	PV panel design selection decision:.....	16
3.4	Mathematical modeling of a PV cell.....	18
3.4.1	Equivalent Circuit	18
3.4.2	Solar Cell Model.....	18
3.4.3	Solar Module Model	19
3.4.4	Solar Array Model	20
3.5	Working principle of PV (photovoltaic) driven milk chiller.....	23
CHAPTER-4: METHODOLOGY		24
4.1	Data collection and analysis.....	24
4.1.1	Solar radiation analysis	24
4.1.2	Estimation of hourly radiation from daily data	26
4.1.3	Optimum tilt angle of the PV panel	27
4.1.4	Solar radiation on the optimally tilted PV panel	28
4.1.5	Hourly absorbed solar radiation.....	29
4.1.6	Ambient temperature analysis	30
4.2	Cooling Load Estimation	30

4.2.1	Transmission load	30
4.2.2	Infiltration load	31
4.2.3	Product load.....	33
4.3	Standard Sizing and Design Steps for Components of PV System.....	34
4.3.1	Calculate total watt-hours per day for each heat gain.....	34
4.3.2	Calculate total watt-hours needed from the PV modules.....	35
4.3.3	Calculate the total watt-peak rating needed from PV module.....	35
4.3.4	Calculate the number of PV panels for the system.....	35
4.3.5	Electrical Characteristics of AKT-180-M Solar Panel	39
4.3.6	Influence of Cell Temperature.....	41
4.3.7	Wiring and Voltage Management.....	42
4.3.8	Charge controller sizing	43
4.3.9	Battery sizing	45
4.4	Selection of Refrigeration Cycle Components	49
4.4.1	Design requirement of the system	49
4.4.2	Refrigerator Compressor Selection.....	50
4.4.3	Selecting Condenser Temperature.....	53
4.4.4	Selecting Evaporator Temperature	53
4.4.5	ASHREA-HBP Cooling Capacity of the Compressor at the Selected Operating Temperature of Evaporator and Condenser.....	53
4.4.6	Modeling of CASCADE17-0244Y3 Compressor at its Operating Temperature	54
4.4.7	Isentropic Power Consumption of the Compressor at ASHREA-HBP Test Condition	55
CHAPTER-5: MATHEMATICAL MODELING.....		59
5.1	Vapor-Compression refrigeration cycle	59
5.2	Thermodynamics Analysis of the System	60
5.3	Mathematical Model of Sub-Components.....	61
5.3.1	Compressor.....	61
5.3.2	Condenser	62
5.3.3	Expansion valve.....	63
5.3.4	Evaporator	63

5.4	Radiation and Convection heat loss from the PV panel.....	63
5.4.1	The Radiation heat loss to from the PV to the sky temperature at <i>T_{sky}</i>	64
5.4.2	The convection heat loss from the PV by wind.....	64
5.4.3	Energy balance of the PV module	64
5.4.4	Refrigeration System Energy Performance	65
5.4.5	Hourly Milk temperature.....	66
5.4.6	Overall Energy Balance of the Refrigeration system	66
CHAPTER-6: RESULTS AND DISCUSSION		67
6.1	Results	67
CHAPTER-7: CONCLUSION AND RECOMMENDATION.....		73
7.1	Conclusion.....	73
7.2	Recommendation.....	74
REFERENCES		75
Appendix A: Electrical and Mechanical Characteristics under STC’(AKT-180-M)		78
Appendix B: MATLAB code		79
Appendix B ₁ : Code to model the I-V, P-V electrical characteristics of the PV module for single AKT-180-M as well as for four AKT-180-M connected in series and I-V intersection of PV module and the Compressor.....		79
Appendix B ₂ : Code to model the Total Efficiency variation of Refrigerator Compressor with Rpm		82
Appendix B ₃ : Code to model Monthly average Solar Radiation on inclined surface, Hourly PV surface temperature, Hourly Electrical Energy output of the System, Hourly temperature of the Milk and Monthly Cop of the System.		84
Appendix C: Performance Coefficients of CASCADE17-0244Y3 Compressor		90
Appendix D: Properties of Some Materials used		91
Appendix D ₁ : Thermo-physical properties		91
Appendix E: Peak Sunshine, daily extra-terrestrial solar radiation and daily solar radiation and Hour for October Month		92

Lists of Figures

Figure 1-1 solar radiation distribution [2]	2
Figure 1-2 Spectral distribution of black body radiation and sun radiation [3].....	3
Figure 2-1 Schematic drawing of incident light on pv cell	9
Figure 3-1 Photovoltaic system [25].....	15
Figure 3-3 Connecting PV cells in series.....	19
Figure 3-4 Connecting PV cells in parallel	19
Fig. 3.5 solar cell arrays consists of M_p parallel branches, with M_s modules in series in each branch.....	20
Fig. 4.1 Pyranometer	28
Fig. 4.2 Ratio of beam radiation on tilted surface to horizontal radiation	29
Fig. 4.3 Algorithm of MATLAB program used to model a PV panel	38
Fig. 4.4 I-V curve characteristics of single AKT-180-M Solar Panel at STC for different radiation at constant cell temperature.....	39
Fig. 4.6 P-V curve characteristics of single AKT-180-M Solar Panel at STC for different radiation at constant cell temperature.....	40
Fig. 4.8 A typical load variation with voltage.....	43
Fig. 4.9 FLEXmax 30/40 series charge controller.....	45
Fig. 4.10 LiFePo4 24V/360Ah battery	47
Fig. 4.12 CASCADE17-0244Y3 VSDC (variable speed direct current compressor)	50
Fig. 4.13 Cooling capacity Vs Power consumption and RPM of compressor	55
Fig. 4.14 Thermodynamic cycle of the refrigerator at selected evaporator and condenser temperature at ASHRAE-HBP test condition.....	56
Fig. 4.15 Efficiency of compressor variation with RPM.....	57
Fig. 4.16 I-V intersection point of PV module and compressor	58
Fig. 5.1 Single stage vapor compression refrigeration cycle.....	59
Fig. 5.2 T-S Diagram of real vapor compression refrigeration cycle.....	60
Fig. 5.3 Thermal network of a typical PV model.....	63
Fig. 5.4 Heat transfer of two sides of the PV panel	64
Fig. 6.1 Monthly average solar radiation on inclined surface	68
Fig. 6.2 Hourly PV surface temperature.....	69
Fig. 6.3 Hourly Electrical Energy output of the system	70
Fig. 6.4 Hourly Temperature of Milk	71
Fig. 6.5 Monthly Cop of the system	72

Lists of table

<i>Table 3-1:- Multi criteria decision making for solar panel</i>	17
<i>Table 4-1:- Recommended average day of month, declination angle and value of n by month</i>	25
<i>Table 4-2:- Electrical and Mechanical characteristics of AKT-180-M solar panel under STC</i> .	37
<i>Table 4-3:- Multi-criteria of Pulse-width modulation (PWM) Vs Maximum power point tracking (MPPT) (source Solarcraft, 2014 (Vader, 2014)</i>	43
<i>Table 4-4:- Multi-criteria decision of Deep-cycle Lead-acid battery Vs Lithium-ion battery (source: 12VMONSTER)</i>	46
<i>Table 4-5:- Reference for further information on battery charging current (*At minimum operating environment temperature, ** At 25°c environment temperature</i>	48
<i>Table 4-6:- Optional fixed resistor speed chart (source master flux)</i>	51
<i>Table 4-7:- Cooling capacity (Watt) of the compressor for (24V) at ASHRAE-HBP test condition (source Masterflux)</i>	51
<i>Table 4-8:- Power consumption (Watt) of the compressor for (24V) at ASHRAE-HBP test condition (source Masterflux)</i>	52
<i>Table 4-9:- Current consumption (Amp) of the compressor for (24V) at ASHRAE-HBP test condition (source Masterflux)</i>	52
<i>Table 4-10:- performance of CASCADE17-0244Y3 for different RPM, condenser temperature 49°c and evaporator temperature 0°c</i>	54

NOMENCLATURES

<i>COP</i>	<i>Coefficient of Performance</i>
<i>C_p</i>	<i>Specific heat</i>
<i>E_g</i>	<i>Band gap Energy</i>
<i>EOT</i>	<i>Equation of time</i>
<i>G_n</i>	<i>nominal Solar radiation</i>
<i>PV</i>	<i>photovoltaics</i>
<i>MCC</i>	<i>milk cooling center</i>
<i>I_{ph}</i>	<i>light current</i>
<i>I_o</i>	<i>diode current</i>
<i>I_{sh}</i>	<i>shunt current</i>
<i>R_s</i>	<i>resistors in series</i>
<i>R_p</i>	<i>resistors in parallel</i>
<i>I_{sc,n}</i>	<i>nominal short circuit current</i>
<i>V_{op,n}</i>	<i>nominal open circuit voltage</i>
<i>V_{mpp}</i>	<i>maximum power point voltage</i>
<i>I_{mpp}</i>	<i>maximum power point current</i>
<i>STC</i>	<i>standard test condition</i>
<i>K_v</i>	<i>open circuit voltage temperature coefficient</i>
<i>K_i</i>	<i>short circuit current temperature coefficient</i>
<i>P_{max,e}</i>	<i>maximum experimental peak output power</i>
<i>V_t</i>	<i>thermal circuit voltage</i>
<i>H_o</i>	<i>extraterrestrial solar radiation</i>
<i>G_{sc}</i>	<i>solar constant</i>
<i>VCR</i>	<i>vapor compression refrigeration</i>
<i>V_w</i>	<i>wind speed</i>
<i>T_d</i>	<i>sunshine and sunset hour angle</i>
<i>Z</i>	<i>elevation of the site</i>
<i>W_s</i>	<i>hourly angle</i>

<i>rt</i>	<i>ratio of hourly to daily diffuse solar radiation</i>
<i>δ</i>	<i>declination angle</i>
<i>φ</i>	<i>latitude of the site</i>
<i>θ</i>	<i>incidence angle</i>
<i>β</i>	<i>tilt angle</i>
<i>R_b</i>	<i>ratio of beam radiation on tilted surface to horizontal radiation</i>
<i>U</i>	<i>overall heat transfer coefficient</i>
<i>ACH</i>	<i>air change per hour</i>
<i>C_p</i>	<i>specific heat capacity</i>
<i>PWM</i>	<i>pulse width modulator</i>
<i>MPPT</i>	<i>maximum power point tracker</i>
<i>DOD</i>	<i>depth of discharge</i>
<i>FAO</i>	<i>food and agriculture organization</i>
<i>HBP</i>	<i>high back pressure</i>
<i>N</i>	<i>rotation speed of compressor</i>
<i>σ_{pv}</i>	<i>absorptivity of photovoltaic module</i>
<i>ε</i>	<i>effectiveness</i>
<i>K</i>	<i>thermal conductivity</i>

Subscripts

<i>amb</i>	<i>Ambient</i>
<i>b</i>	<i>Beam</i>
<i>con</i>	<i>Consumption</i>
<i>cond</i>	<i>Condenser</i>
<i>d</i>	<i>diffuse</i>
<i>e</i>	<i>Evaporator</i>
<i>f</i>	<i>Final</i>
<i>min</i>	<i>Milk inlet</i>
<i>max</i>	<i>Maximum</i>
<i>mpp</i>	<i>Maximum power point</i>
<i>n</i>	<i>Nominal</i>

<i>oc</i>	<i>Open circuit</i>
<i>p</i>	<i>Parallel</i>
<i>pv</i>	<i>Photovoltaic</i>
<i>r</i>	<i>refrigerant</i>
<i>ref</i>	<i>Refrigerant</i>
<i>s</i>	<i>Series</i>
<i>sc</i>	<i>Short circuit</i>
<i>sys</i>	<i>System</i>

© GSJ

CHAPTER-1: INTRODUCTION

1.1 Renewable energy

The energy which is harvested from the natural resources like sunlight, wind, tides, geothermal heat etc. is called Renewable Energy. As these resources can be naturally replenished, for all practical purposes, these can be considered to be limitless unlike the tapering conventional fossil fuels. The global energy crunch has provided a renewed impulsion to the growth and development of Clean and Renewable Energy sources. Clean Development Mechanisms (CDMs) are being adopted by organizations all across the globe. Another advantage of utilizing renewable resources over conventional methods is the significant reduction in the level of pollution associated. Powering the system with PV panels and batteries at night is the most reasonable option to run the DC compressor. Most of the solar cooling projects include AC compressor and inverter system which inverts the DC current input taken from the PV panels to AC. However, this system is inefficient and energy is wasted while DC current is converted into AC by the inverter. Whereas, DC compressor is more efficient in terms of power efficiency and power consumption and moreover the cost of conventional energy is rising and solar energy has emerged to be a promising alternative. They are abundant, pollution free, distributed throughout the earth and recyclable. PV arrays consist of parallel and series combination of PV cells that are used to generate electrical power depending upon the atmospheric specifics (e.g. solar insolation and temperature).

1.2 Distribution of solar radiation

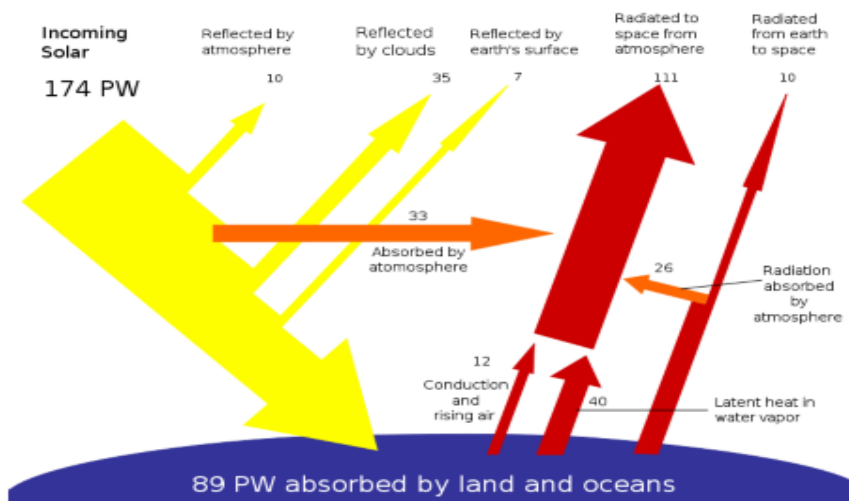


Figure 1-1 solar radiation distribution [2]

From the above Figure of solar radiation, earth receives 174 Peta-watts (PW) of incoming solar radiation at the upper atmosphere. Approximately 30% is reflected back to space and only 89 pw is absorbed by oceans and land masses [1]. The spectrum of solar light at the Earth's surface is generally spread across the visible and near-infrared region with a small part in the near-ultraviolet. The total solar energy absorbed by Earth's atmosphere, oceans and land masses is approximately 3,850,000 EJ per year [3].

1.3 Solar radiation reaching earth surface

The intensity of solar radiation reaching earth surface which is 1369 watts per square meter is known as Solar Constant. It is important to realize that it is not the intensity per square meter of the Earth's surface but per square meter on a sphere with the radius of 149,596,000 km and with the Sun at its centre.

The total amount solar radiation intercepted by the Earth is the Solar Constant multiplied by the cross section area of the Earth. If we now divide the calculated number by the surface area of the Earth, we shall find how much solar radiation is received in an average per square meter of the Earth's surface [3].

1.4 Spectrum of sun

The performance of Photovoltaic device is reliant on the spectral distribution of solar radiation. The standard spectral distribution is mainly used as reference for evaluation of PV devices. There are two standard terrestrial distribution defined by the American Society for Testing and Materials (ASTM), global AM1.5 and direct normal. The solar radiation that is perpendicular to

a plane directly facing the sun is known as direct normal. The global corresponds to the spectrum of the diffuse radiations. Diffuse radiations are the radiations which are reflected on earth's surface or influenced by atmospheric conditions. To measure the global radiations an instrument named pyranometer is used. This instrument is designed in such a way that it responds to each wavelengths and so that we get a precise value for total power in any incident spectrum [2].

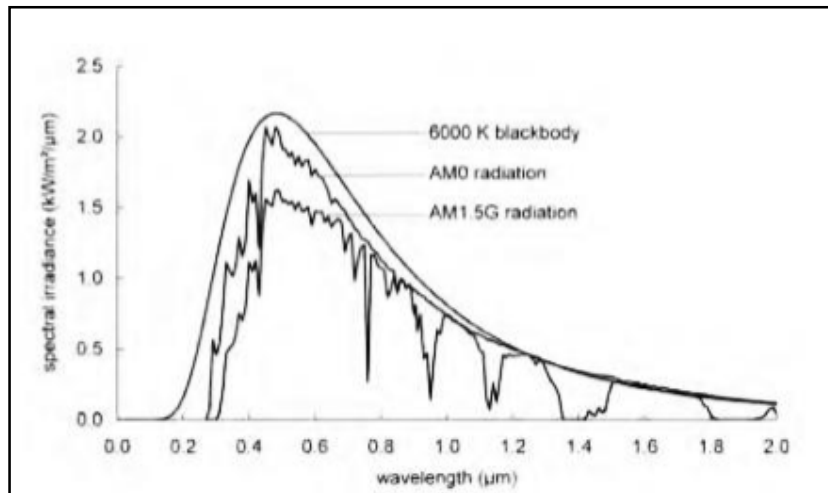


Figure 1-2 Spectral distribution of black body radiation and sun radiation [3]

The AM initials in the above Figure stands for air mass. The air mass in this circumstance means the mass of air between a surface and the sun. The length of the path of solar radiation from the sun through the atmosphere is indicated by the number AMx. The longer the path the more is the deviation of light. The AM0 in the above figure means the spectral distribution and intensity of sunlight in near-earth space without atmospheric attenuation.[3]

1.5 Background of the Study

Milk, be it from cows, buffaloes, goats, sheep or camels, is a highly nourishing food and has been harvested by humankind for thousands of years. Milk contains numerous nutrients and makes a significant contribution to meeting the human body's needs for calcium, magnesium, selenium, riboflavin, vitamin B12 and pantothenic acid (vitamin B). Milk is a complex food containing numerous nutrients required for daily human nutrition [4]. Milk and dairy products play a key role in healthy human nutrition and development throughout life, especially in childhood. However, raw fresh milk is highly perishable and is an excellent growth media for the microorganisms that cause spoilage. [5]

Milk and agro processing has a potentially important role in the economic development of developing countries.[6] India is the world's largest producer of milk and claims 20% of the world's total milk Production. According to milk production data by the National Dairy

Development Board, milk production in India has increased by approximately 51% from 80.6 million tons to 121.8 million tons. Nearly 820 million people live and work in rural India, and almost 10% of rural families 80 million work in dairy production.[7,8]

Ethiopia is reported to be endowed with the largest livestock population in Africa. According to the 2010 report of the Central Statistical Agency (CSA), the cattle population was estimated at about 50.9 million with a capacity of producing 3.2billion liter of milk annually. The indigenous breeds accounted for 99.19 percent, while the hybrids and pure exotic breeds were represented by 0.72 and 0.09 percent, respectively. From the total cattle population, 45.13 percent are males and 54.87 percent females. This indicates the importance of male cattle particularly oxen for draft power. However, in the crop/livestock mixed farming system, oxen work for a maximum of 100 days in a year. This means that for the rest of the year oxen compete for the meagre feed resources though unproductive. An appropriate alternative strategy needs therefore to be put in place to reserve the feed for dairy cows that produce not only milk but also replacement stock. The total estimated goat population was about 22 million with indigenous breeds accounting for 99.98 percent and hybrid and pure exotic breeds for about 0.02 percent. The male and female goat population accounted for 30.83 and 69.17 percent, respectively. The total camel population was estimated to be 807 581 with the proportion of male and female camels being 33.88 and 66.12 percent, respectively (CSA, 2010a). However, 20-25% of the total milk production is spoiled due to improper preservation.[9] This may be a great loss to the farmers and the country. The spoilage can be reduced by implementing suitable preservation strategies in the places where it is produced.[10,11]

The major approved methods of milk preservation are refrigeration and/or heat treatment, although both methods have limitations with respect to processing.[12] Fresh milk, after milking, normally has a temperature of 33°C. Proper milk cooling is essential to ensure good quality, because bacteria multiply rapidly when milk is cooled too slowly or if it is stored at temperatures above 4°C. Cooling and storage is very important, especially if there is a long delay (more than 2 h) between milking and delivery at the collection center.[13]

The vapor compression refrigeration system working with conventional energy has been used for most of the cooling applications. In recent years, the focus of the nations is shifted to renewable energy technologies because of the issues associated with conventional sources of energy.

To overcome the problem of continuous grid supply of electricity and diesel generator sets, renewable energy based refrigeration system for milk cooling at society level is quiet feasible and found competitive with lower energy related cost, minimum losses in the post-harvest and green house gas emissions. This can be achieved through taking energy efficiency steps,

reducing overall energy consumption and generating energy through renewable energy resource of photovoltaic based chillers [14].

Currently, lack of competitive small-scale PV (photovoltaic) driven chillers in most rural areas of developing countries is responsible for mismatched demand and supply of chilled milk [15].

1.6 Statement of Problem

Milk leaves the udder at a temperature of about 37°C. Fresh milk from a healthy cow is practically free from bacteria but must be protected against contaminating bacteria's as soon as it leaves the udder. Micro-organisms capable of spoiling the milk are everywhere from being on the udder to the milker's hands, on air-borne dust particles and water droplets, on straw and chaff, on the cow's hair and in the soil as well. Milk contaminated in this way must be filtered and careful attention must be paid to hygiene in order to produce milk of high bacteriological quality.

However, despite all precautions, it is impossible to completely exclude bacteria from milk. Milk is in fact an excellent growth medium for bacteria as it contains all the nutrients they need, so as soon as bacteria get into milk they start to multiply. Although the milk leaving the teats contains original bactericides which protect the milk against the action of micro-organisms during the initial period, it is a matter of time that the micro-organisms adapt this environment and starts to grow dramatically.

Unless the milk is chilled in a constant manner, it will be quickly spoiled by micro-organisms, which thrive and multiply most vigorously at temperatures around 33-37°C. milk should therefore be chilled quickly to about 4°C immediately after it leaves the cow where at this temperature the level of activity of micro-organisms is very low to cause humans life-risking disease. Therefore efficient cooling right after milking is the best way of preventing bacterial growth.

In most circumstance of developing countries of rural areas where large volume of milking takes place, lack of conventional grid supply or being too far from milking center also plays a major role in not achieving immediate cooling that results for spoilage of 20-25% of the total milk production due to improper preservation.

In general non-availability of cooling or chilling system and high ambient temperature are the main constrains in milk collection and distribution. These conditions decrease or shorten the shelf life of raw milk.

This paper aims to solve this mega-problem by using PV driven milk chiller on small-scale bases as to save endangered human's health especially of children's and to reduce production loss(evening milk) by chilling the milk to the desired temperature for use.

1.7 Objectives

1.7.1 General objective

- To design and simulate small-scale PV (photovoltaic) driven milk chiller for cooling and preserving milk at 4°C. (i.e PV system design as well as chiller components selection).

1.7.2 Specific objectives

- To collect and analyze data.
- Selecting operating temperature of condenser and evaporator based on ambient temperature of Semera.
- Selecting an appropriate size of compressor based on cooling load.
- Selecting size of the PV panel, battery, and charge controller based on cooling load estimation.
- Modeling electrical characteristics (such as I-V and P-V) of the selected PV panel from the manufacturer's specification
- To model refrigeration sub-components
- To simulate the performance of small-scale milk chiller with MATLAB software.

1.8 Scope and Delimitations

The scope of this particular research includes designing and simulating small-scale milk chillers by using solar radiation collected in PV cells, selection of refrigerator compressor, designing of an efficient thermodynamic cycle which is similar to the test condition of the compressor's manufacturer, modeling of the hourly performance variation of the solar refrigeration system, and transient heat transfer analysis of the preservation process of the milk by the power from PV electricity. The science of mechanical engineering (mostly thermal engineering) and electrical engineering to some extent will be dealt to come up with the desired cooling effect. The actual chiller manufacturing work won't prevail in this paper due to lack of ample time and shortage of budget as main limitations.

1.9 Thesis Organization

This thesis contains eight chapters where chapter one deals with how the solar energy is distributed on the earth's surface and how much of it is received and with in-depth sight on enormous benefits of milk despite facing huge spoilage risks. Chapter two brings us the details of PV cell science and the different technologies related to it with its historical background as

well. Chapter three observes the design of photovoltaic refrigeration system together with mathematical modeling of PV cell with its equivalent circuit and the basic working principle of PV driven milk chiller. Chapter four deals with data collection and analysis, cooling load estimation, sizing and design steps of PV system and appropriate component selection of refrigeration cycle based on condenser and evaporator temperature. Chapter five is all about the mathematical modeling of refrigeration cycle sub-components. Chapter six wraps-up all the works done in the previous chapters in the result and discussion part. Chapter seven deals with summarizing part of the work in the conclusion and recommendation chapter.



CHAPTER-2: LITERATURE REVIEW

2.1 Definitions of PV (photovoltaic) Chiller

A PV chiller is a device that will transfer heat from a low temperature environment to a high temperature environment by converting light energy from solar radiation to electricity using semiconducting materials that exhibit the photovoltaic effect.

2.2 Historical Background of PV

Solar technology isn't new. Its history spans from the 7th century B.C to today with starting by concentrating sun's heat with glass and mirrors to light fires. Today we have everything from solar-powered building to solar-powered vehicle. A physical phenomenon allowing light –electricity conversion (the photovoltaic effect) was discovered in 1839 by the French physicist, Alexandre Edmond Becquerel. Experimenting with metal electrodes and electrolyte he discovered that conductance rises with illumination. Willoughby Smith discovered the photovoltaic effect in selenium in 1873. In 1876, with his student Richard E. Day, William G. Adams discovered that illuminating a junction between selenium and platinum also has a photovoltaic effect. These two discoveries formed a foundation for the first selenium solar cell construction, which was built in 1877. Henceforth, the first solar cell was made by Charles Fritts in the year 1883 through the use of selenium but comprehensive theoretical work about the photovoltaic effect was written by Albert Einstein who described the phenomenon to receive the Noble prize in 1904. [16]. Another major breakthrough, which would have significant implications of the later manufacturing of Pv panels was the ability to create single crystal silicon by Jan Czochralski in the year 1918. Therefore in the solar photovoltaic area, many works start to be done ones the above mentioned science of progress adverts. Thomachan A. Kattakayam and K. Srinivasan has manufactured a refrigerator which is powered by field of photovoltaic panels, a battery tank and inverter and it's shown that there is no degradation in the performance when a non-sinusoidal waveform AC source is used to operate the refrigerator.[17]

2.3 PV cell Science

The most common PV cells are made of single-crystal silicon. An atom of silicon in the crystal lattice absorbs a photon of the incident solar radiation, and if the energy of the photon is high enough, an electron from the outer shell of the atom is freed. This process thus results in the formation of a hole–electron pair, a hole where there is a lack of an electron and an electron out in the crystal structure. These normally disappear spontaneously as electrons recombine with holes. The recombination process can be reduced by building into the cells a potential barrier, a

thin layer or junction across which a static charge exists. This barrier is created by doping the silicon on one side of the barrier with very small amounts (of the order of one part in 10^6) of boron to form p-silicon, which has a deficiency of electrons in its outer shell, and that on the other side with phosphorus to form n-silicon, which has an excess of electrons in its outer shell. The barrier inhibits the free migration of electrons, leading to a buildup of electrons in the n-silicon layer and a deficiency of electrons in the p-silicon. If these layers are connected by an external circuit, electrons (i.e., a current) will flow through that circuit. Thus free electrons created by absorption of photons are in excess in the n-silicon and flow through the external circuit to the p-silicon. Electrical contacts are made by metal bases on the bottom of the cell and by metal grids or meshes on the top layer (which must be largely uncovered to allow penetration of photons). A schematic section of a cell of this type and a schematic of a cell in a circuit are shown below

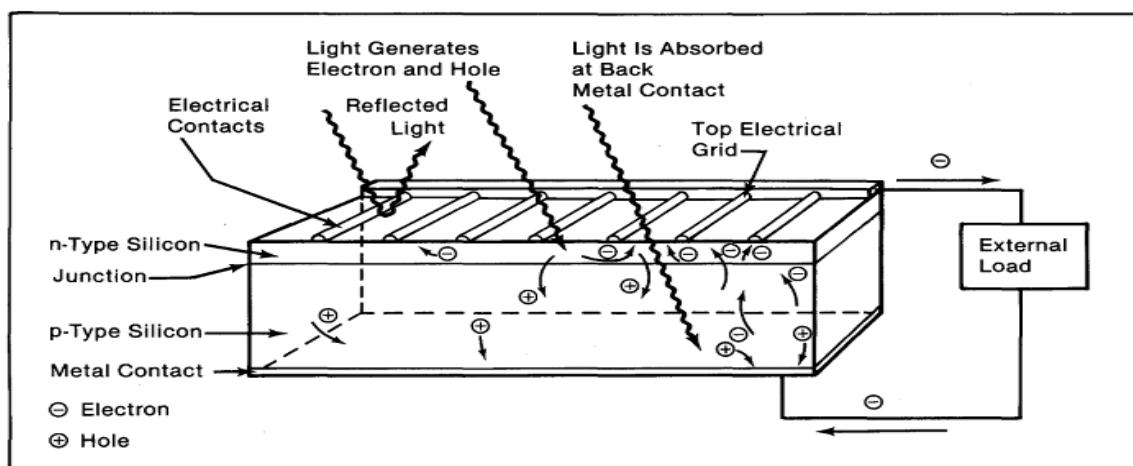


Figure 2-1 Schematic drawing of incident light on pv cell

General PV system energy flow path schematic drawing



Figure 2-2 Schematic drawing of stand-alone PV system

Advantages

- Minimal maintenance
- Power generation is silent
- Technology is improving rapidly
- No moving parts required
- Longer life
- Highly portable due to light weight
- Power output matches very well with peak load demands
- Generates electricity directly
- Well suited for distribution generation

Disadvantages

- Intermittency
- Relatively high cost especially with storage
- Requires relatively large amount of open space
- Relatively low efficiency

2.4 Different types of Solar Refrigeration Technologies

Solar refrigeration offers a wide variety of cooling techniques powered by solar collector-based thermally driven cycles and photovoltaic (PV)-based electrical cooling systems. In comparison with conventional electrically driven compression systems, substantial primary energy Savings can be expected from solar cooling, thus aiding in conserving energy and preserving the environment.

Solar refrigeration technology engages a system where solar power is used for cooling purposes. Henceforth, this paper aims at PV based electrical cooling system and also highlights others cooling techniques to some extent. According to Kim and Ferreira(2008), cooling can be achieved through four basic methods

2.4.1 Solar thermo-electrical cooling

In solar thermo-electric cooling, power produced by the solar PV devices is supplied to the peltier cooling systems. It is possible to produce cool by thermo-electric processes, using the principle of producing electricity from solar energy through thermoelectric effect and the principle of producing cool by Peltier effect. Thermo-electric generator consists of a small number of thermocouples that produce a low thermo-electric power but which can easily produce a high electric current. It has the advantage that can operate with a low level heat source and is therefore useful to convert solar energy into electricity[18].

The thermoelectric refrigerator is a unique cooling system, in which the electron gas serves as the working fluid. In recent years, concerns of environmental pollution due to the use of CFCs in conventional domestic refrigeration systems have encouraged increasing activities in research and development of domestic refrigerators using Peltier modules[19].

2.4.2 Solar thermo-mechanical cooling

In the thermo-mechanical solar cooling system, the thermal energy is converted to the mechanical energy. Then the mechanical energy is utilized to produce the refrigeration effect by compressing the working fluid in a vapor compression cycle directly (ejector cooling cycle) or indirectly (coupled with an organic Rankine cycle)[20].

2.4.3 Solar thermal cooling technologies

Solar thermal cooling is becoming more popular because a thermal solar collector directly converts light into heat. Sorption technology is utilized in thermal cooling techniques. The cooling effect is obtained from the chemical or physical changes between the sorbent and the refrigerant.[21]

2.4.4 Solar photovoltaic cooling systems

A PV cell is basically a solid-state semiconductor device that converts light energy into electrical energy. To accommodate the huge demand for electricity, PV-based electricity generation has been rapidly increasing around the world alongside conventional power plants over the past two decades[22].

While the output of a PV cell is typically direct current (DC) electricity, most domestic and industrial electrical appliances use alternating current (AC). Therefore, a complete PV cooling system typically consists of four basic components: photovoltaic modules, a battery, an inverter circuit and a vapor compression AC unit [23].

- The PV cells produce electricity by converting light energy (from the sun) into DC electrical energy.
- The battery is used for storing DC voltages at a charging mode when sunlight is available and supplying DC electrical energy in a discharging mode in the absence of daylight. A battery charge regulator can be used to protect the battery from overcharging.
- The inverter is an electrical circuit that converts the DC electrical power into AC and then delivers the electrical energy to the AC loads.
- The vapor compression AC unit is actually a conventional cooling or refrigeration system that is run by the power received from the inverter.

There have been many papers in the open literature enumerating the various advantages of each of the above methods as a feasible approach of refrigeration, however, in the present study; only solar photovoltaic refrigeration using the vapor compression system has been the main focus. Solar PV vapor compression refrigeration has gained much popularity because of their simplicity and high COPs. The energy supplied in the system is provided by an array of solar cells which convert the incident solar radiation to electricity. The later is used to drive the compressor and excess charges a battery system for use at periods at low or no insolation.

2.5 Previous Researches on PV cooling

Among the various technologies mentioned above, solar thermal and solar photovoltaics are mainly used in small-scale milk cooling operations and MCC's (milk cooling centers) according to [24] Some researchers conducted experiments on the performance analysis of photovoltaic driven vapour compressor refrigeration system. Kattakayam *et al.* (1996) studied the electrical characteristics of a 100W AC operated domestic refrigerator using R-12 powered by a field of SPV panels, a battery bank and an inverter. A minimum current region was observed in the mains voltage range of 180– 190V and at the inverter voltage range of 210–230 V. Charters and Oo (2003) suggested its use in developing countries for essential purposes such as vaccine serum storage at medical clinics in remote regions. Eltawil and Samuel (2007) stated that refrigerated storage, was believed to be best method for storing the fruits and vegetables in fresh form, which were not available in rural or remote locations where grid electricity was almost not available. Fatehmulla *et al.* (2011) designed and developed low power refrigeration system using PV modules, 2 modules each of 36 solar cells. Yilanci *et al.* (2011) studied the energy an analysis of a refrigerator, powered by a photovoltaic investigated to obtain efficient operation conditions based on experimental data. Sobamowo *et al.* (2012) designed and developed photovoltaic-powered dc vapour compression refrigeration system for developing countries such as Nigeria and showed that its applicability to different climatic regions in Africa and could be used for perishable food storage, improvement in the health services and living conditions in remote and rural areas which were unable to access electricity from the grid.

According to (Yesilata and Isiker,2006), PV refrigeration system are economical and reliable solution for remote or urban areas where the supply of electricity is non-reliable such as found in developing countries.

According to Obeng and Hans-Dieter (2009), the presence of solar PV powered icemakers in rural communities can assist micro enterprises in fishing, sale of ice cubes and cold stores, especially small rural stores in the tropical and sub-tropical countries such as Ghana and

Ethiopia to expand their inventory by adding items that can be preserved using solar-powered refrigerators.

Modi, et al. (2009) described the fabrication, experimentation and simulation stages of converting a 165L domestic electric refrigerator to a solar powered one. The conventional domestic refrigerator used in their experiment was redesigned by adding battery tank, inverter and a charge controller, and powered by photovoltaic panels and a maximum COP of 2.102 was observed at 7AM.

Biligili (2011), proposed and investigated the performance of a solar electric vapor compression refrigeration system under different evaporating temperatures and months in Adana city located in the southern of Turkey. Conventional refrigerator was operated by solar PV system via a battery, it was found the proposed system driven by solar PV can be successfully operated in the chosen province in Turkey and it may be more applicable and encouraged when the cost of solar panel system decreases.

According to (Kim and Ferriera, 2008), the biggest advantage of using solar panel for refrigeration is the simplicity in construction and high overall efficiency when combined with a conventional vapor compression system.

Thomachan and Kattakayam (2000), also presented the cool-down, warm-up and steady state performance of a 100Watt AC operated domestic refrigerator powered by a field of photovoltaic panel, a battery and an inverter. The author noted that there was no degradation in the performance when a non-sinusoidal waveform AC source is used to operate the refrigerator although it may involve only a slight additional heating of the hermetic compressor.

According to Aprea et al. (2009), PV systems are the most appropriate system for small capacity refrigeration plants used for food or medical applications in areas far from conventional energy sources where a high level of solar radiation is present.

This paper aims at using PV panel for cooling milk due to the many advantages it has like direct electricity production and low running cost which is vital for milk cooling in most rural areas and developing countries where grid system isn't available or at far distance. Moreover in Ethiopia, there hasn't been such cooling technology for the past decades which is the main gap that needs to be addressed to largely minimize post-harvest losses.

CHAPTER-3: DETAILS OF PHOTOVOLTAIC ARRANGMENT AND MODULE SELECTION

In this chapter, the detail working principle of the PV cell, module and array of the system will be presented as our main element in the cooling of milk to a desired temperature and the components of the refrigeration will be selected appropriately. The PV arrangement, materials used in a cell, different types of PV panels and their selection criteria, mathematical modeling of PV cell will also be dealt.

3.1 Photovoltaic Arrangement

3.1.1 Photovoltaic cells

PV cells are made of semiconductor materials, such as silicon. For solar cells, a thin semiconductor wafer is specially treated to form an electric field, positive on one side and negative on the other. When light energy strikes the solar cell, electrons are knocked loose from the atoms in the semiconductor material. If electrical conductors are attached to the positive and negative sides, forming an electrical circuit, the electrons can be captured in the form of an electric current - that is, electricity [25].

3.1.2 Photovoltaic module

Due to the low voltage generated in a PV cell (around 0.5V), several PV cells are connected in series (for high voltage) and in parallel (for high current) to form a PV module for desired output. Separate diodes may be needed to avoid reverse currents, in case of partial or total shading, and at night. The p-n junctions of mono-crystalline silicon cells may have adequate reverse current characteristics and these are not necessary. Reverse currents waste power and can also lead to overheating of shaded cells. Solar cells become less efficient at higher temperatures and installers try to provide good ventilation behind solar panels.[26]

3.1.3 Photovoltaic array

The power that one module can produce is not sufficient to meet the requirements of home or business. Most PV arrays use an inverter to convert the DC power into alternating current that can power the motors, loads, lights etc. The modules in a PV array are usually first connected in series to obtain the desired voltages; the individual modules are then connected in parallel to allow the system to produce more current [23]

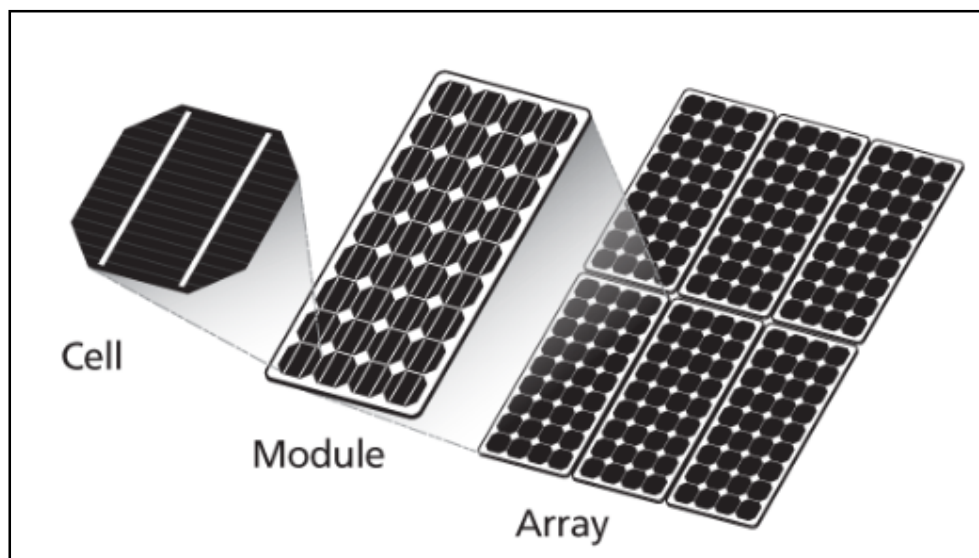


Figure 3-1 Photovoltaic system [25]

3.2 Materials used in a cell

The materials used in PV cells are as follows:

➤ **Single-crystal silicon**

Single-crystal silicon cells are the most common in the PV industry. The main technique for producing single-crystal silicon is the Czochralski (CZ) method. High-purity polycrystalline is melted in a quartz crucible. A single-crystal silicon seed is dipped into this molten mass of polycrystalline. As the seed is pulled slowly from the melt, a single-crystal ingot is formed. The ingots are then sawed into thin wafers about 200-400 micrometers thick (1 micrometer = 1/1,000,000 meter). The thin wafers are then polished, doped, coated, interconnected and assembled into modules and arrays [27]

➤ **Polycrystalline silicon**

Consisting of small grains of single-crystal silicon, polycrystalline PV cells are less energy efficient than single-crystalline silicon PV cells. The grain boundaries in polycrystalline silicon hinder the flow of electrons and reduce the power output of the cell. A common approach to produce polycrystalline silicon PV cells is to slice thin wafers from blocks of cast polycrystalline silicon. Another more advanced approach is the “ribbon growth” method in which silicon is grown directly as thin ribbons or sheets with the approach thickness for making PV cells [27].

➤ **Gallium Arsenide (GaAs)**

A compound semiconductor made of two elements: Gallium (Ga) and Arsenic (As). GaAs has a crystal structure similar to that of silicon. An advantage of GaAs is that it has high level of light absorptivity. To absorb the same amount of sunlight, GaAs requires only a layer of few

micrometers thick while crystalline silicon requires a wafer of about 200-300 micrometers thick. Also, GaAs has much higher energy conversion efficiency than crystal silicon, reaching about 25 to 30%. The only drawback of GaAs PV cells is the high cost of single crystal substrate that GaAs is grown on [27].

➤ Cadmium Telluride (CdTe)

It is a polycrystalline compound made of cadmium and telluride with a high light absorbability (i.e a small thin layer of the compound can absorb 90% of solar irradiation). The main disadvantage of this compound is that the instability of PV cell or module performance. As it a toxic substance, the manufacturing process should be done by extra precaution [27].

➤ Copper Indium Diselenide (CuInSe)

It is a polycrystalline compound semiconductor made of copper, indium and selenium. It delivers high energy conversion efficiency without suffering from outdoor degradation problem. It is one of the most light-absorbent semiconductors. As it is a complex material and toxic in nature so the manufacturing process face some problem [27].

3.3 PV panel types and Multi-criteria selection

3.3.1 PV panel design selection decision:

There are three basic types of PV panels.

i. **Mono-crystalline panels:**

Mono-crystalline solar panels are made of premium-grade silicon crystals, which contain very few impurities. These panels are therefore far more efficient than other types of solar panel [28].

Advantages (28)

- The average efficiency of mono-crystalline solar panels ranges from 15 to 20 percent.
- Mono-crystalline silicon solar panels make efficient use of space and are economical. As they have higher power outputs, they can be smaller than any other type of solar panel.
- They are highly durable. Most producers of mono-crystalline solar panels provide guarantees of 20–25 years.

Disadvantages (28)

- Is expensive and recommended mainly for small spaces when high power density is required.
- Shade affects their efficiency and power production.
- Sensitive to temperature. High temperatures decrease the efficiency of mono-crystalline solar panels.

ii. Polycrystalline panels:

These are slightly less efficient and expensive than mono-crystalline cells. They are easier to manufacture than mono-crystalline panels.

Advantages

- Manufacturing process is less complicated than that of mono-crystalline panels.
- The polycrystalline process does not include the Czochralski process, so generates less silicon waste than the mono-crystalline process does.
- Cheaper than mono-crystalline panels.

Disadvantages

- Lesser efficiency compared to mono-crystalline panels with average efficiency of around 12 to 17 percent due to higher impurity of silicon used to make polycrystalline panel.
- It needs more space than mono-crystalline panels.
- More sensitive to temperature than mono-crystalline

iii. Thin film panels:

Thin-film solar panel technology is cheaper to produce than either mono- or polycrystalline silicon cells, but thin-film panels have far lower efficiency.

Advantages [29]

- Thin-film panels are economical and simple to produce.
- High temperatures and shade have less impact on their performance and efficiency.
- They can be fully integrated into existing structures and building elements.

Disadvantages [29]

- Efficiency is in the range of only 7–13 percent.
- Because of this low efficiency, thin-film technology requires a lot of space.
- The low efficiency and need for space increases the cost of thin-film PV equipment, such as support structures and cables.
- They are less durable than mono- and polycrystalline solar panels.

Table 3-1:- Multi criteria decision making for solar panel

Candidate materials	Criteria					Total percentage
	Cost (30%)	Efficiency (30%)	Size (15%)	Durability (15%)	Temp. and shade effect (10%)	Total (100%)
Mono-crystalline	15	23	15	15	5	73
Poly-crystalline	20	18	10	10	7	65
Thin film	25	13	7	5	10	60

As shown in the table, efficiency, durability and simplicity of mono-crystalline panel makes it with higher percentage in the multi-criteria decision. Therefore mono-crystalline panel is selected for our PV design.

3.4 Mathematical modeling of a PV cell

3.4.1 Equivalent Circuit

A PV module consists of a number of solar cells connected in series and parallel to obtain the desired voltage and current output levels. Each solar cell is basically a p-n diode. As sunlight strikes a solar cell, the incident energy is converted directly into electrical energy without any mechanical effort. For simplicity, the single-diode model [30] is used in this paper. This model offers a good compromise between simplicity and accuracy with the basic structure consisting of a current source and a parallel diode. The equivalent electrical circuit is shown in Figure 3-2 below. Series resistors R_s and parallel (shunt) R_{sh} that limit the performance of the cell are added to the model to take into account the dissipative phenomena at the cell (internal losses) [31].

R_s : Series resistor, mainly due to losses by Joule effect through grids collection and to the specific resistor of the semiconductor, as well as bad contacts (Semi conductor, electrodes).

R_p : Parallel resistor, called 'Shunt' comes from the recombination losses mainly due to the thickness, the surface effects and the non-ideality of the junction.

An assessment of the operation of solar cells and the design of power systems based on solar cells must be based on the electrical characteristics, that is, the voltage-current relationships of the cells under various levels of radiation and at various cell temperatures. The electrical characteristics of a PV (photovoltaic) module is very vital in the determination of compressor's cooling effect level as it has direct relationship with the operating RPM of the compressor.

3.4.2 Solar Cell Model

The model is developed using basic circuit equations of the Photovoltaic (PV) Solar cells including the effects of solar irradiation and temperature changes. A PV cell can be represented by a current source connected in parallel with a diode, since it generates current when it is illuminated and acts as a diode when it is not. The equivalent circuit model also includes a shunt and series internal resistance that can be represented by resistors R_s and R_{sh} as shown below

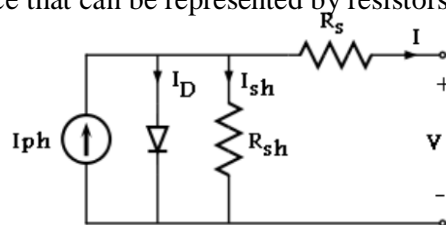


Figure 3-2 The equivalent PV cell circuit model

The physical structure of a solar cell is similar to that of a diode in which the p–n junction is subjected to sun exposure. The basic semi-conductor theory is captured in the following equations:

$$I = I_{ph, cell} - I_d \dots\dots\dots 3.1$$

$$I_d = I_{0, cell} [\exp (\frac{qV}{aKT}) - 1] \dots\dots\dots 3.2$$

Where:

$I_{ph, cell}$: is the current generated by the incident light (it is directly proportional to the Sun irradiation), I_d : is the Shockley diode equation, $I_{0, cell}$ is the reverse saturation or leakage current of the diode, q is the electron charge ($1.60217646 \times 10^{-19}$ C), K is the Boltzmann constant ($1.3806503 \times 10^{-23}$ J/K), T (in Kelvin) is the temperature of the p – n junction, and a is the diode ideality constant.

3.4.3 Solar Module Model

To increase total voltage of the module, cells have to be connected in series as shown in fig. 3.3, ($V_{out}=V_1+V_2+\dots$). Connecting PV cells in parallel, as shown in fig. 3.4, increases the total current generated by the module ($I_{out}=I_1+\dots$).The total current is equal to sum of current produced by each cell.

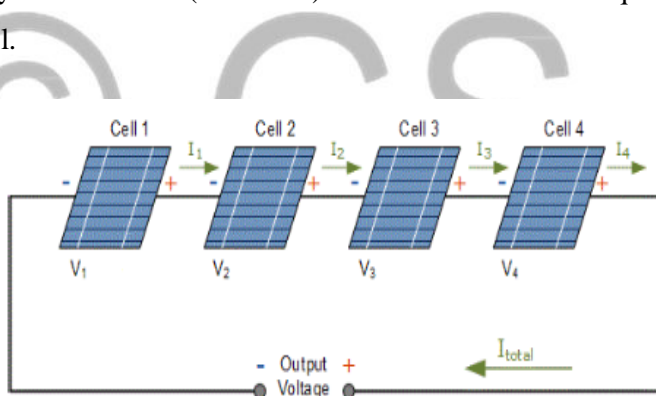


Figure 3-3 Connecting PV cells in series

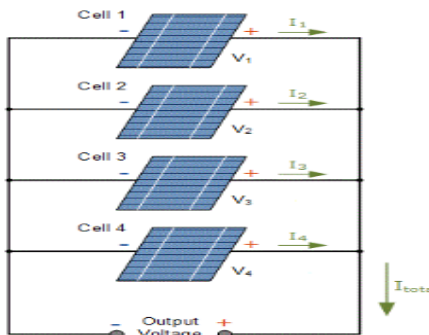


Figure 3-4 Connecting PV cells in parallel

For N_p cells branches in parallel and N_s cells in series, the total shunt resistances ($R_{sh,Module}$) and series resistances(R) in module are equal to:

$$R_{sh,module} = \frac{N_p}{N_s} * R_{sh,cell} \dots \dots \dots 3.3$$

$$R_{s,module} = \frac{N_s}{N_p} * R_{s,cell} \dots \dots \dots 3.4$$

Where: $R_{sh,module}$ is total shunt resistance of the module, $R_{s,module}$ is total series resistance of the module (Ohm), $R_{sh,cell}$ is Shunt resistance in one photovoltaic cell, $R_{s,cell}$ is Series resistance in one photovoltaic cell, N_p is Number of cells branches in parallel and N_s is number of cells in series.

The module current has an implicit expression depending on the following variables expressed in function of a single cell parameters and this is approximation method [32]

$$I_{sc,module} = N_p * I_{sc,cell} \dots \dots \dots 3.5$$

$$V_{oc,module} = N_s * V_{oc,cell} \dots \dots \dots 3.6$$

Where: $I_{sc,module}$ is Total short circuit current of the photovoltaic module, Amp, $V_{oc,module}$, Total open circuit voltage of the photovoltaic module, V, $I_{sc,cell}$, Short circuit current of one photovoltaic cell, and $V_{oc,cell}$, short circuit voltage of one photovoltaic cell.

3.4.4 Solar Array Model

The modules in a PV system are typically connected in arrays. Fig. 3.5 illustrates the case of an array with M_p parallel branches each with M_s modules in series.

The applied voltage at the array's terminals is denoted by V^A , while the total current of the array is denoted by

$$(I)^A = \sum_{i=0}^{M_p} I_i \dots \dots \dots 3.7$$

Where: A is the branch number

It is assumed that the modules are identical and the ambient irradiation is the same on all the modules, then the array's current is:

$$(I)^A = M_p * I^M \dots \dots \dots 3.8$$

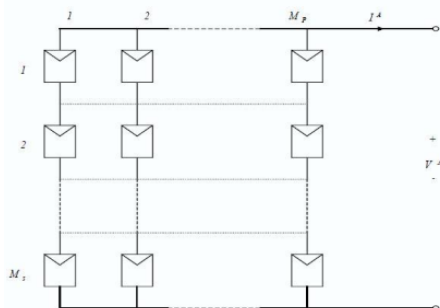


Fig. 3.5 solar cell arrays consists of M_p parallel branches, with M_s modules in series in each branch

Manufacturers of PV arrays, instead of the $I-V$ equation, provide only a few experimental data about electrical and thermal characteristics. Unfortunately, some of the parameters required for adjusting PV array models cannot be found in the manufacturer's datasheets, such as the light generated or PV current, the series and shunt resistances, the diode ideality constant, the diode reverse saturation current, and the band gap energy of the semiconductor. All PV array datasheets bring basically the following information: the nominal open-circuit voltage ($V_{oc,n}$) the nominal short-circuit current ($I_{sc,n}$), the voltage at the Maximum power point (V_{mmp}), the current at Maximum power point (I_{mmp}), the open-circuit voltage/temperature coefficient (K_v), the short circuit current/temperature coefficient (K_I), and the maximum experimental peak output power ($P_{max,e}$). This information is always provided with reference to the nominal condition or standard test conditions (STCs) of temperature and solar irradiation. So, it is necessary to derive the electrical parametric equation ($I-V$ and $P-V$ equation) from the manufacturer's data sheet.

Since the basic equation of Kirchhoff (3.1) of the elementary PV cell does not represent the $I-V$ characteristic of a practical PV array, practical arrays are composed of several connected PV cells and the observation of the characteristics at the terminals of the PV array requires the inclusion of additional parameters to the basic equation [33].

$$I = I_{ph} - I_o \left[\exp\left(\frac{V+IR_s}{v_t a}\right) - 1 \right] - \frac{V+IR_s}{R_{sh}} \dots\dots\dots 3.9$$

Where I_{ph} and I_o are the photovoltaic (PV) and saturation currents, respectively, of the array and $v_t = N_s * K * T / q$ is the thermal voltage of the array with (N_s) number of cells connected in series. The diode saturation current I_o and its dependence on the temperature and expressed as [32].

$$I_o = I_{o,n} \left(\frac{T}{T_n}\right)^3 \exp\left[\frac{qE_g}{aK} \left(\frac{1}{T_n} - \frac{1}{T}\right)\right] \dots\dots\dots 3.10$$

Where: Where E_g is the band gap energy of the semiconductor ($E_g = 1.12 \text{ eV}$ or $1.794 \times 10^{-19} \text{ J}$) for the mono-crystalline Si at 25 °C) and $I_{o,n}$ is the nominal saturation current, the value of diode ideality constant is usually between $1 \leq a \leq 1.5$ and for mono-silicon material is around 1.2 [34]

$$I_{o,n} = \frac{I_{sc,n}}{\exp\left(\frac{V_{oc,n}}{aV_{t,n}}\right) - 1} \dots\dots\dots 3.11$$

Where: $V_{t,n}$ is the thermal voltage of N_s series-connected cells at the nominal temperature T_n . The light-generated current of the PV cell depends linearly on the solar irradiation and is also influenced by the temperature according to the following equation [33]

$$I_{ph} = (I_{ph,n} + K_I \Delta T) \frac{G}{G_n} \dots\dots\dots 3.12$$

Where: $I_{ph,n}$ (in Amp) is the light-generated current at the nominal condition (i.e 25°C and 1000W/m²), $\Delta T = T - T_n$ (T and T_n are the actual and nominal temperatures (K), respectively),

K_I is the short circuit temperature coefficient usually given by the manufacturers and also calculated by

$$K_I = \frac{I_{sc}(T_2) - I_{sc}(T_1)}{T_2 - T_1} \dots\dots\dots 3.13$$

G is the irradiation on the PV panel (W/m²) and G_n is the nominal irradiation (i.e 1Suns=1000W/m²).

The nominal light generated current $I_{ph,n}$ is given accurately by the following equation [33].

$$I_{ph,n} = \frac{R_p + R_s}{R_p} I_{sc,n} \text{ or } I_{ph,n} = I_{sc}(T_n) * \frac{G}{G_n} \dots\dots\dots 3.14$$

The series resistance R_s was included; which represents the resistance inside each cell in the connection between cells.

$$R_s = \frac{-dV}{dI_{Voc}} - \frac{1}{X_V} \dots\dots\dots 3.15$$

$$X_V = I_o(T_n) * \frac{q}{A * K * T_n} \exp\left(\frac{qV_{oc,n}}{A * K * T_n}\right) - \frac{1}{X_V} \dots\dots\dots 3.16$$

Therefore equation (3.9) can be expressed with the known values given by the manufacturer's datasheet ($I_{sc,n}$ and $V_{oc,n}$), the constants (a, q, K and Eg) and the external influential factors of radiation and temperature (T, G), but the internal influencing parameters (R_s and R_p) are still unknown.

Marcelo G. et al.[33], proposed an interesting method for adjusting R_s and R_p based on the fact that there is an only pair $\{R_s, R_p\}$ that warranties that $P_{max,m} = P_{max,e} = V_{mpp} I_{mpp}$ at the (V_{mpp}, I_{mpp}) point of the I-V curve, i.e., the maximum power calculated by the I-V model of equation (3.9), ($P_{max,m}$) is equal to the maximum experimental power from the datasheet ($P_{max,e}$) at the MPP (where MPP is a maximum power point, which means a point where the power output of the solar panel will be maximum).

Using the help of the method proposed by *Marcelo G*, a mat-lab program is developed which is capable of determining the electrical characteristics of any solar panel from the specification of the manufacturer data sheet.

The calculated maximum current output of the solar panel at nominal temperature and solar radiation (at 25°C and 1000 W/m²) could be expressed using equation (3.9) as

$$I_{mpp} = I_{ph,n} - I_{o,n} \left[\exp\left(\frac{V_{mpp} + R_s I_{mpp}}{V_{t,n} a}\right) - 1 \right] - \frac{V_{mpp} + R_s I_{mpp}}{R_p} \dots\dots\dots 3.17$$

Where: V_{mpp} is the voltage at MPP (Maximum power point), the thermal voltage of the array at STC I_{mpp} is current at MPP.

Rearranging equation (4.51) to express the shunt resistor with other variables will be

$$R_p = \frac{V_{mpp} + R_s I_{mpp}}{I_{ph,n} - I_{o,n} \left[\exp\left(\frac{V_{mpp} + R_s I_{mpp}}{V_{t,n} a}\right) - 1 \right] - I_{mpp}} \dots\dots\dots 3.18$$

3.5 Working principle of PV (photovoltaic) driven milk chiller

General working principle summary

- 1 Solar radiation from the sun is collected through PV modules where they will be changed to electricity.
- 2 The PV generated electricity should be controlled before passing to the battery tank in order to safe functioning of the battery from overly charged and to avoid deep discharge.
- 3 The battery tank stores the power during the sunlight period and uses the stored energy in the night time when insufficient power prevails.
- 4 Here the actual milk chilling effect will be achieved by the electricity received to the compressor just same like vapor-compression refrigeration system



CHAPTER-4: METHODOLOGY

In this chapter, four main steps for the design of PV panel and selecting components of the chiller will be undertaken primarily based on the cooling load requirement. The steps to be followed are data collection and analysis, cooling load estimation, standard sizing and design steps of PV system and selection of PV refrigerator components.

4.1 Data collection and analysis

Semera which is located in afar region has been selected for implementing the design case study has the following geographical coordinates together with five year sunshine hour data as collected from the National Metrology Agency of Ethiopia.

Latitude = 11° 47' 36" N

Longitude = 41° 12' 4" E

Elevation above sea level = 433m =1420 ft

4.1.1 Solar radiation analysis

First we start to calculate the extraterrestrial solar radiation on horizontal surface as a platform for estimating our daily solar radiation value for horizontal surface. Therefore by using the following correlation, we calculate daily solar radiation daily extraterrestrial solar radiation H_o (kW hr /m²/day)

$$H_o = \frac{24 * G_{sc}}{\pi} * \left(1 + 0.033 \cos \frac{360n}{365}\right) * (\cos \phi \cos \delta \sin \omega_s + \frac{\pi \omega_s}{180} \sin \phi \sin \delta) \dots \dots \dots 4.1$$

Where H_o : extraterrestrial solar radiation (i.e solar radiation that would be received in the absence of atmosphere),

$G_{sc} = 1367$ w/m² is solar constant,

n : the number of days of the year,

ϕ is the latitude of semera,

δ sun declination angle and

ω_s : sunset or sunrise hour angle which is given by

$$\omega_s = \cos^{-1}(-\tan \phi \tan \delta)$$

Table 4-1:- Recommended average day of month, declination angle and value of n by month

Month	n for i th Day of month	For Average Day of month		
		date	n	δ
January	I	17	17	-20.9
February	31+i	16	47	-13.9
March	59+i	16	75	-2.4
April	90+i	15	105	9.4
May	120+i	15	135	18.8
June	151+i	11	162	23.1
July	181+ i	17	198	21.2
August	212+i	16	228	13.5
September	243+i	15	258	2.2
October	273+i	15	288	-9.6
November	304+i	14	318	-18.9
December	334+i	10	344	-23.0

Once the extraterrestrial solar radiation is found, the daily total solar radiation will be calculated by using Angstrom regression equation

$$\frac{H}{H_o} = a + b * \frac{s}{T_d} \dots\dots\dots 4.2$$

Where H: daily total solar radiation on horizontal surface,

a and b are the empirical constant parameters, which express as a function of latitude and sunshine hours

$$a = -0.309 + 0.539 * \cos\phi - 0.0693 * z + 0.29 * \frac{s}{T_d} \dots\dots\dots 4.3$$

$$b = 1.449 - 0.553 * \cos\phi - 0.694 * \frac{s}{T_d} \dots\dots\dots 4.4$$

Where s: is sunshine hour in a day,

Z: is elevation of the site above sea level = 433m and T_d is the time of sun set or rise, its equation is given below

$$T_d = \frac{2}{15} * \omega_s = \frac{2}{15} \cos^{-1}(-\tan\phi \tan\delta) \dots\dots\dots 4.5$$

Where hourly angle is:

$$\omega_s = \cos^{-1}(-\tan\phi \tan\delta) \dots\dots\dots 4.6$$

The daily total solar radiation on horizontal surface (H) has two components, daily solar beam radiation (H_b) and daily solar diffuse radiation (H_d) components. Calculating the sunrise or sunset hour angle (ω_s) from equation (6), ω_s is greater than 81.4° for all months of the year, the clearance index K_t are in the range of 0.3 to 0.8. Therefore average daily diffuse radiation on the surface is given by Liu and Jordan correlation [34].

$$\frac{H_d}{H} = 1.311 - 3.022K_t + 3.427K_t^2 - 1.821K_t^3 \dots\dots\dots 4.7$$

Where $k_t = \frac{H}{H_o}$

Therefore we can calculate the daily beam radiation from the total daily solar radiation by:

$$H = H_b + H_d \dots\dots\dots 4.8$$

4.1.2 Estimation of hourly radiation from daily data

Once we know the daily average solar irradiation on, we'll change this daily average data to hourly solar irradiance for each and every month in a year for the sake of easily understanding of the transient nature of the solar intensity within a day. In order to do so we'll use the following correlation [34]

$$r_t = \frac{I}{H} \dots\dots\dots 4.9$$

Where: I is hourly solar radiation on horizontal surface,

H is daily solar radiation on horizontal surface,

r_t is the ratio of hourly to daily total solar radiation and also expressed as follow:

$$r_t = \frac{\pi}{24} (a + b \cos \omega) \left(\frac{\cos \omega - \cos \omega_s}{\sin \omega_s - \left(\frac{\pi \omega_s}{180}\right) \cos \omega_s} \right) \dots\dots\dots 4.10$$

Where: ω is the hour angle in degree and ω_s is the sunset hour angle.

The coefficient of a, b and ω is given as:

$$a = 0.409 + 0.5016 * \sin (\omega_s - 60) \dots\dots\dots 4.11$$

$$b = 0.6609 - 0.4767 * \sin (\omega_s - 60) \dots\dots\dots 4.12$$

$$\omega = (12 - ST) * 15^\circ \dots\dots\dots 4.13$$

Therefore the ratio of hourly to daily solar radiation (r_t) will be calculated using excel or Matlab

Since $r_t = \frac{I}{H}$

$$I = H * r_t \dots\dots\dots 4.14$$

Hourly solar radiation will be calculated for every hour of the months in a year by using the above equation which is vital to depict the transient nature of power fluctuation from the solar radiation available.

4.1.3 Optimum tilt angle of the PV panel

Semera which is found in the northern hemisphere should face towards the south in order to receive ample irradiation. The collector must face towards the equator with tilt angle of the local latitude of the site is recommended [35]. The solar radiation reaches pick at solar noon when the sun just becomes at meridian of the point. So, to utilize this pick solar radiation, our solar panel must face south with zero azimuth angle (i.e. no tilting of the panel towards west or east).

For south facing panels incident angle of solar rays is given as [36]

$$\cos\theta = \sin(L - \beta) \sin(\delta) - \cos(L - \beta) \cos(\delta) \cos(\omega) \dots\dots\dots 4.15$$

Where: θ is incident angle of solar radiation on the PV panel which is tilted by β angle from horizontal surface to south, L is latitude angle of the point, ω is hour angle, and δ is declination angle.

At solar noon (as it is important reference for almost all solar calculation [35] the hour angle (ω) will be zero. So, equation (4.15) will be:

$$\cos(\theta) = \sin(L - \beta) \sin(\delta) - \cos(L - \beta) \cos(\delta) \cos(0)$$

$$\cos(\theta) = \sin(L - \beta) \sin(\delta) - \cos(L - \beta) \cos(\delta)$$

Which can be further reduced using cosine law

$$\cos(\theta) = -\cos(L - \beta + \delta) \dots\dots\dots 4.16$$

$$\theta = \pi - (L - \beta + \delta) \dots\dots\dots 4.17$$

Taking summer solstice or fall equinox as reference, the declination angle δ will be fixed to zero,

and equation (4.17) will be:

$$\theta = \pi - (L - \beta) \dots\dots\dots 4.18$$

The incident angle (θ) of equation (4.4) will become optimum when its value is zero. So, does the tilt angle of the panel.

$$0 = \pi - (L - \beta_{optimum})$$

$$\beta_{optimum} = L - \pi \dots\dots\dots 4.19$$

Equation (4.20) indicates the need for tilting of the solar panel at the same latitude angle but to the opposite direction (i.e. if the latitude position is north to face the panel to south).

In our case, Semera is found 11.76 degree of north. Hence the solar panel should face 11.76 to south.

4.1.4 Solar radiation on the optimally tilted PV panel

The sunshine hour solar data from the National Metrology Agency of Ethiopia must be analyzed in such a way that the irradiation output should be based on the tilted angle of the PV. Since we already know the optimum tilt angle, now we should come up with the amount of irradiation it receives hourly. Unfortunately the device Pyranometer in fig. 4.1 is used to measure only the global solar radiation falling on horizontal surface since its sensor has a horizontal radiation-sensing surface that absorbs solar radiation energy from the whole sky (i.e. a solid angle of 2π sr) and transforms this energy into heat.



Fig. 4.1 Pyranometer

For purposes of solar process design and performance calculations, it is often necessary to calculate the hourly radiation on a tilted surface of a collector from measurements or estimates of solar radiation on a horizontal surface. So far the equations we have seen above works best for the horizontal surface, we can't proceed with it. Since the PV panel is not placed horizontally facing the sky, some amendment will be done in the following part to accurately estimate the solar radiation incident on the tilted PV panel. The radiation on the tilted surface considers three components: beam, isotropic diffuse and solar radiation diffusively reflected from the ground. A surface tilted at slope β from the horizontal has a view factor to the sky $F_{c-s} = \frac{(1+\cos\beta)}{2}$, view factor to the ground $F_{c-g} = \frac{(1-\cos\beta)}{2}$ and if the surroundings have a diffuse reflectance of ρ_g for the total solar radiation, the reflected radiation from the surrounding on the surface will be

$$I * \rho_g \left(\frac{1-\cos\beta}{2} \right)$$

Therefore the total solar radiation on the tilted surface is given by Liu-Jordan diffuse assumption [24]

$$H_T = H_b R_b + H_d \frac{(1+\cos\beta)}{2} + H \rho_g \frac{(1-\cos\beta)}{2} \dots\dots\dots 4.20$$

Where: H_T : total solar radiation on tilted surface,

H_b : daily solar beam radiation on horizontal surface,

R_b : ratio of beam radiation on tilted surface/beam radiation on horizontal surface,

H_d : daily diffuse solar radiation on horizontal surface,

H : daily solar radiation on horizontal surface,

ρ_g : diffuse reflectance of the ground,

β : tilt angle

4.1.5 Hourly absorbed solar radiation

The monthly average hourly radiation incident on the collector is given by

$$I_T = (Hr_t - H_d r_d)R_b + H_d \left(\frac{1+\cos\beta}{2} \right) + H\rho_g r_t \left(\frac{1-\cos\beta}{2} \right) \dots\dots\dots 4.21$$

Where r_d : is the ratio of hourly diffuse radiation to total diffuse radiation on horizontal surface and is given by

$$r_d = \frac{\pi}{24} \left(\frac{\cos\omega - \cos\omega_s}{\sin\omega_s - \left(\frac{\pi\omega_s}{180} \right) \cos\omega_s} \right) \dots\dots\dots 4.22$$

Ratio of beam radiation on tilted surface to that of horizontal surface (R_b) is given by

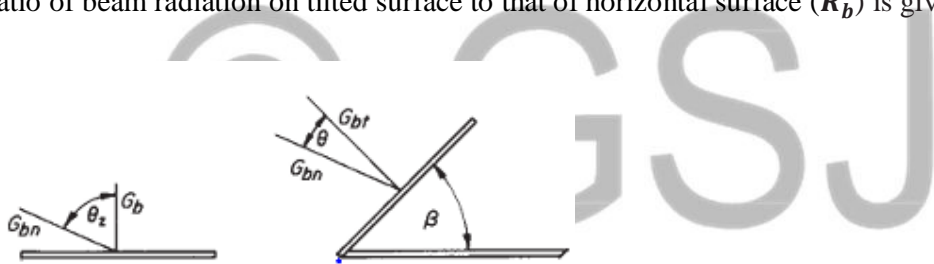


Fig. 4.2 Ratio of beam radiation on tilted surface to horizontal radiation

$$R_b = \frac{G_{bT}}{G_b} = \frac{G_{bn} \cos\theta}{G_{bn} \cos\theta_z} = \frac{\cos\theta}{\cos\theta_z} \dots\dots\dots 4.23$$

Where: θ is incidence angle on the surface which is given by

$$\cos\theta = \sin\delta \sin\phi \cos\beta - \sin\delta \cos\phi \sin\beta \cos\gamma + \cos\delta \cos\phi \cos\beta \cos\omega + \cos\delta \sin\phi \sin\beta \cos\gamma \cos\omega + \cos\delta \sin\beta \sin\gamma \sin\omega$$

$$\cos\theta = \cos\theta_z \cos\beta + \sin\theta_z \sin\beta \cos(\gamma_s - \gamma)$$

θ_z is zenith angle and is given by

$$\cos\theta_z = \cos\phi \cos\delta \cos\omega + \sin\delta \sin\phi$$

Where: γ is surface azimuth angle,

γ_s is solar azimuth angle

Daily solar beam radiation on horizontal surface (H_b) is can be found from equation(4.8)

$$H = H_b + H_d \dots\dots\dots 4.24$$

$$H_b = H - H_d \dots\dots\dots 4.25$$

Where: H_d from equation (4.7) = $(1.311 - 3.022K_t + 3.427K_t^2 - 1.821K_t^3) * H$

4.1.6 Ambient temperature analysis

The hourly variation of temperatures can be predicted from the daily maximum and daily minimum temperatures using the sine-exponential model (Brandsma Koñnen 2006). The method is developed by Parton and Logan (1981). This model describes the diurnal cycle by a sine function during daytime connected to a decreasing exponential function during nighttime.

A, for day light hours

$$T(H) = (T_{MAX} - T_{MIN}) \sin\left(\frac{\pi * m}{y + 2a}\right) + T_{MIN} \dots\dots\dots 4.26$$

B, for night _time hours

$$T(H) = T_{MIN} + (T_{SUNSET} - T_{MIN}) \text{EXP}\left(\frac{-b * n}{z}\right) \dots\dots\dots 4.27$$

Where $T(H)$ is the temperature at any hour of the day or night period determined from m and n , y is day length (h), z is night length (h), T_{SUNSET} is temperature at sunset ($^{\circ}\text{C}$), m is number of hours between time at T_{MIN} and sunset (h), n is number of hours from sunset to the time of T_{MIN} (h), a is lag coefficient for $T_{MAX}=1.80(\text{h})$, b is night –time temperature coefficient = $2.2.0(\text{h})$

4.2 Cooling Load Estimation

The total cooling load must be estimated in order to size our PV panel optimally. The four types of load we should consider are as follows

4.2.1 Transmission load

The rate of heat transfer through a particular wall, floor, or ceiling section of milk storage tank can be determined from

$$Q_{trans} = U * A_o * \Delta T (W) \dots\dots\dots 4.28$$

Where: A_o : outside surface area of the storage tank

ΔT : temperature difference between the outside air and the air inside the refrigerated space

U : overall heat transfer coefficient

According to ASHRAE (2002), the overall heat transfer coefficient (U) is determined from

$$U = \frac{1}{\frac{r_o}{h_i * r_i} + \frac{r_o * \ln(r_o / r_i)}{K_{steel}} + \frac{r_o * \ln(R_o / r_o)}{K_{ins}} + \frac{1}{h_o}} \dots\dots\dots 4.29$$

Where : r_i and r_o ; inside and outside radius of the milk storage tank respectively

R_o is radius of the storage tank including the insulation thickness and is given by

$$R_o = r_o + \text{insulation thickness}$$

h_i and h_o is the inner and outer surface convective heat transfer respectively.

The overall heat transfer coefficient for natural convection falls in the range of $0.15 \frac{w}{m^2K}$ to $0.28 \frac{w}{m^2K}$ and convective heat transfer coefficient range from $5 \frac{w}{m^2K}$ to $25 \frac{w}{m^2K}$. [35]

- From the standard milk storage tank dimension (Refrigerated milk tank, G1; Alfred and Co.), we consider the size of the cylindrical milk storage tank for 50 liter to be stainless steel with Height = 57cm, Diameter = 35cm, $r_o = 17.5cm$, $r_i = 17.2cm$ and Weight = 53kg
- Extruded polystyrene insulator is used $R = 5 \frac{m^2.K}{w}$ per 1" of thickness and insulation thickness to be 1" = 0.0254m
- All sides of the storage tank are well insulated.

Calculating the transmission load as follows

$$Q_{trans} = U * A_o * \Delta T \text{ (W)}$$

$$U = \frac{1}{\frac{r_o}{h_i * r_i} + \frac{r_o * \ln(r_o / r_i)}{K_{steel}} + \frac{r_o * \ln(R_o / r_o)}{K_{ins}} + \frac{1}{h_o}}$$

A_o = area of all insulated sides of the storage tank

$$A_o = \pi * D * H + \pi r^2$$

$$A_o = \pi * 0.35 * 0.57 + \pi * 0.175^2 = 0.723m^2$$

ΔT = temperature difference between the outside and inside temperature = $37^\circ C - 4^\circ C = 33^\circ C$

Therefore transmission load $Q_{transmission} = 0.185 \frac{w}{m^2.K} * 0.723m^2 * 33K = 12.75$

$$Q_{trans} = 4.41 \text{Watt}$$

4.2.2 Infiltration load

This is the heat gain through warm outside air which occurs during opening the hood of the storage tank either when filling the tank with milk to be cooled or when dispatching chilled milk from the storage tank.

A practical way of determining the infiltration load is to estimate the rate of air infiltration in terms of air changes per hour (ACH), which is the number of times the entire air content of the storage tank is replaced by the infiltrating air per hour. Once the number of air changes per hour is estimated, the mass flow rate of air infiltrating into the room is determined from [38]

$$\dot{m}_{air} = (V_{room}/v_{air}) * ACH \left(\frac{kJ}{hr}\right) \dots\dots\dots 4.30$$

Where

V_{room} : is the volume of the tank and

v_{air} : is the specific volume of the dry air in the tank. Once \dot{m}_{air} is available, the sensible and latent infiltration loads of the cold storage tank can be determined from

$$Q_{inf,sensible} = \dot{m}_{air} (h_{amb} - h_{room}) \left(\frac{kJ}{hr}\right) \dots\dots\dots 4.31$$

$$Q_{inf,latent} = (\omega_{amb} - \omega_{st,air}) \dot{m}_{air} h_{fg} \left(\frac{kJ}{hr}\right) \dots\dots\dots 4.32$$

where

ω : is the humidity ratio of air (the mass of water vapor in 1 kg of dry air),

h : is the enthalpy of air, and h_{fg} is the heat of vaporization of water.

The values of specific volume v , enthalpy h , and the humidity ratio ω can be determined from the psychrometric chart when the temperature and relative humidity (or wet-bulb temperature) of air are specified.

Assumptions[38]

- Ideal gas properties of air is considered from table $h_{amb} = h@37oc = 310.45kJ/kg$,
 $h_{room} = h@4oc = 277.3kJ/kg$ and $v = \frac{1}{\rho} = 1/1.2kg/m^3 = 0.833m^3/kg$
- Atmospheric pressure condition, $h_{fg} = 2257kJ/kg$ from saturated steam table
- Since the storage tank volume is small, air change per hour(ACH) to be 1.04

Therefore mass flow rate of the air entering the tank will be

$$\dot{m}_{air} = (V_{room}/v_{air}) * ACH = \left(\frac{0.1m^3}{0.833\frac{m^3}{kg}}\right) * \frac{1.04}{hr} = 0.125 \frac{kg}{hr}$$

$$Q_{inf,sensible} = 0.125 \frac{kg}{hr} \left(310.45 \frac{kJ}{kg} - 277.3 \frac{kJ}{kg}\right)$$

Or we can use also

$$Q_{inf,sensible} = \dot{m}_{air} * C_{pair} * (T_{amb} - T_{inside}) = 0.125 \frac{kg}{hr} * 1 \frac{kJ}{kg.K} * 33K = 4.142 \frac{kJ}{hr}$$

$$Q_{inf,sensible} = 4.14kJ/hr = 1.15Watt$$

$$Q_{inf,latent} = (\omega_{amb} - \omega_{st,air}) \dot{m}_{air} h_{fg}$$

$$\omega_{amb} : \text{humidity ratio of the ambient air} = 0.622 * \frac{\%Mv}{(100 - \%Mv)}$$

$$\%Mv \text{ (moisture by volume)} = \frac{\text{partial pressure of water vapor}}{\text{total pressure}} = \frac{P_{\text{water vapor}}}{P_{\text{total}}}$$

To find the partial pressure of water vapor we use Antoine equation as follows

$$\log P_{\text{water vapor}} = 8.07131 - \left(\frac{1730.63}{233.426+T}\right) \dots\dots\dots 4.33$$

Where T in $^{\circ}c$ and $P_{w,vapor}$ in torr

for ambient temperature $T = 37^{\circ}c$

$$\log P_{w,vapor} = 8.07131 - \left(\frac{1730.63}{233.426+37}\right) = 1.67166$$

$$P_{w,vapor} = 46.95 \text{ torr} = 46.95 * 133.322pa = 6259.82pa \dots\dots\dots 1 \text{ torr} = 133.322Pa$$

$$\%Mv \text{ (moisture by volume)} = \frac{6259.82}{101325} = 0.06177 = 6.177\%$$

$$\omega_{amb,at37oc} = \frac{0.622 * \%Mv}{(100 - \%Mv)} = \frac{(0.622 * 6.177)}{(100 - 6.177)}$$

$$\omega_{amb,at37oc} = 0.041$$

For storage tank temperature $T = 4^{\circ}c$

$$\log P_{\text{water vapor}} = 8.07131 - \left(\frac{1730.63}{233.426+4}\right) = 0.782$$

$$P_{\text{water vapor}} = 6.053 \text{ torr} = 6.053 * 133.332pa = 807.1pa$$

$$\%Mv = \frac{P_{w,vapor}}{P_{total}} = \frac{807.1}{101325} = 0.00796 = 0.796\%$$

$$\omega_{amb,at37oc} = \frac{0.622 * \%Mv}{(100 - \%Mv)} = \frac{0.622 * 0.796}{(100 - 0.796)}$$

$$\omega_{amb,at37oc} = 0.00499$$

Therefore

$$\begin{aligned} Q_{inf,latent} &= (\omega_{ambient} - \omega_{storage\ tank,air}) \dot{m}_{air} h_{fg} \\ &= (0.041 - 0.00499) * 0.125 \frac{kg}{hr} * 2257 \frac{kJ}{kg} \\ &= (0.041 - 0.00499) * 0.125 \frac{kg}{hr} * 2257 \frac{kJ}{kg} \end{aligned}$$

$$Q_{inf,latent} = 10.15 \frac{kJ}{hr} = 2.82 \text{ Watt}$$

4.2.3 Product load

The heat removed from the milk to refrigeration temperature is the product load

$$Q_{cooling,m} = m_m * cp_m * (T_1 - T_2) (kJ) \dots\dots\dots 4.34$$

Where m_m : mass of the milk = 50 liter = $0.001m^3 * 50 = 0.05m^3$

$$\rho_m = 1035 \frac{kg}{m^3}; \text{ density of the milk}$$

$$cp_m : \text{specific heat capacity of the milk} = 3.93 \frac{kJ}{kg.K}$$

$$T_1 : \text{milk temperature before refrigeration} = 37 \text{ } ^\circ c$$

$$T_2 : \text{milk temperature after refrigeration} = 4 \text{ } ^\circ c$$

$$Q_{cooling,m} = m_m * cp_m * (T_1 - T_2) = \left(0.05m^3 * 1035 \frac{kg}{m^3}\right) * 3.93 * \frac{kJ}{kg.K} (37 - 4)K$$

$$= 6,711.45kJ$$

Since our refrigeration system has to fulfill the FAO milk preservation requirement (i.e. temperature of the milk shall be down to 4 °C within three to four-hour time period).

$$Q_{cooling,m} = \frac{6,711.45kJ}{(4*3600)s} = 466 \text{ watt}$$

Since milk is refrigerated inside a storage tank, the product load also includes cooling the storage tank itself. Therefore the amount of heat that needs to be removed from the storage tank is given by the same formula as above

$$Q_{s,t} = m_{s,t} * cp_{s,t} * (T_1 - T_2) \text{ (kJ)} \dots\dots\dots 4.35$$

Assumptions [39]

- Specific heat capacity of storage tank made from stainless steel $cp_{storage\ tank} 0.5 \frac{kJ}{kg.K}$
- From the standard specification based on the size and the thickness of the storage tank, *Net mass = 53 kg* is taken [37].

$$Q_{cooling,t} = 53 \text{ kg} * 0.5 \frac{kJ}{kg.K} * (37 - 4)K = 874kJ$$

The same happens for the storage tank too that it should be lowered from atmospheric temperature to milk temperature within four hours. So we will have

$$Q_{cooling,t} = \frac{874}{(4*3600)} \frac{kJ}{s} = 60.7 \text{ Watt}$$

Therefore the total cooling load will be

$$Q_{total} = Q_{trans} + Q_{inf,sensible} + Q_{inf,latent} + Q_{cooling,m} + Q_{cooling,t} \dots\dots\dots 4.36$$

$$Q_{total} = 12.75 + 1.15 + 2.82 + 466 + 60.7 \approx 535 \text{ Watt}$$

After knowing the total cooling load, now the PV system sizing will be calculated as follows

4.3 Standard Sizing and Design Steps for Components of PV System

The first step in designing a solar PV system is to find out the total power and energy consumption of all loads that need to be supplied by the solar PV system as follows:

4.3.1 Calculate total watt-hours per day for each heat gain

$$Q_{transmission} = 4.41 \text{ Watt} * 4hr = 18 \text{ Watt - hours}$$

$$Q_{infiltration,sensible} = 1.15 \text{ Watt} * 4hr = 4.6 \text{ Watt - hours}$$

$$Q_{infiltration,latent} = 2.82Watt * 4hr = 11.28 Watt - hours$$

$$Q_{cooling,milk} = 535Watt * 4hr = 2174 Watt - hours$$

$$Q_{cooling,storage\ tank} = 60Watt * 4hr = 240 Watt - hours$$

$$Q_{total} = 2.415 kwh$$

4.3.2 Calculate total watt-hours needed from the PV modules

Assuming the energy lost in the PV system due to

- Temperature losses
- DC cables losses
- Shadings losses
- Losses at weak radiation
- Losses due to dust

Consider a correction factor 1.3 [40]

Multiply the total Watt-hours per day times 1.3 (the energy lost in the system) to get the total Watt-hours per day which must be provided by the panels

$$Q_{total} = 2415 Watt - hours * 1.3 = 3.14 kwh$$

4.3.3 Calculate the total watt-peak rating needed from PV module

Divide the total Watt-hours per day needed from the PV modules by “**peak sun hour**” to get the total Watt-peak rating needed for the PV panels used to operate the cooling. In order to do so, first we look for the lowest daily solar irradiation value so as to be sure that at this value the PV system can provide the required power for cooling the milk and from the calculated value of daily solar radiation incident on the surface of PV panel, we found that October 5th is with lowest solar radiation with an average peak sun hour for October month is 5.9hrs.(Appendix E)

Therefore total Watt-Peak will be given by

$$\begin{aligned} \text{Total Watt - Peak} &= \frac{\text{total Watt-hours per day}}{\text{peak sunhour}} \dots\dots\dots 4.37 \\ &= \frac{3140}{5.9} = 540.62 \approx 541 Wp \end{aligned}$$

4.3.4 Calculate the number of PV panels for the system

Divide the total Watt-Peak by the rated output watt-peak of the PV modules (180 Wp PV modules is selected from manufacturer)

$$\begin{aligned} \text{No of pv panels} &= \frac{\text{total watt-peak}}{\text{rated output watt-peak of module}} \dots\dots\dots 4.38 \\ &= \frac{541}{180} = 3.01 \text{ (rounded to 4)} \end{aligned}$$

Therefore the system should be powered by at least 4 PV modules of 180Wp. (180W AKT solar panel, 180W, 10.29A and 17.5V)

Features of AKT-180-M solar panel

- High performance, high efficiency mono-crystalline silicon cells
- Bypass diode to avoid hot-spot effect
- Made from 72(125*125) high performance, high efficiency mono-crystalline solar cells
- Complete with 5m of flexible solar cable and MC4 connectors.
- Top of the range 180 Watt solar panel with excellent performance
- 3.2mm tempered glass and rigid anodized aluminum alloy for exceptional strength
- Voltage optimized for use in 12v systems
- Cells guaranteed 25 year power-output
- 180W $\pm 5\%$ power output
- CE certification
- Waterproof for permanent outdoor use

Applications

- Powering fridge, television, laptop and lighting
- Perfect for caravans, boats and off-grid PV applications

© GSJ

Table 4-2:- Electrical and Mechanical characteristics of AKT-180-M solar panel under STC

Electrical characteristics under STC' (AKT-180-M solar panel)	
	For single solar panel
Max. power at STC (Wp)	180 ±5%
Open-circuit voltage (V_{oc})	21.6 V
Voltage at max. power (V_{mp})	17.5 V
Short-circuit current (I_{sc})	11.31 Amp
Current at max. power (I_{mp})	10.29 Amp
Operating temperature	-40 °c to +85 °c
Max. system voltage	1000 V dc
Temperature dependence of I_{sc}, V_{oc} and W_p	
Nominal operating cell temperature (NOCT)	47 °c ± 2 °c
Temperature coefficient of V_{oc}	-0.6 ± 0.002%/°c
Temperature coefficient of I_{sc}	0.034 ± 0.005%/°c
Temperature coefficient of W_p	0.0045 ± 0.05%/°c
Mechanical characteristics and dimensions	
Solar cells	Mono-crystalline 125× 125
No of cells in serious	36
Dimensions	1580× 808 × 35 mm

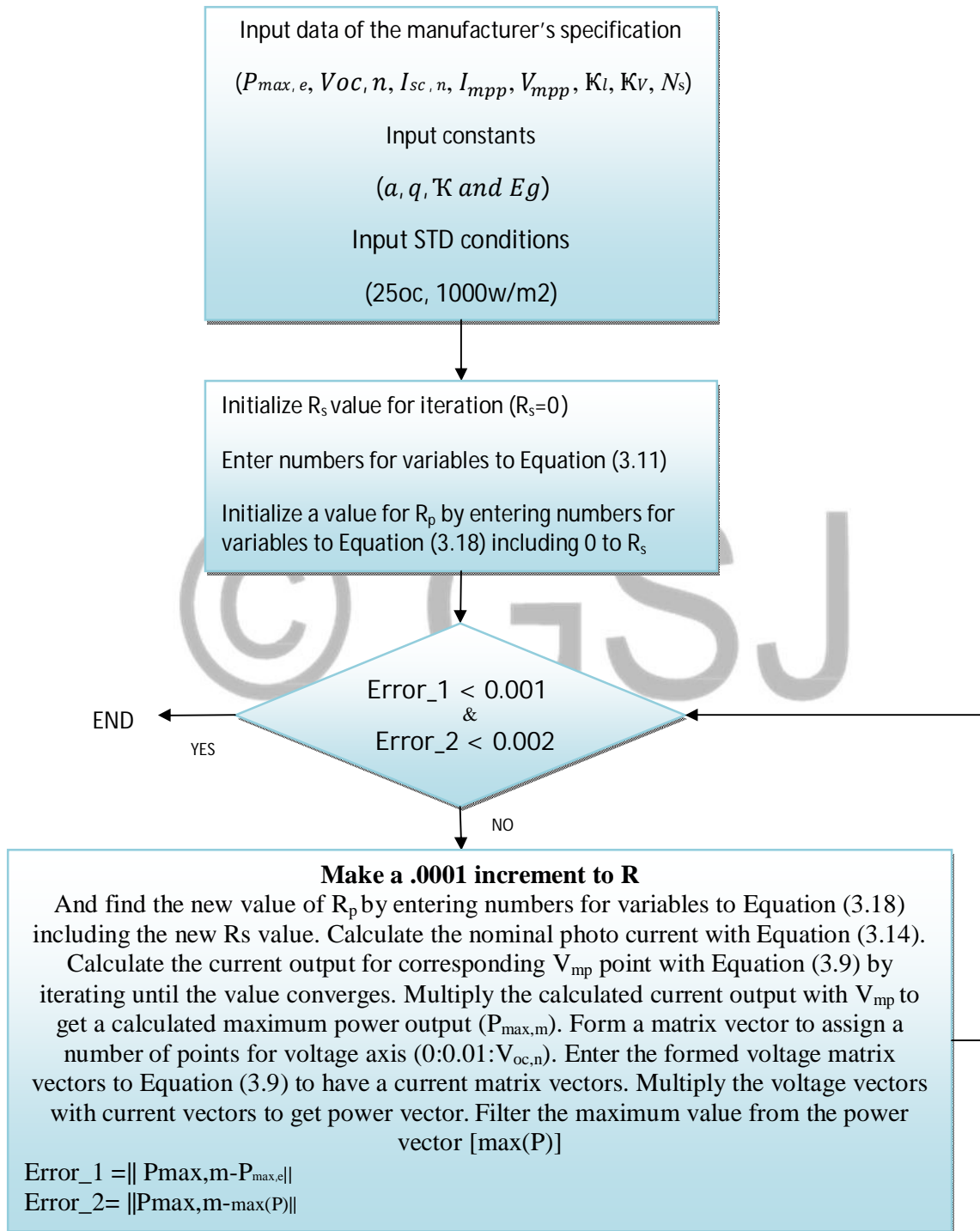


Fig. 4.3 Algorithm of MATLAB program used to model a PV panel [41]

4.3.5 Electrical Characteristics of AKT-180-M Solar Panel

The electrical characteristics of the PV module will be depicting in I-V and P-V curves at STC (standard test condition). The following I-V and P-V curve of AKT-180-M Solar Panel is achieved based on the mathematical modeling shown in section 3.4 and the values from the table above using Mat-lab simulation.

4.3.5.1 I-V curve characteristics of AKT-180-M Solar Panel

The figure below shows the I-V curve of the solar module selected above for different solar radiation.

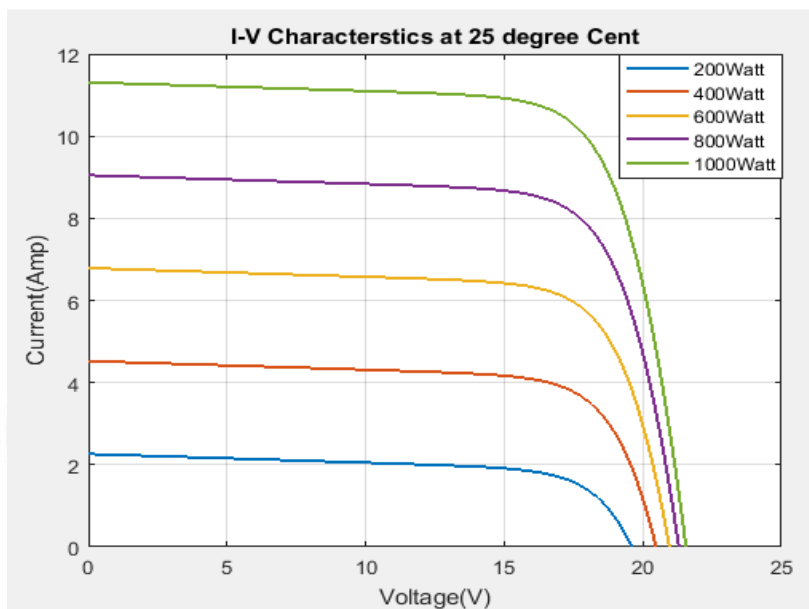


Fig. 4.4 I-V curve characteristics of single AKT-180-M Solar Panel at STC for different radiation at constant cell temperature

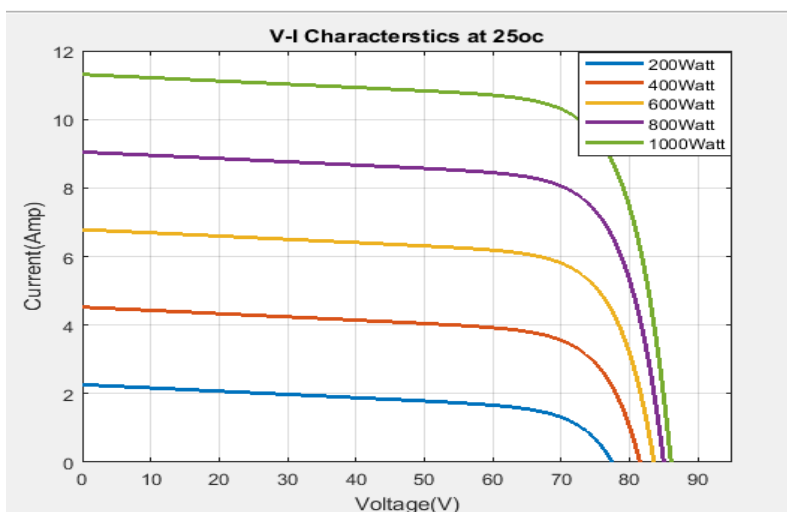


Fig. 4.5 I-V curve characteristics of 4 AKT-180-M Solar Panel connected in series at STC for different radiation at constant cell temperature

4.3.5.2 P-V curve characteristics of AKT-180-M Solar Panel

The figure below shows the P-V curve of the solar module selected above for different solar radiation.

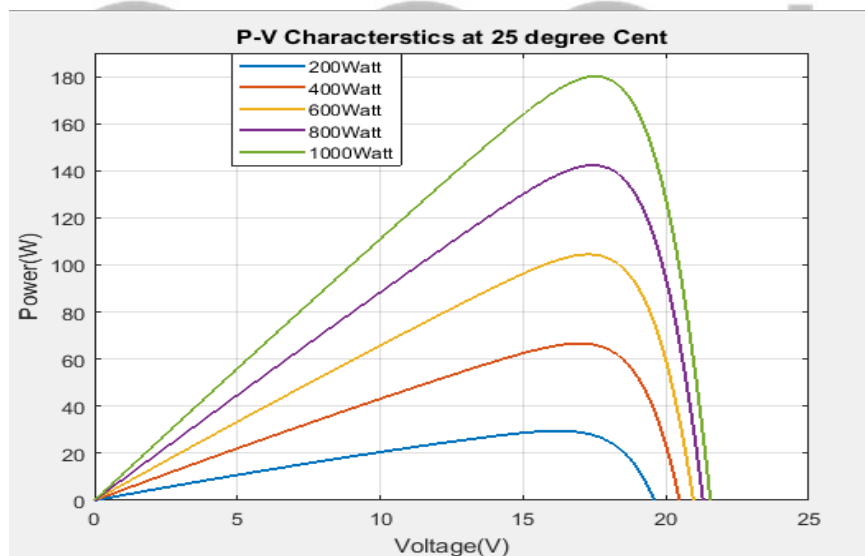


Fig. 4.6 P-V curve characteristics of single AKT-180-M Solar Panel at STC for different radiation at constant cell temperature

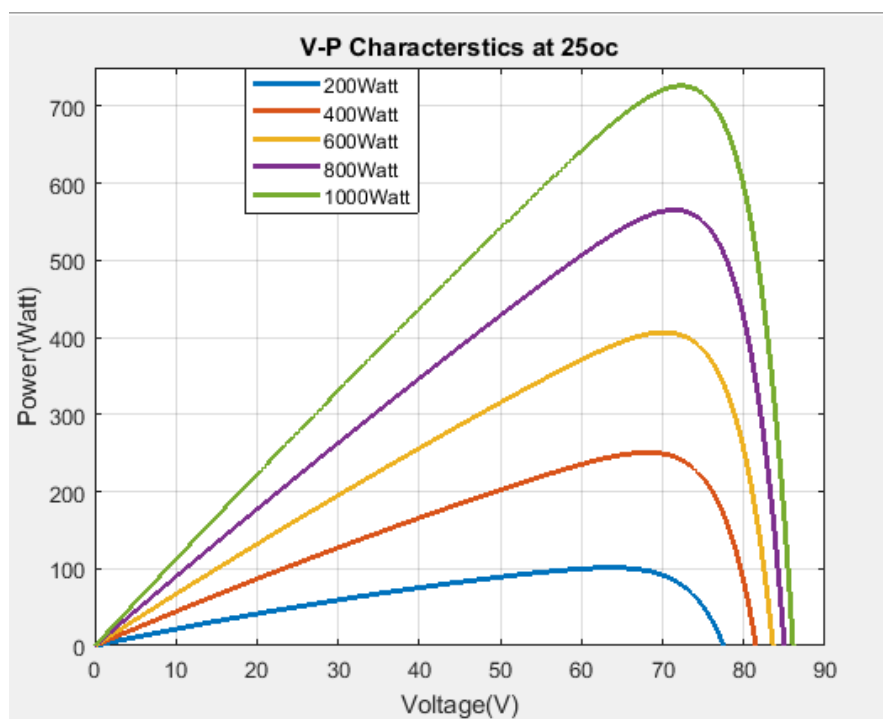


Fig. 4.7 P-V curve characteristics of 4 AKT-180-M Solar Panel connected in series at STC for different radiation at constant cell temperature

The above four figures show the power and current output of the PV module with respect to voltage. Further in depth simulation of the current and power output will be simulated hourly for the whole year in the later chapters to see the real effect of fluctuation in transient nature of both solar irradiation and temperature of the PV cell. The MATLAB algorithm for the above graphs is presented in appendix B₁.

4.3.6 Influence of Cell Temperature

The solar energy that is absorbed by the module is converted into thermal energy and electrical energy. The electrical behavior of the PV module was described in the previous chapter. Here the influence of the cell temperature on the I-V characteristic is analyzed. To determine the cell temperature of a PV module, an energy balance is made.

$$\tau * \alpha * G_T = \eta_c * G_T + u_L (T_c - T_a) \dots\dots\dots 4.39$$

Where τ is the transmittance of the cover

α is the absorption coefficient

G_T is the incident solar radiation

η_c is efficiency of the module

u_L is the loss coefficient of the module

T_a is the ambient temperature

The ratio $\frac{\tau\alpha}{u_L}$ is assumed to be constant. To determine this ratio the nominal operating cell temperature (NOCT) is measured. The NOCT conditions are an incident solar radiation $800 \frac{W}{m^2}$, a wind speed of $1 \frac{m}{s}$ and an ambient temperature of $20^\circ C$. the measurement is made under no load conditions. In this case the efficiency, η_c is zero which leads to equation 4.41 for the ratio $\frac{\tau\alpha}{u_L}$. Once we know this, equation 4.42 will be used to calculate the cell temperature at any operating conditions

$$\frac{\tau\alpha}{u_L} = \frac{(T_{c,NOCT} - T_{a,NOCT})}{G_{T,NOCT}} \dots\dots\dots 4.40$$

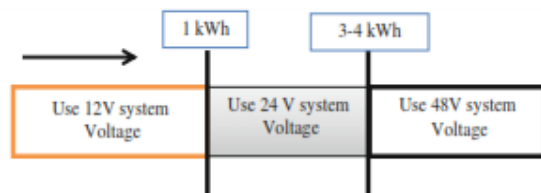
$$T_c = T_a + (G_T * \frac{\tau\alpha}{u_L}) * (1 - \frac{\eta_c}{\tau\alpha}) \dots\dots\dots 4.41$$

Rearranging equation 4.42 gives us

$$T_c = T_a + (\tau\alpha - \eta_c) \frac{(G_T)}{u_L} \dots\dots\dots 4.42$$

4.3.7 Wiring and Voltage Management

Since the total power needed from the PV panel is known, we now proceed to see the system connection wiring to match the 543 Watt. Therefore 4 AKT-180-M (180Watt, 10.29Amp and 17.5V) solar panel must be wired in series to come up with the required 543 Watt to cool the milk to the desired temperature. Hence before proceeding with any subsequent PV system component sizing, we must be sure first that the range of voltage for our PV system is the most appropriate and cost-wise one. The first and foremost advantage of wiring the PV panels in series is since mostly the distance between the charge controller and the PV panels is about more than 100 feet away from the charge controller, the cost for the copper cable will significantly decrease as the current is much smaller compared to when connected in parallel. Secondly our selected AKT-180-M solar panel has by-pass diode so we don't worry which in case the shading or hot spot effect of one module fails to deliver the current and power intermittency won't prevail. In addition the backside of the panels frame is equipped with drainage holes in order to eliminate the risk that rain or snow water may accumulate in the frame causing damage to the frame in cold season.



(source PV standard procedure)

Fig. 4.8 A typical load variation with voltage

As shown in the above figure, determining the system voltage is totally based on the load of the system and since our total load calculated in section 4.3.2 is 3225Wh, our system voltage will be 24V system.

4.3.8 Charge controller sizing

The charge controller is a key component of a solar PV system. It is basically a voltage and/or current regulator in the PV power system in order to protect batteries from overcharging or completely draining. Despite the variety in charge controllers, there are two types that are most commonly used in PV power installations. The first one is the pulse width modulation (PWM) and the second one is the maximum power point tracking (MPPT). To specify the suitable one for the system, some requirements have to be analyzed. Both of them adjust charging rates and monitor the battery's temperature to prevent overheating. Also each one of them has its own advantages.

Thus, the selection depends on system components, site condition, size of array and load, and the cost. The following table demonstrates a comparison between the two types of charge controller.

Table 4-3:- Multi-criteria of Pulse-width modulation (PWM) Vs Maximum power point tracking (MPPT) (source Solarcraft, 2014 (Vader, 2014)

Multiple-criteria	Pulse-width modulation (PWM)	Maximum power point tracking (MPPT)
Array voltage	PV voltage and battery voltage have to be matched	PV array voltage can be higher than battery voltage
Battery voltage	Good performance in warm temperature and when battery is almost fully charged	It can be operated above battery voltage so that, it enhances the performance in cold temperature and when the charge in battery is lower
System voltage	More suitable in small system	It has capacity to handle more than what the PWM regulator does.
PV array sizing method	PV array sized in Amps (based on current produced when PV array is operating at battery voltage)	The temperature compensated Voc of the array should be less than the maximum input voltage of the regulator.
Grid connection	Off-grid	Off-grid and on-grid
Cost	Low	Comparatively high

Therefore based on the above multi-criteria decision, Maximum power point tracking (MPPT) charge controller has been selected for our PV system.

The solar charge controller is typically rated against Amperage and voltage capacities of the solar array. We will follow the following steps for calculating the appropriate MPPT charge controller size for our PV panel

- The current of the charge controller will be 125% of the max. allowed PV current (I_{sc}) to allow for cold temperatures, light reflection and round up. To get the current of the charge controller, we'll look for the output current of the system and from the common power equation we have

$$P = v * I$$
 Since we have 4 AKT-180-M solar panel, the power output is known and the voltage of the battery is also known for our design. Therefore the current will be $I = \frac{P}{v} = \frac{720}{24} = 30Amp$ (the output current of the system and we consider the factors mentioned above $30Amp * 1.25 = 37.5 \approx 40Amp$).
- The voltage of a charge controller will be 120% of max. allowed PV voltage (V_{oc}) and since 4 AKT-180-M connected in series with V_{oc} value of 21.6Volt each, it will be $(86.4Volt + 17.28 = 103.68 \approx 105Volt)$

Since the system PV voltage (V_{oc}) is above 52Volt while connected in series, MPPT charge controller which can handle about 150V_{oc} dc is selected for safe operation of the battery. Therefore the charge controller is rated with 150V and 40Amp. (Blue pacific solar,2018) Outback FLEXmax 30/40(MPPT), 5200078(part number)(Photovoltaic solar system). The controller supports a wide range of nominal battery voltages from 12V to 60VDC and has the ability to step-down a higher voltage solar array to recharge a lower voltage battery tank.

4.3.8.1 MPPT Technology

Due to the nonlinear characteristics of solar array, there is a maximum energy output point (Maximum power point) on its curve. Traditional controllers, with switch charging technology and PWM charging technology can't charge the battery at the maximum power point so the maximum energy available can't be harvested from the PV array. The FLEXmax 30/40 series controller utilizes maximum power point tracking (MPPT) technology to extract maximum power from the solar modules. The tracking algorithm is fully automatic and does not require user adjustment. It will track the maximum power point voltage (V_{mp}) as it varies with weather conditions, ensuring that maximum power is harvested from the array.

FLEX-max 30/40 series charge controller features

- It charges and discharges the battery in off grid solar application
- The smart tracking algorithm of the controller maximizes PV cell energy returns

- The FLEXmax 30/40 charging process optimizes battery life and improves overall system performance
- The self diagnostic and electronic protection features minimize possible damage from installation mistakes or system faults.
- It offers protection from high temperature, over charging, PV and load short, PV (battery) reversed and over current
- Widely used with automatic recognition during the day or at night
- Supports firmware updates
- Supports multiple load control modes: manual, light (on/off), light(on/off/timer) and time controlled



Fig. 4.9 FLEXmax 30/40 series charge controller

4.3.9 Battery sizing

Solar storage batteries are essential component of the solar PV system. It stores the excess energy which is produced by PV panels. This energy would compensate the leakage of power during the cloudy days and/or use during the night.

*Table 4-4:- Multi-criteria decision of Deep-cycle Lead-acid battery Vs Lithium-ion battery
 (source: 12VMONSTER)*

Multiple-criteria	Deep cycle Lead-acid battery	Deep cycle Lithium-ion battery
Weight	Heavier	30% lighter than lead-acid batteries
Charging time	0.2c (have charging time of only 0.2 times of its capacity)	0.5c (have almost half of the current is used for charging)
Discharge	Have less than 80% of charge-discharge efficiency	Have almost 100% charge-discharge with even the worst have 80% efficiency
Cycle lifetime	Have an average of 400-1500 cycle	Have an average of 2000-4000 cycles
Voltage stability	Voltage constantly drop over its discharge (sloping voltage)	Almost 100% stable in terms of voltage
Safety and Environmental impact	The lead content can damage the environment	Much cleaner and safe for the environment
Cost	Cheapest	Expensive

Therefore based on the above multi-criteria, the battery type recommended for using in solar PV system is Lithium-ion battery by sacrificing for its cost. Lithium-ion battery is specifically designed for to be discharged to low energy. So once we select our battery type we'll start to size it by the following steps based on standard design procedure of PV.

- Calculate the total Watt-hours per day used by appliances

$$\text{Already calculated } Q_{total(Wh)} = 3225 \text{ Watt} - \text{hours}$$

- Divide the total Watt-hours per day used by 0.85 for battery loss

$$Q_{total(Wh)} = \frac{3225 \text{ Watt} - \text{hours}}{0.85} = 3795 \text{ Watt} - \text{hour}$$

- Divide the answer obtained above by 0.9 for depth of discharge(DOD)

$$\frac{3795 \text{ Watt} - \text{hour}}{0.9} = 4217 \text{ Watt} - \text{hour}$$

- Divide the answer obtained above by the nominal battery voltage

$$\frac{4217 \text{ Watt} - \text{hour}}{24v} = 175.7 \approx 180Ah$$

- Multiply the answer obtained above with days of autonomy (since Semera has almost sunny weather throughout the year we generally take a minimum days of autonomy to be 2)

$$180 * 2 = 360 Ah$$

$$Battery\ capacity\ (Ah) \frac{(total\ \frac{Wh}{day} * days\ of\ autonomy)}{0.85 * 0.9 * nominal\ battery\ voltage} = 360Ah \dots\dots\dots 4.43$$

Therefore, our system should contain a Lithium-ion (LiFePo4) battery with rated capacity of 24V, 360Ah for 2-day autonomy.(source: photovoltaic solar system)

Features of LiFePo4 battery

- Cell level under/over voltage detection
- End compression plated to prevent cell expansion
- Battery isolation capability
- Positive cell retention in case of rollover
- 500amp safety fuse on positive terminal
- Cell level shunt regulation for cell balancing
- Estimated 2,000 cycles to 90% DOD
- The battery pack is intended to be used with a separately provided BMS (battery management system) which protects the battery from over charge and discharge condition



Fig. 4.10 LiFePo4 24V/360Ah battery

4.3.9.1 Battery charging current

The charging current of the battery is basically comes from the PV array. Due to the nature of the solar radiation fluctuation instantly, the charging current also varies accordingly. Here we look at two vital cases to consider in reality.

- i. PV array actual power ≤ controller rated charge power; the controller will charge the battery at the actual maximum power point.
- ii. PV array actual power > controller rated charge power; the controller will charge the battery at rated power.

Table 4-5:- Reference for further information on battery charging current (*At minimum operating environment temperature, ** At 25°C environment temperature

Battery Charging Current					
Model	Rated charge current (I_{bat})	Rated discharge current	Rated charge power	MAX. PV power (P_{max})	MAX. PV open circuit voltage
FLEXmax30	30A	20A	390W/12V 780W/24V	1170W/12V 2340/24V	150V*
FLEXmax40	40A	20A	520W/12V 1040W/24V	1560W/12V 3120W/24V	138V**

Since our actual power of 4 AKT-180-M solar panel total powers is with maximum of 720W which is less than the rated charge power for FLEXmax40 in the above table, the controller will charge the battery at the actual maximum power point. Therefore we will calculate the charging current of the battery as we know already our battery capacity is 360Ah.

The charging current should be 10% of the Ah rating of the battery, i.e $360Ah * 0.1 = 36Amp$
 Therefore the charging time for 360Ah battery will be

$$Charging\ time = 360Ah / 36Amp = 10hrs \dots\dots\dots 4.44$$

But this is ideal case; practically 40% of losses occur in case of battery charging. So we need to take account that value

$$360 * \left(\frac{40}{100}\right) = 144 \dots (360 * 40\% \text{ of losses})$$

$$360Ah + 144Ah = 504Ah$$

$$Now\ the\ charging\ time\ of\ the\ battery = \frac{504Ah}{36A} = 14hrs$$

Therefore to fully charge the battery, it will take 14hrs with 36A charging current.

4.3.9.2 Battery storage and Ultra-capacitor (Energy storage system)

Battery storage sizing is very important. There are three main parameters that need to be considered for every installation of battery storage system: the depth of discharge (DOD), state of charge (SOC) and state of health (SOH), as well as battery capacity, maximum battery charge and discharge power and the utility rating type (Aichhorn et al. 2012).

The battery transient equation can be represented by

$$\frac{dE_b}{dt} = P_b(t) \dots\dots\dots 4.45$$

Where E_b : represent the amount of electricity stored at t time and P_b the charging or discharging rate

4.3.9.3 Backup time of the Battery

Since we already have our LiFePo4 battery is rated with 24V and 360Ah, the Watt-hour of the battery will be

$$\text{Battery watt - hour} = 24V * 360Ah = 8,640Wh \dots\dots\dots 4.46$$

The milk to be chilled is inside the chiller for maximum of four hours at full load. Therefore during this period of time, maximum load (543Watt) needs to be chilled from 33°C to 4°C in the refrigerator.

$$\text{Backup time} = \frac{8640Wh}{543w} = 15.92hr \dots\dots\dots 4.47$$

In equation 4.47 above, we can see that the battery has the ability to run for almost 16hrs at maximum load while running for four straight hours.

4.4 Selection of Refrigeration Cycle Components

4.4.1 Design requirement of the system

This system is focused in designing and simulating of a vapor compression refrigeration system using PV system for preserving 50liters of milk within four hours of milk’s introduction into the system. The refrigerator compressor will use the DC current produced from the PV panels to compress the refrigerant to pressurize it up to condenser pressure. The most commonly used compressors for PV driven refrigeration is reciprocating compressors same as domestic refrigerators.

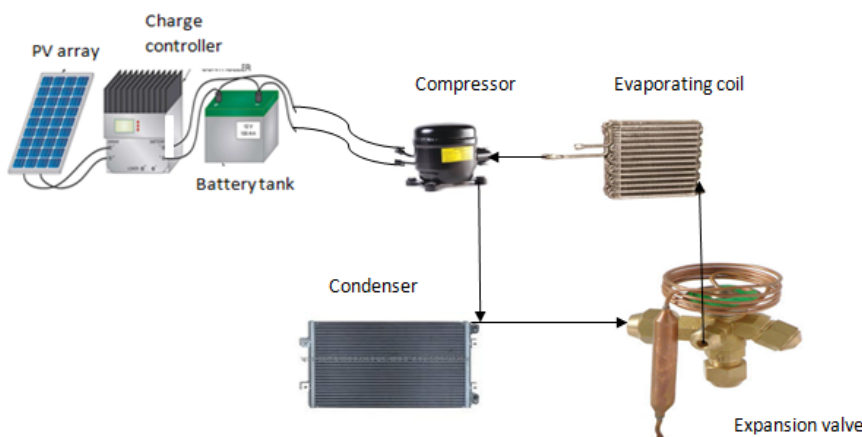


Fig. 4.11 Schematic diagram of solar refrigeration system

4.4.2 Refrigerator Compressor Selection

The selection of appropriate compressor of vapor compression refrigeration system is the heart of the system. The refrigerator's compressor selection shall be done in such a way that our refrigeration system has to fulfill the FAO milk preservation requirement (i.e. temperature of the milk shall be down to 4°C within three to four-hour time period). Since we already calculated the total cooling load $Q_{total} = 543$ Watt, our compressor size should have to be greater than this value in order to chill the milk effectively within the required time. The compressor used in this thesis project is 'DC compressor' since they have brushless motors, their power consumption is low compared to motors with brush which make them more efficient. CASCADE17-0244Y3 model, variable speed DC(VSDC), high back pressure which is a product of Master-flux Company is suggested for the system as it has high cooling capacity of 618Watt which makes it favorable especially in the areas of Semera region where temperature will rise above expected.

4.4.2.1 Description of CASCADE17-0244Y3 VSDC Compressor and Electronic control unit

The CASCADE17-0244Y3 model compressor is ideally suited for battery powered stationary and mobile applications. It is designed for connection of 12, 24 or 48v DC power supply with refrigerant type to be used R-134a.

Typical application for this model includes for commercial refrigeration for foods and beverages, make and store ice, residential refrigerator and freezer, and air conditioning in transport, military, medical, telecom and many others.

This compressor is applicable for evaporator temperature range of -40°C to 15°C and condenser temperature range of 26.7°C to 65.6°C.



(source masterflux)

Fig. 4.12 CASCADE17-0244Y3 VSDC (variable speed direct current compressor)

The electronic controller unit features are as follows

4-poles sensor-less/brushless variable speed BLDC motor controller. 1.0-4.75V analog speed set input (resistor programmable for fixed speed). The rpm range is 1800-4200 where the controller will shut down the motor when the power reaches the maximum condition of 618Watt with in-

built controlling mechanism. Now if we need to operate the compressor in off/on mode by fixing the rpm of the motor, a resistor will be introduced between the ground and speed input terminals to provide 1.0-4.75V analog speed input (i.e the motor is resistor programmable for fixed speed).

Table 4-6:- Optional fixed resistor speed chart (source master flux)

Resistor value(OHMS)	Motor speed(RPM)
200	1800
242	1900
287	2000
388	2200
510	2400
659	2600
847	2800
1090	3000
1.4k	3200
1.88k	3400
2.58k	3600
3.8k	3800
6.36k	4000
15.3k	4200

The following tables are experimental outputs of ASHRAE-HBP test condition with all points are at 35°C ambient temperature, 18.33°C suction temperature, 8.33°C sub-cooling and at condenser temperature of 54.4°C.

Table 4-7:- Cooling capacity (Watt) of the compressor for (24V) at ASHRAE-HBP test condition (source Masterflux)

RPM	Evaporator temperature(°c)						
	-7°c	-1°c	2°c	4°c	7°c	10°c	13°c
1800	114	162	188	214	240	267	294
2400	158	219	250	283	316	350	384
3000	218	287	324	362	400	440	479
3600	273	350	391	432	475	519	563
4200	308	389	433	477	523	570	618

Table 4-8:- Power consumption (Watt) of the compressor for (24V) at ASHRAE-HBP test condition (source Masterflux)

	Evaporator temperature(°c)						
RPM	-7°c	-1°c	2°c	4°c	7°c	10°c	13°c
1800	83	92	97	101	106	110	114
2400	105	115	121	126	131	136	142
3000	129	143	150	157	165	173	181
3600	155	174	184	195	206	218	230
4200	181	209	224	239	255	272	290

Table 4-94:- Current consumption (Amp) of the compressor for (24V) at ASHRAE-HBP test condition (source Masterflux)

	Evaporator temperature(°c)						
RPM	-7°c	-1°c	2°c	4°c	7°c	10°c	13°c
1800	3.45	3.85	4.04	4.22	4.4	4.57	4.73
2400	4.37	4.81	5.02	5.24	5.46	5.68	5.91
3000	5.38	5.94	6.24	6.54	6.86	7.19	7.54
3600	6.44	7.24	7.67	8.12	8.59	9.08	9.59
4200	7.56	8.7	9.32	9.96	10.63	11.33	12.07

All the above tables show the performance information of CASCADE17-0244Y3 compressor for different evaporating temperature at ASHRAE-HBP test condition at condensing temperature of 54.4°C.

4.4.2.2 Performance Equation of the Compressor at ASHRAE-HBP test condition

Table 4.7, table 4.8 and table 4.9 on the previous section have depicted the performance of the refrigerator at various evaporator temperature and operating RPM of the compressor but with fixed condenser temperature of 54.4°C. So Master-flux Company provided more flexible performance equation with coefficients which is capable of expressing cooling capacity, refrigerant mass flow rate, power consumption, and current consumption of the compressor.

Here is the characteristics equation provided by the manufacturer

$$Y = C_1 + C_2x_1 + C_3x_1^2 + C_4x_1^3 + C_5x_2 + C_6x_2^2 + C_7x_2^3 + C_8x_3 + C_9x_3^2 + C_{10}x_3^3 + C_{11}x_1x_2x_3 + C_{12}x_1^2x_2x_3 + C_{13}x_1x_2^2x_3 + C_{14}x_1x_2x_3^2 + C_{15}x_1x_2 + C_{16}x_1x_3 + C_{17}x_2x_3 +$$

$$C_{18}x_1^2x_2 + C_{19}x_1x_2^2 + C_{20}x_1^2x_3 + C_{21}x_1x_3^2 + C_{22}x_2^2x_3 + C_{23}x_2x_3^2 \dots\dots\dots 4.48$$

x_1 = RPM

x_2 = Evaporator temperature in degree Fahrenheit

x_3 = Condenser temperature in degree Fahrenheit

Y= performance characteristics like refrigerant mass flow rate, cooling capacity, current consumption, power consumption of the CASCADE17-0244Y3 compressor.

4.4.3 Selecting Condenser Temperature

The ambient temperature of Semera region reaches as high as 43°C based on the collected Metrological data collected. Hence our refrigerator condenser must operate at a temperature greater than this value in order to release heat to the surrounding. So it will be convenient to fix the condenser temperature to 49°C, which results a 5.5°C minimum temperature difference between the ambient and the operating temperature of the condenser. Selection of condenser temperature is carried out considering the highest ambient temperature of Semera, and also by taking the experimental test of SIERRA01-0716Y3XA condenser by the manufacturer as a benchmark. The condenser was tested at 48.9°C operating temperature against 43.3°C ambient temperature, which is similar to our selection.

4.4.4 Selecting Evaporator Temperature

Here since our milk must cool down to 4°C according to FAO, the evaporator temperature must not be far away below this temperature because of freezing of milk might occur. Therefore as the difference between the operating temperature of evaporator and condenser is lower, the cooling capacity of the refrigerator’s compressor will be higher. So, in order to obtain a higher cooling capacity of the refrigerator system, we have to fix the operating temperature of evaporator in such a way that as near as possible to condenser temperature.

As it is stated in section 4.4.2.1 of this chapter, the compressor is applicable for evaporator with maximum operating temperature of 15°C or 59°F; though we won’t select this as it must be below 4°C, hence we are limited to select the possible maximum operating temperature of the evaporator which is 0°C.

4.4.5 ASHREA-HBP Cooling Capacity of the Compressor at the Selected Operating Temperature of Evaporator and Condenser

Evaporator and condenser temperatures of this system have been selected, that means x_2 and x_3 of equation (4.48) are known, and hence it is possible to determine the performance characteristics of the compressor at any desired RPM of the compressor. Putting the selected

average operating temperature of the condenser ($T_c = x_3 = 49^\circ\text{C}$) and average evaporator temperature ($T_e = x_2 = 0^\circ\text{C}$) of the refrigerator with respective performance coefficients from appendix C altogether into equation (4.48), we got the maximum cooling capacity of the refrigerator under the selected operating temperature of the condenser and evaporator (49°C and 0°C respectively).

$$\dot{Q}_{cooling_{max}} = 618\text{Watt}$$

Since this calculated cooling capacity of the compressor at selected evaporator and condenser temperature is greater than the cooling power required by the milk which is calculated in section 4.2.3, hence it is possible to design the refrigeration system with CASCADE17-0244Y3 hermetically sealed reciprocating compressor.

4.4.6 Modeling of CASCADE17-0244Y3 Compressor at its Operating Temperature

Since the performance data of CASCADE17-0244Y3 compressor which is provided by the manufacturer is experimental result at ASHRAE –HBP test condition, we can calculate the real performance of our selected compressor by using equation 4.48 at the selected condenser(49°C) and evaporator(0°C) temperature with the result tabulated below

Table 4-10:- performance of CASCADE17-0244Y3 for different RPM, condenser temperature 49°C and evaporator temperature 0°C

RPM	COOLING CAPACITY(Watt)	POWER CONSUMPTION(Watt)	MASS FLOW RATE(gm/sec)
1800	163.78	89.5	1.0637
1900	173.78	92.93	1.1202
2000	186.10	96.509	1.1818
2200	209.24	104.1	1.3177
2400	262.66	112.25	1.4668
2600	322.96	120.96	1.6247
2800	375.65	130.22	1.7868
3000	412.89	140.01	1.9488
3200	450.23	150.31	2.106
3400	500.23	161.13	2.254
3600	530.12	172.44	2.3883
3800	562.74	184.24	2.5045
4000	595.02	196.51	2.5979
4200	618.07	209.25	2.6641

As we can see from the table above as the rpm of the compressor increases, the cooling capacity, the power consumption and as well as the mass flow rate of the refrigerant will increase accordingly till the maximum rpm is reached.

Therefore based on the above calculated data value, the following Mat-lab graph is plotted for the operating temperature of evaporator and condenser.

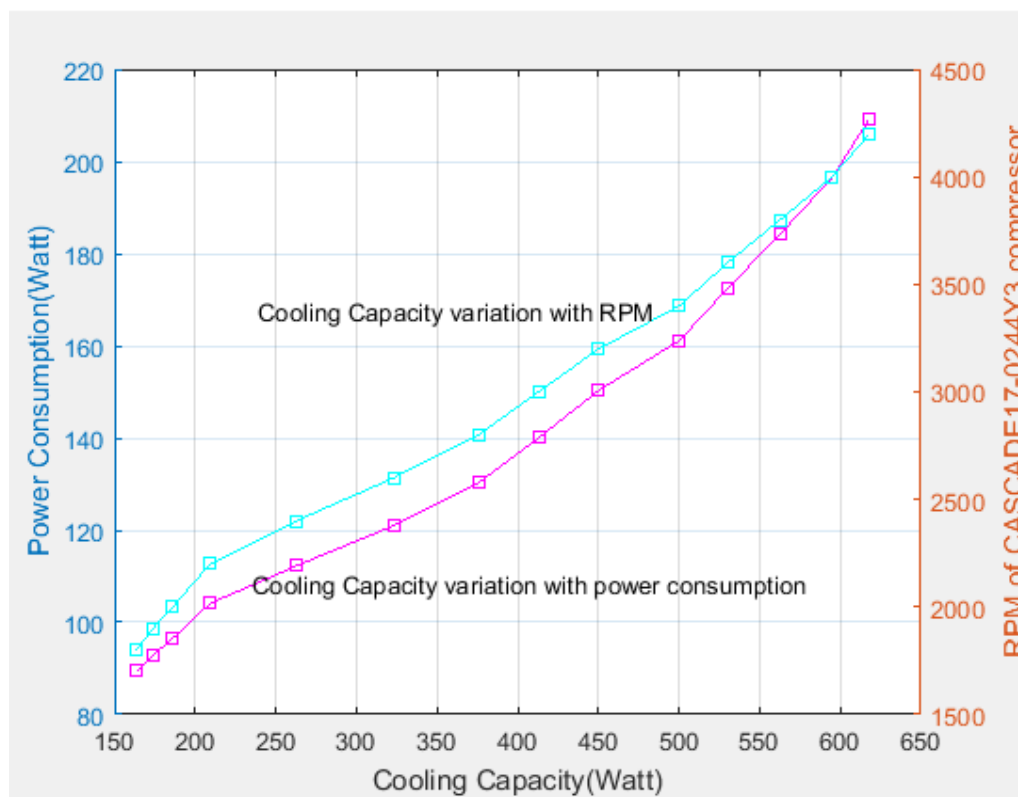


Fig. 4.13 Cooling capacity Vs Power consumption and RPM of compressor

The above figure depicts both power consumption and cooling capacity of the compressor gets increasing starting from the compressor start-up rpm value which is 1800. The minimum power consumption is 89.5Watt for the lowest rpm value and the maximum is 209.25Watt for the highest rpm value which is 4200rpm at the operating evaporator and condenser temperature; whereas the minimum and maximum cooling capacity of the CASCADE17-0244Y3 compressor is 163.78 and 618.07Watt respectively. Similarly based on the tabulated table value, we can see the relationships between any of the parameters graphically.

4.4.7 Isentropic Power Consumption of the Compressor at ASHREA-HBP Test Condition

The following figure depicts thermodynamic cycle of the refrigerator at ASHREA-HBP test condition. Process 1-2 is the compression process of the refrigerator inside the compressor;

process 2-3 is heat rejection process from the refrigerant into the (32.2°C) temperature ambient in the condenser; process 3-4 is the throttling process; process 4-1 is a heat absorption process by the refrigerator at the evaporator coil.

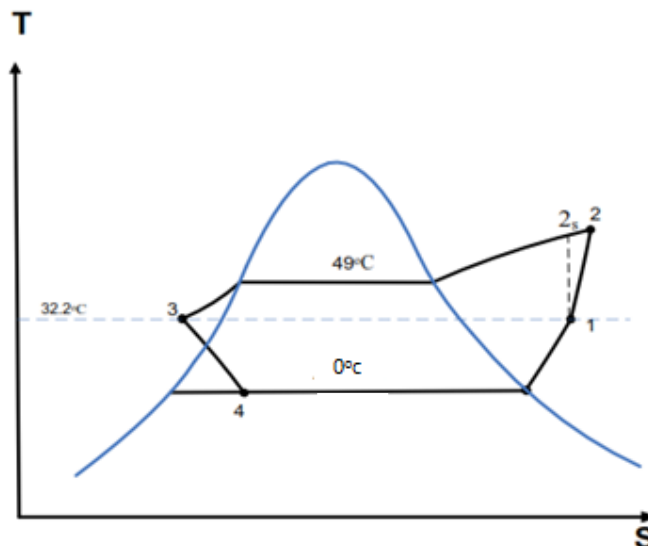


Fig. 4.14 Thermodynamic cycle of the refrigerator at selected evaporator and condenser temperature at ASHRAE-HBP test condition

Process 1-2s

Process 1-2s is an isentropic compression of the refrigerant in the compressor. The saturated pressure of the refrigerant at evaporator temperature is 293kPa but since the refrigerant should enter at state 1 (compressor) at superheated state, we'll look from the superheated property table for R134a to get the thermodynamic properties at state 1 after interpolation is as shown below

$$\text{At state 1 } U_1 = 257 \frac{\text{kJ}}{\text{kg}}, V_1 = 0.1294 \frac{\text{m}^3}{\text{kg}}, S_1 = 1.0716 \frac{\text{kJ}}{\text{kg.K}}, h_1 = 281 \frac{\text{kJ}}{\text{kg}}$$

The saturated pressure at condenser temperature is 1287 kPa and hence the refrigerant at this state is superheated one, we'll find the superheated property table for state 2s as well.

$$\text{Since the entropy is constant from state 1-2s, } s_1 = s_{2s} = 1.0716 \frac{\text{kJ}}{\text{kg.K}}$$

$$U_{2s} = 303.7 \frac{\text{kJ}}{\text{kg}}, V_{2s} = 0.0207 \frac{\text{m}^3}{\text{kg}}, h_{2s} = 330.2 \frac{\text{kJ}}{\text{kg}}, T_{2s} = 98.70\text{c}$$

Where: h is specific enthalpy, u is specific internal energy, s is specific entropy, and v is specific

volume of the refrigerant; and T calculated temperature of the refrigerant at point 2s.

The isentropic specific work done by the compressor to the fluid is calculated as:

$$w_{1-2s} = h_{2s} - h_1 \dots\dots\dots 4.48$$

$$w_{1-2s} = 49.2 \frac{\text{kJ}}{\text{kg}}$$

The total efficiency of the compressor at the operating conditions will be given by

$$\eta_t = \frac{p_{isentropic}}{p_{act}} \dots\dots\dots 4.49$$

$$p_{isen} = \dot{m}_{ref} * w_{1-2s} \dots\dots\dots 4.50$$

$$\eta_t = \frac{p_{isentropic}}{p_{act}} = \frac{\dot{m}_{ref} * w_{1-2s}}{p_{act}} \dots\dots\dots 4.51$$

Where: $p_{isentropic}$ is the ideal power consumption of the refrigerator (i.e. the isentropic work consumption of the compressor), and p_{act} is the actual electrical power consumption of the compressor, \dot{m}_{ref} is refrigerant mass flow rate, w_{1-2s} is the calculated isentropic specific work consumption of the refrigerator.

Therefore based on the above equation coupled with table 4.12, we can plot in MATLAB for the total efficiency of the compressor by using the tabulated data of column third and fourth for various rpm values of the compressor

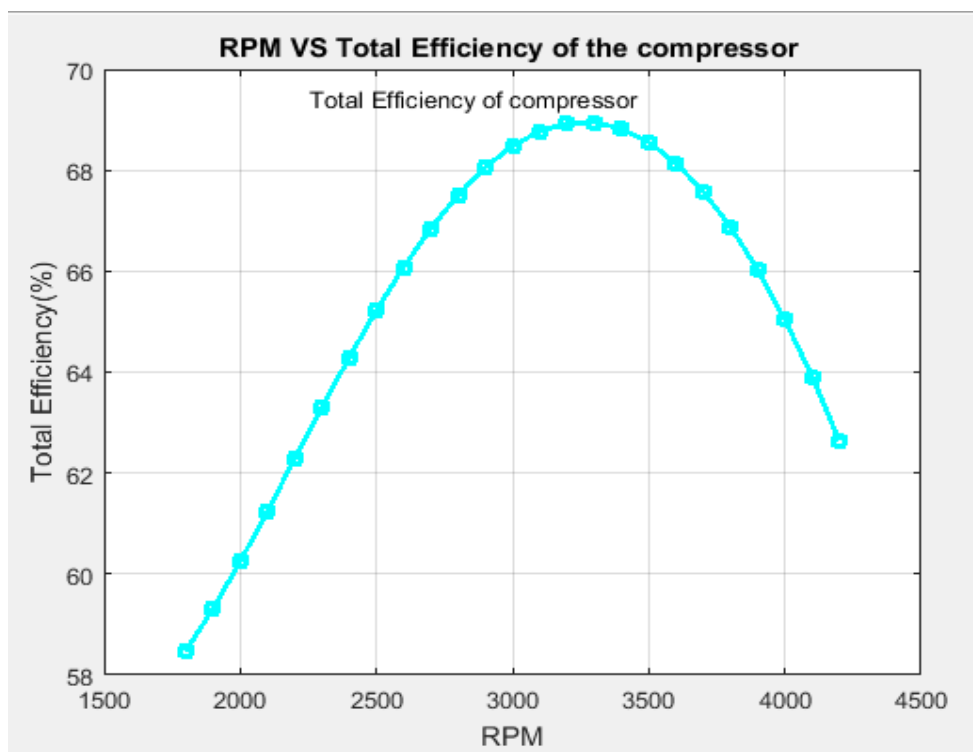


Fig. 4.15 Efficiency of compressor variation with RPM

From section 4.3 we already have the I-V and P-V electrical characteristics graphs for different solar power and also we calculated the hourly solar data in section 4.1. Hence from the many hourly data generated, it's wise to know the minimum power required to drive the system. Our compressor needs minimum of 89.5Watt as calculated earlier and tabulated in table 4.12. Therefore using equation (3.12), it's possible to calculate the I-V electrical characteristics of the compressor at its lowest rpm and the power consumption is expressed below

$$I = \frac{89.5\text{Watt}}{v} \dots\dots\dots 4.52$$

Since the temperature of Semera is usually much closer to 32°c during 10AM to 11AM, we assume this temperature in order to calculate the minimum solar power needed to drive our system by increasing our PV power until the I-V curve of the PV module gets in touch with the I-V curve of the compressor in the above equation.

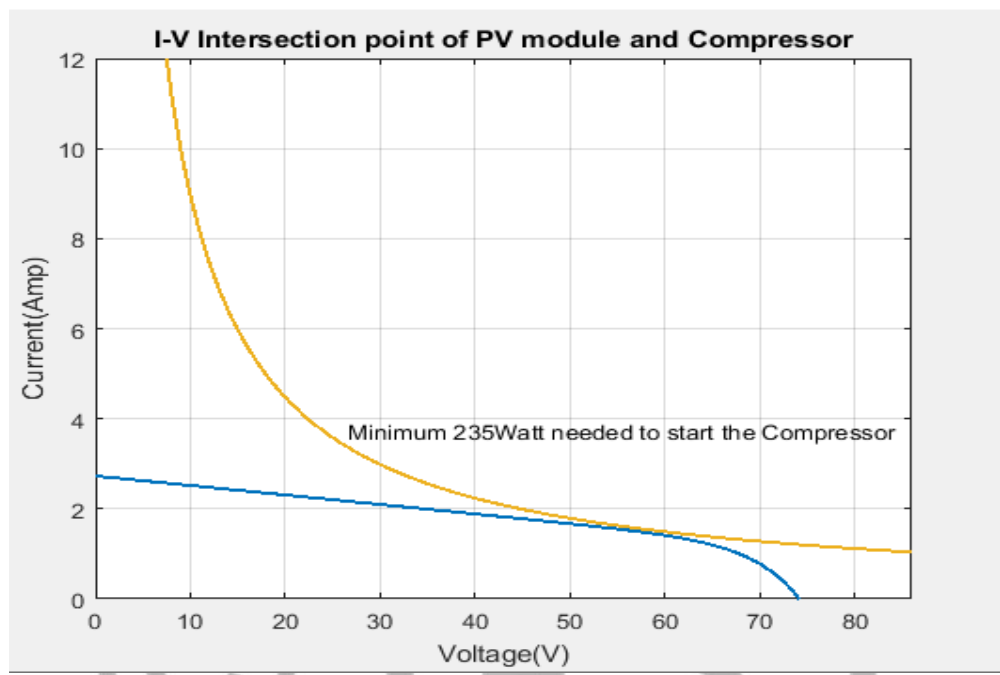


Fig. 4.16 I-V intersection point of PV module and compressor

As shown above the I-V curve of the CASCADE17-0244Y3 compressor intersects the four AKT-180-M PV modules connected in series at around 235Watt in order to drive the compressor at its lowest rpm. Therefore the system requires a minimum of 235Watt in order to operate at least with lower rpm value (1800).

CHAPTER-5: MATHEMATICAL MODELING

5.1 Vapor-Compression refrigeration cycle

Vapor-compression refrigeration (VCR) cycles are considered to be the most commonly used in domestic and industrial refrigeration and air-conditioning (Jain, Kachhwaha, & Sachdeva, 2013) (Mopab & Shapiro, 2000) (Dincer & Kanoglu, 2010). The term vapor compression refers to the way the cooling liquid is circulated through the system components. The four key components of the (VCR) system are; the compressor, the condenser, the evaporator, and the throttling device (Silbrestein,2015). PV driven vapor compression cycle works exactly same as that of domestic refrigerator where PV driven electricity is used only. The system efficiency of PV driven vapor compression is much higher than the different solar cooling technologies explained in chapter two. The following figure shows the single stage vapor compression refrigeration cycle

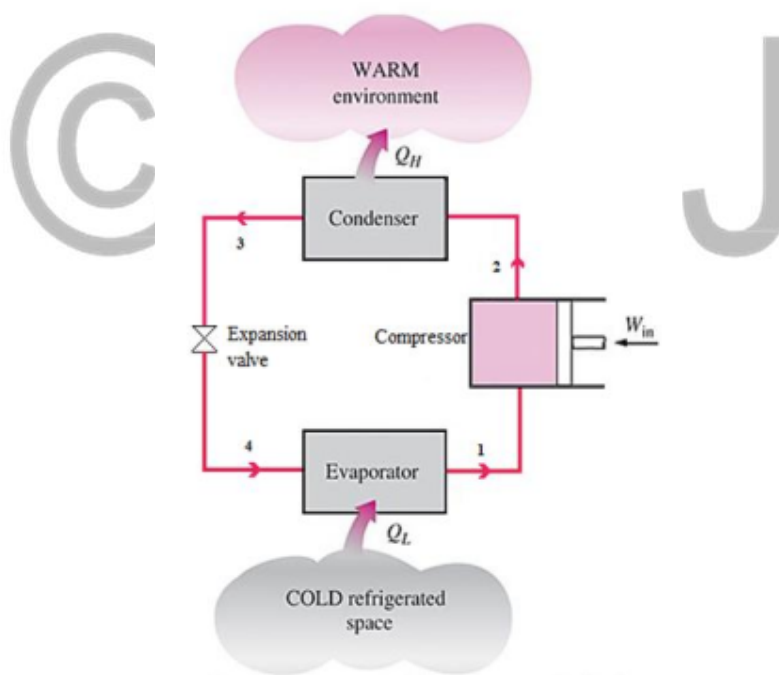


Fig. 5.1 Single stage vapor compression refrigeration cycle

5.2 Thermodynamics Analysis of the System

The thermodynamics of the vapor compression cycle can be analyzed on a temperature versus entropy diagram as depicted in the figure below

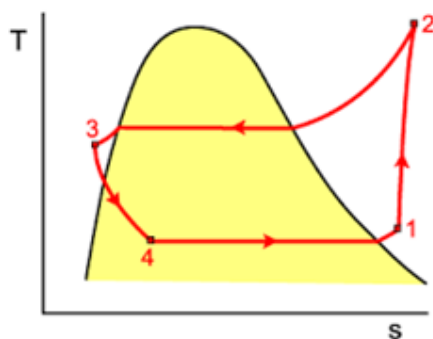


Fig. 5.2 T-S Diagram of real vapor compression refrigeration cycle

At point 1 in the diagram the refrigerant enters the compressor as a super-saturated vapor.

From point 1-2: the vapor is isentropically compressed and exits the compressor as a superheated vapor.

From point 2-3: the vapor travels through the condenser and is condensed into a saturated liquid. The condensation takes place at constant pressure.

From point 3-4: the saturated liquid refrigerant passes through the expansion valve and undergoes an abrupt decrease of pressure and this process results in the adiabatic flash evaporation and auto-refrigeration of a portion of the liquid (typically, less than half of the liquid flashes.)

The adiabatic flash evaporation process is isenthalpic (occurs at constant enthalpy).

From point 4-1: the cold and partially vaporized refrigerant travels through the coil or tubes in the evaporator where it is totally vaporized by the warm milk in the storage tank.

Notice that the above process works best for ideal vapor-compression refrigeration cycle which doesn't take into account the real world items like frictional pressure drop in the system, slight internal irreversibility during compression of the refrigerant vapor. In the practical VCR cycle, there are two processes which should be considered. The first process is superheating which refers to superheating of the refrigerant vapor in the evaporator before it enters compressor. The second process is sub-cooling which refers to sub-cooling of the refrigerant liquid in the condenser. But for the sake of simplicity and minimize complexity of the modeling system, sub-cooling and superheating will be neglected as these process requires extra source of energy.(Dincer & Kanoglu, 2010).

Therefore a thermodynamics analysis of a PV driven vapor compression refrigeration cycle modeling is based on the following assumption;

- Evaporator and condenser are at constant pressure devices ($P1=P4$ and $P2=P3$)
- Pressure drops in the refrigerant pipes are negligible.
- Saturated vapor at the evaporator outlet (point 1)
- Saturated liquid at the condenser outlet (point 3)
- $\Delta ke = \Delta pe = 0$
- Adiabatic process in expansion valve ($h3=h4$)

5.3 Mathematical Model of Sub-Components

The thermodynamic equations of respective components are based on mass flow rate of the refrigerant, overall heat transfer coefficient and enthalpy by applying mass and energy balance for each component. Therefore the mathematical relations for the refrigeration cycle of evaporator temperature 0°C and condenser temperature 49°C :

$$\sum \dot{m}_{out} h_{out} - (\sum \dot{m}_{in} h_{in} + \sum \dot{m}_{in} (\frac{h_{zis}-h_{in}}{\eta_{is}})) = \sum \dot{Q} \dots\dots\dots 5.1$$

Where: m is mass flow rate (kg/s) and h is specific enthalpy (kJ/kg) and Q is heat transfer rate.

5.3.1 Compressor

Compression process is described with volumetric efficiency, to define the refrigerant mass flow rate and overall efficiency to obtain electric power for compressor process. Both are obtained from manufacturer's report data for the mass flow rate and power consumption of the compressor with condensation temperature of $30-65^{\circ}\text{C}$ and evaporating temperature range from $-6.7-15^{\circ}\text{C}$ as seen in chapter four section 4.4.2.2.

Refrigerant mass flow rate is obtained from compressor displacement (V_{cyc}), compressor rotation speed (N), volumetric efficiency (η_{vol}) and the refrigerant density at the suction line (ρ_l)

$$\dot{m}_{ref} = V_{cyc} * \eta_{vol} * \rho_l * (\frac{N}{60}) \dots\dots\dots 5.2$$

From manufacturer's Technical datasheet, CASCADE17-0244Y3 hermetically sealed reciprocating compressor has V_{cyc} , η_{vol} , and N $32.7 * 10^{-6} \text{m}^3$, 0.76 and 1800-4200rpm respectively where ρ_l is density of refrigerant, $4.25 \frac{\text{kg}}{\text{m}^3}$.

In fact the rpm (N) of the compressor can also be found by

$$N = \frac{f_{comp}}{P_{motor}} * (1 - s_m) * 60 \dots\dots\dots 5.3$$

Where: f_{comp} is frequency of compressor P_{motor} is motor power and s_m is slip of motor which is assumed to be 5%.

Total energy supply for compression process is obtained from overall efficiency and

isentropic power of compressor. Here the transient nature of the PV based electricity production is the one that drives the compressor to compress the refrigerant from point 1 to point 2 as shown in fig. 5.2.

$$\dot{W}_{ele} = \dot{m}_{ref} * \left(\frac{h_{2s} - h_1}{\eta_{is}} \right) \dots \dots \dots 5.4$$

Where: h_{2s} is compressor outlet enthalpy, h_1 is enthalpy at compressor inlet, η_{vol} is volumetric efficiency of compressor.

The power coming to the PV is given by:

$$I_n = R_b * (H_b - H_d) + (H_d * 0.5 * (1 + \cos(\beta))) + (0.5 * rho * ((1 - \cos(\beta)) * H_b)) \dots \dots \dots 5.5$$

Where: rho is ground reflection, H_d and H_b is diffuse and beam radiation respectively, R_b is ratio of beam radiation on tilted surface to horizontal and β is tilt angle.

Solar energy arrived in the module and absorbed by the PV module

$$I_c = I_n * \alpha_{pv} \dots \dots \dots 5.6$$

Where: α_{pv} is absorptivity of PV panel

Therefore the compressor will use this power to compress the refrigerant.

5.3.1.1 Thermal loss in compressor

The compressor heat release rate to the surrounding is given by

$$\dot{Q}_{comp} = U_{comp} * A_{comp} * (T_{2s} - AT) \dots \dots \dots 5.7$$

Where: U_{comp} : overall heat transfer coefficient, A_{comp} : is area of compressor, AT : ambient temp.

5.3.2 Condenser

The heat transfer rate from the refrigerant to the cooling medium (air) is obtained by applying energy balances for each stream

$$\dot{Q}_{con} = \dot{m}_{ref} * (h_2 - h_3) \dots \dots \dots 5.8$$

Where: \dot{m}_{ref} is mass flow rate of refrigerant, h_2 and h_3 is enthalpy at condenser inlet and outlet, ϵ : is effectiveness of the condenser and is given by

$$\epsilon = 1 - \exp * (-Ntu) = \frac{Ntu}{1 + Ntu} \dots \dots \dots 5.9$$

Where: $Ntu = \frac{U * A}{(C_{min})}$ is the number of transfer unit (Keys and London, 1984). ($\epsilon = 0.91$ for the selected copper coil for the condenser material).

Condenser heat release rate to the surrounding will be

$$\dot{Q}_{con} = U_c * A_c * (T_{2s} - T_3) \dots \dots \dots 5.10$$

Overall heat transfer coefficient of the outer surface of air cooled condenser:

$$k_{c,o} = \frac{\dot{Q}_{con}}{A_{c,o} * (T_{2s} - AT)} \dots \dots \dots 5.11$$

Where: $k_{c,o}$ is overall heat transfer coefficient, $A_{c,o}$ is the condenser area which is given by

$$A_c = \frac{\dot{Q}_{con}}{U_c * (T_{2s} - T_3)} \dots\dots\dots 5.12$$

5.3.3 Expansion valve

It is assumed that the thermostatic valve is perfectly insulated, and the following is valid.

$$h_3 = h_4 \dots\dots\dots 5.13$$

5.3.4 Evaporator

Evaporator's cooling capacity of refrigerant side given by following equation:

$$\dot{Q}_e = \dot{m}_{ref} * (h_1 - h_4) \dots\dots\dots 5.14$$

$$\dot{Q}_e = \dot{m}_{ref} * cp_{ref} * \varepsilon * (T_1 - T_4) \dots\dots\dots 5.15$$

Evaporator cooling capacity inside the milk storage tank

$$\dot{Q}_e = U_e * A_e * (T_m - T_e) \dots\dots\dots 5.16$$

Where: U_e : overall heat transfer coefficient, T_e : evaporator temperature and T_m , inlet milk temperature

A_e evaporator area is given by

$$A_e = \frac{\dot{Q}_e}{U_e * (T_m - T_e)} \dots\dots\dots 5.17$$

5.4 Radiation and Convection heat loss from the PV panel

The PV panel which is highly sensitive to temperature change is exposed to radiation and convective heat losses on both the upper and lower part of the PV.

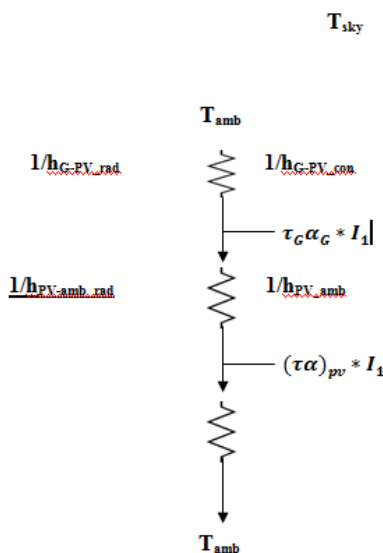


Fig. 5.3 Thermal network of a typical PV model

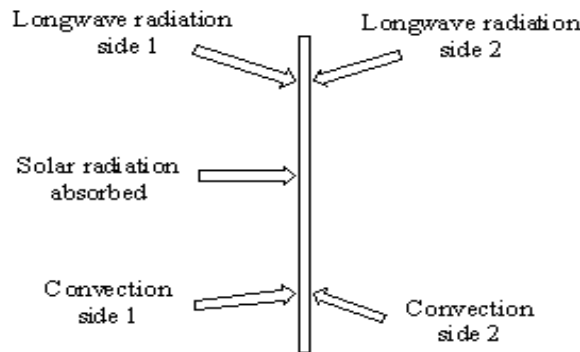


Fig. 5.4 Heat transfer of two sides of the PV panel

5.4.1 The Radiation heat loss to from the PV to the sky temperature at T_{sky}

It is approximated same as the radiation from glass to sky temperature due to the high quality of PV glass emissivity and transmittivity (Beckman,1974). Hence PV radiation loss will be considered twice at the top and bottom side of the PV panel.

$$h_{rad_PV} = \epsilon_{pv} * \sigma * \left(\frac{T_{pv}^4 - T_{sky}^4}{T_{pv} - T_{sky}} \right) \dots\dots\dots 5.18$$

Where: ϵ_{pv} : emissivity of the PV module, T_{pv} : PV temperature, σ : boltzman constant.

T_{sky} is the local air temperature is given by [31]

$$T_{sky} = 0.0552T_a^{1.5} \dots\dots\dots 5.19$$

5.4.2 The convection heat loss from the PV by wind

The convective heat transfer coefficient is approximated by heat transfer coefficient around the PV panel as the nature of the wind is highly unpredictable due to its transient nature of turbulent and laminar flow intermixed continuously [31].

$$h_{wind} = 5.7 + 3.8v \dots\dots\dots 5.20$$

Where: h_{wind} is convective heat transfer coefficient around the upper and lower PV area and v is wind speed(m/s).

5.4.3 Energy balance of the PV module

Here as mentioned in the above section, there is heat loss as well as heat gain from both radiation and convection based on the ambient temperature of the region. This means heat from the PV to the surrounding will be lost when the ambient temperature is lower and heat energy

will be gained when the ambient temperature is higher both for upper and lower side of the PV.

Therefore the energy balance is given by

$$m_{pv} * c_{pv} * \frac{(T_p - T_{pi})}{dt} = A_{pv} * (I_{pv} - E + 2 * (T_a * (h_{rad_{pv}} + h_{wind}))) - 2 * (T_{pi} * (h_{rad_{pv}} + h_{wind})) \dots \dots \dots 5.21$$

Where m_{pv} : mass of the PV module, c_{pv} : specific heat of the PV, A_{pv} : area of the PV module

T_p : final state of PV temperature, T_{pi} : initial PV temperature, dt : change of time

I_{pv} : solar Energy arrived in the module and absorbed by module

E : electrical energy generation

PV surface temperature can be derived from the above equation and be

$$T_p = T_{pi} + \frac{(dt * A_{pv} * (I_{pv} - E + 2 * (T_a * (h_{rad_{pv}} + h_{wind}))) - 2 * (T_{pi} * (h_{rad_{pv}} + h_{wind})))}{m_{pv} * c_{pv}} \dots \dots \dots 5.22$$

5.4.4 Refrigeration System Energy Performance

The COP of the system is given by

$$COP = \frac{\dot{Q}_e}{P_{pv} * \eta_c} \dots \dots \dots 5.23$$

Where \dot{Q}_e is the cooling capacity of the evaporator,

P_{pv} is the useful power generated by the PV panel

η_c is the overall efficiency of the compressor

The evaporator total heat transfer is a function of mass flow rate of the refrigerant which main cooling occurs as well as subjected to the environmental air condition to loss its temperature to the surrounding.

Therefore the evaporative cooling equation becomes

$$\dot{Q}_e = \dot{m}_{ref} * (h_1 - h_4) = U_e * A_e * (T_{milk} - T_e) \dots \dots \dots 5.24$$

The electrical power \dot{W}_{ele} that's coming from the PV is given by

$$P = A_{pv} * I_c * \Delta(\sigma\tau) * p_f * \eta_{pv} * ((1 - T_{c,pv}) * (T_{pv} - T_{rf})) \dots \dots \dots 5.25$$

Where: E is the electrical energy generated, I_c is solar energy absorbed by the module as explained in section 5.3.1, $\Delta(\sigma\tau)$ is difference between absorptivity and transmittivity, p_f is packing factor, η_{pv} is efficiency of PV module, $T_{c,pv}$ temperature coefficient of PV module, T_{pv} is PV temperature and T_{rf} is the reference temperature. Parameters like $T_{c,pv}$, η_{pv} , $\Delta(\sigma\tau)$, p_f are directly taken from the manufacturer's datasheet of AKT-180-M solar panel. It is found in appendix A.

Therefore the COP of the system will be

$$COP = \frac{U_e * A_e * (T_{milk} - T_e)}{A_{pv} * I_c * \Delta(\sigma\tau) * p_f * \eta_{pv} * ((1 - T_{c,pv}) * (T_{pv} - T_{rf})) * \eta_c} \dots\dots\dots 5.26$$

5.4.5 Hourly Milk temperature

The milk temperature at the evaporator outlet is influenced by the cooling capacity of the evaporator [32] and is given by

$$T_{m,out} = T_{m,in} + \frac{Q_{m,out}}{M_m * CP_m} \dots\dots\dots 5.27$$

Where $T_{m,in}$ is inlet milk temperature,

$Q_{m,out}$ is the milk heat energy at outlet and is given by

$$Q_{m,out} = \dot{Q}_e - \dot{Q}_{m,loss} \dots\dots\dots 5.28$$

$$\dot{Q}_{m,loss} = U_{st} * A_{st} * (T_m - T_a) \dots\dots\dots 5.29$$

Where $\dot{Q}_{m,loss}$ is storage tank heat loss

5.4.6 Overall Energy Balance of the Refrigeration system

The energy balance between compressor, evaporator and condenser is found from the first law of thermodynamics:

$$Q_{cond} = Q_e + W \dots\dots\dots 5.30$$



CHAPTER-6: RESULTS AND DISCUSSION

6.1 Results

In the design and simulation of small-scale milk chiller process, the following results are obtained

- Milk chiller has been designed that is able to cool milk from around 33°C to 4°C within four hours of time according to FAO standard.
- Daily solar radiation is converted and analyzed in hourly basis for performing the simulation.
- Condenser and evaporator temperature based on ambient temperature of Semera has been selected.
- After knowing the total cooling load demand by the system, appropriate compressor size is selected.
- Design and selection of PV panels, batteries and charge controllers is done based on cooling load and multiple criteria selection.
- Electrical characteristics the PV and compressor is simulated by using MAT-LAB algorithm.
- Mathematical modeling of refrigeration components are done
- Total design of PV system together with the modeled refrigeration components is depicted with schematic drawing
- Hourly performance of the milk chiller is simulated by using MAT-LAB as shown in the subsequent parts.

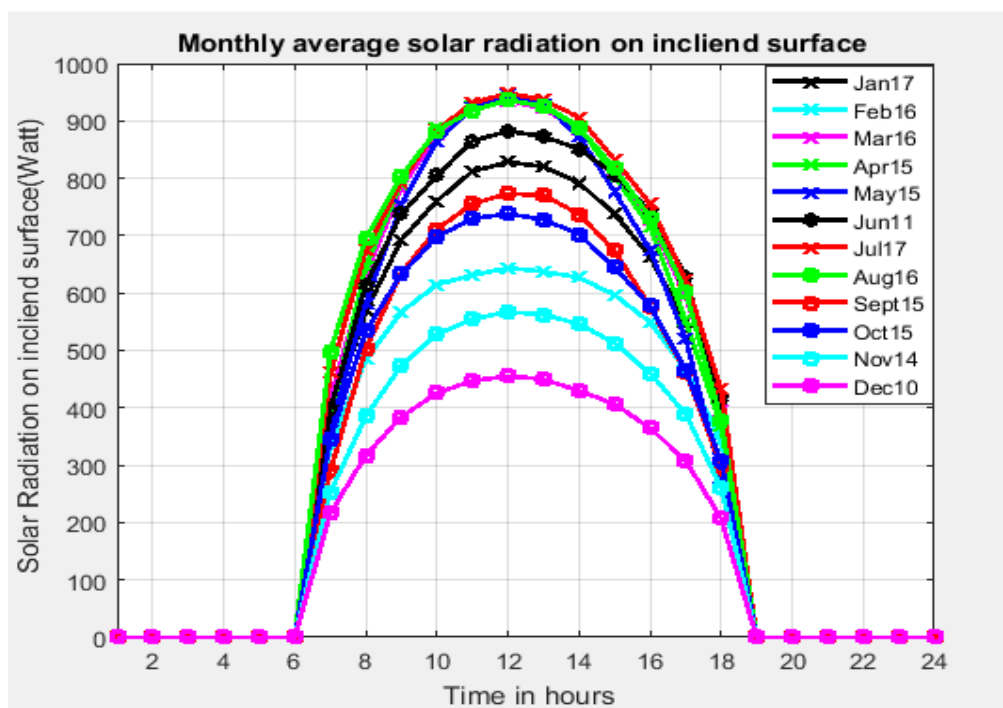


Fig. 6.1 Monthly average solar radiation on inclined surface

As shown in the above figure, monthly average solar radiation on inclined surface varies with time instantly where the highest occurs at noon time when the sun becomes overhead and the lowest radiation counts on the morning and at dawn time. Monthly point of view, August and July have the highest solar radiation while lowest in December. Here also we notice that the maximum hourly solar radiation won't reach the STC value (1000Watt) which is practically convincing.

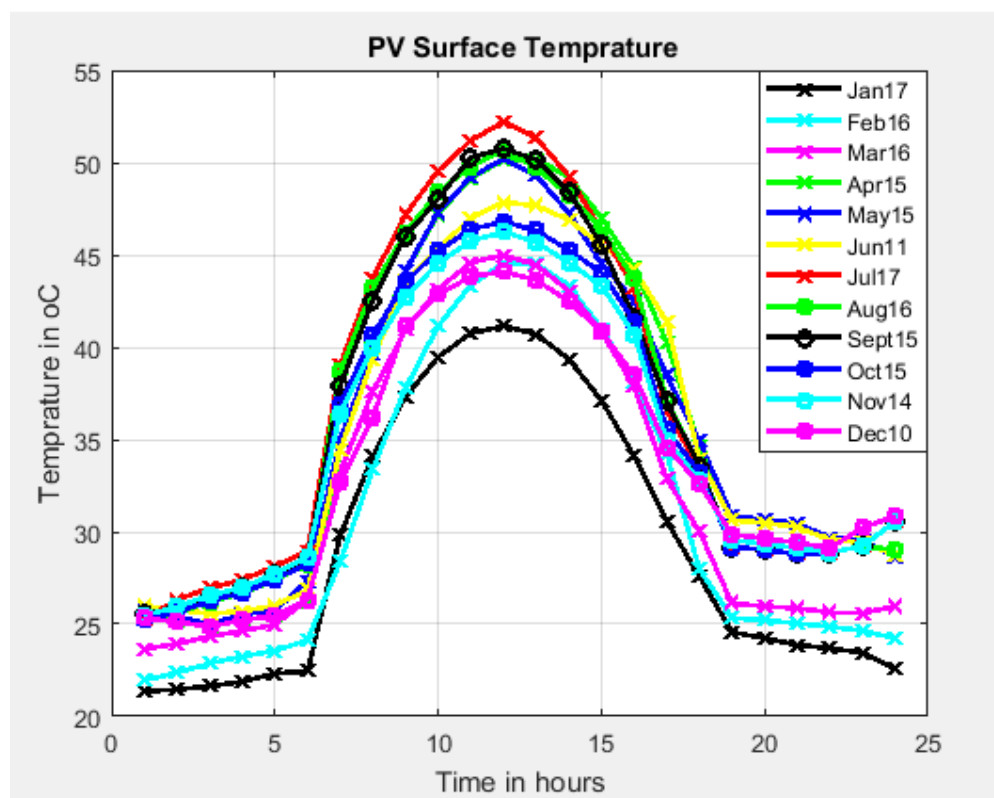


Fig. 6.2 Hourly PV surface temperature

The above fig shows the hourly PV surface temperature. It's high at noon in the middle as usual and low at the two opposite end of the graph (i.e in the morning and evening respectively) but one can see that the morning time (left hand side), the temperature is a bit lower than in the right hand side(from sunset to down) that is due to once the PV surface temperature gets hot enough, its rate of cooling is a bit lower where it doesn't get rid of all its temperature to the surrounding to be equal with exactly the same as morning temperature. The minimum PV surface temperature is just around 21°C as shown above for the month of January and the maximum is around 53°C on July which is good match for Semera region where maximum temperature looms from the month of April to August.

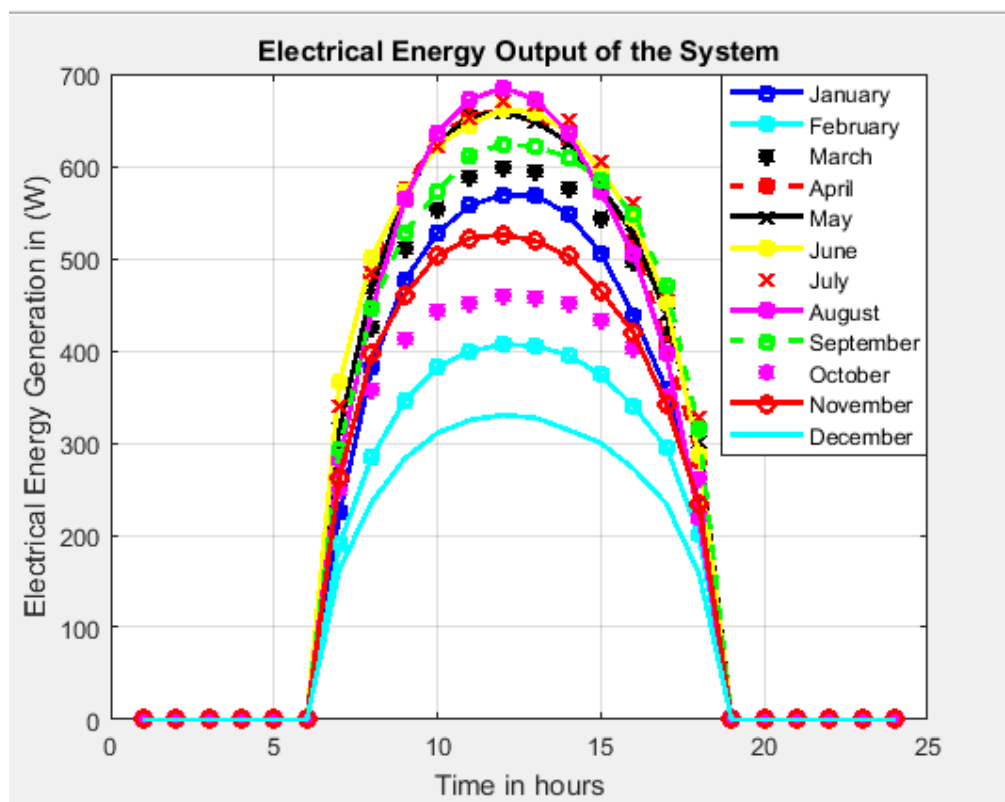


Fig. 6.3 Hourly Electrical Energy output of the system

As shown above the maximum electrical energy output of the system comes for August month around 700Watt and the minimum in December. Generally we can observe for months starting from April to September, maximum electrical energy is harvested by the PV panel and minimum power for months from October to December.

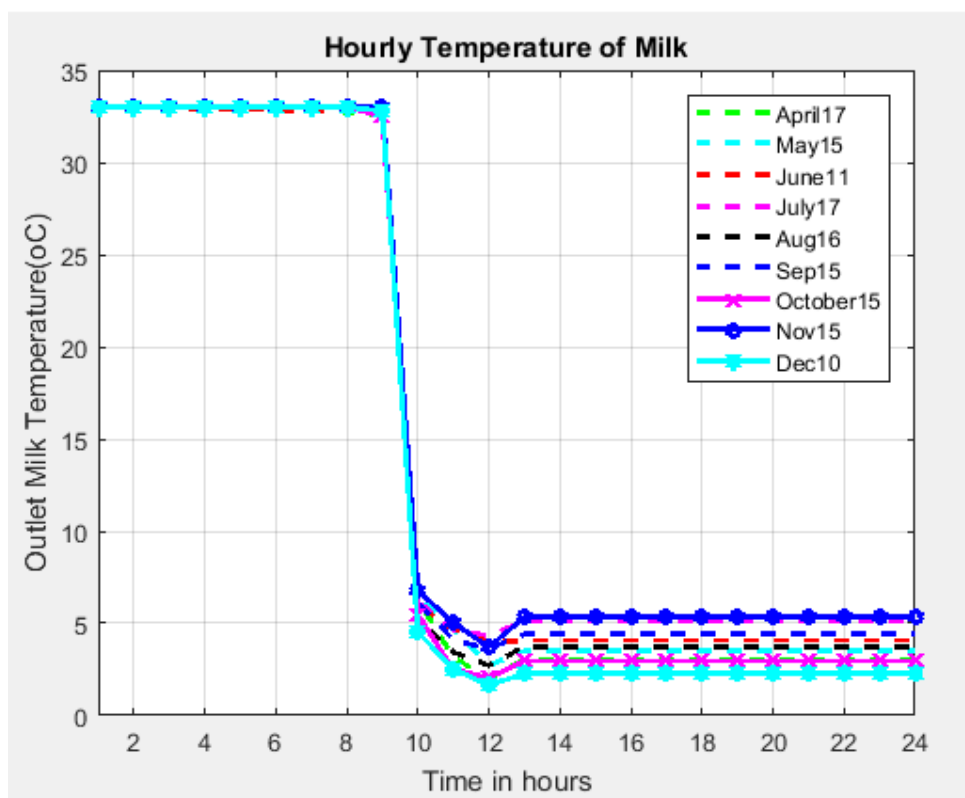


Fig. 6.4 Hourly Temperature of Milk

The hourly milk temperature for various months is shown above where the temperature is just 40c for all months considered. Here the temperature continuously drops as the time goes and reaches the desired milk temperature for longer shelf life. As we can see above, the milk starts to being cool at 9AM in the morning after milking and introduced to the chiller where its temperature will reach to 4°c from 33°c within four hours of period of time and ends at 1PM.

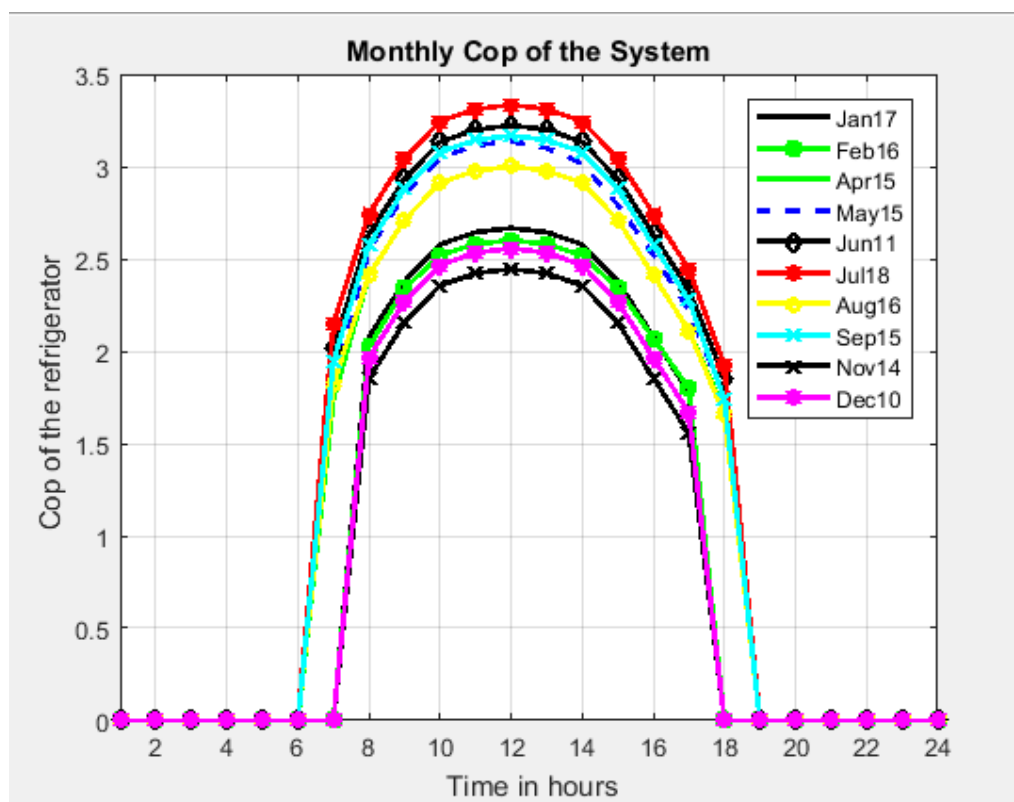


Fig. 6.5 Monthly Cop of the system

The above figure depicts the cop of the system where it falls in the range of roughly from 1.6 to around 3.4 for the months in November and July respectively. We can see that for months from November and February, the cop is lower as well as the Compressor starts operating at 7AM in the morning because of the solar radiation power (less than 235Watt) isn't enough to drive it so it has to wait for an hour until to start operating. In a similar way at 6PM in the afternoon, of course the PV panel produces energy but not enough again and that's why looks as if 0 cop in the figure above. On the contrary to this, for months from April to September; the PV power produced is ample to start the compressor and it already starts for the time between 12AM and 7AM as well as between 6PM and 7PM in the afternoon time.

CHAPTER-7: CONCLUSION AND RECOMMENDATION

7.1 Conclusion

A refrigeration system for milk cooling, which is powered directly by a photovoltaic array was designed. In doing so, solar data for Semera region has been collected and analyzed from Ethiopian Metrology Agency and the hourly solar radiation data was used for the simulation of monthly average solar radiation data on inclined surface, PV surface temperature, electrical energy output of the PV, and temperature of the milk has been obtained by using MATLAB simulation. The designed PV system also uses an MPPT FLEXmax 30/40 charge controller for tracking maximum power point while charging and in order to have safe and long-lasting battery. LiFePo₄ Battery with a back-up time of 15.92hrs for cloudy and night time. In addition the electrical characteristics of the AKT 180-M PV panel was proposed to run the compressor and the optimum tilt angle that improves the annual performance of the PV panel was calculated, and a detail mathematical analysis on solar radiation performance of this optimally tilted panel was carried out, and hourly performance variation of the combined system was investigated. Upon doing this paper, Milk with enormous advantages it has in the nourishing process of children's and elders life; can be cooled comfortably by using this small-scale PV driven refrigeration system for 50 liters of milk. In addition this technology shows its vitality especially in the areas where grid supply is unavailable or at great distance as most milk production areas are this kind, in order to preserve the milk for better use and minimize post-harvest loss. Afar area which is well-known for its cattle production by pastoralists as their income means, PV driven milk chiller plays an important role in longer shelf-life of the milk. COP of the system was calculated based on the performance characteristics equation which is given by the manufacture' with minimum value of 1.6 and maximum of 3.4 based on RPM of the compressor. Milk temperature has been lowered from 33°C to 4°C within four hours of cooling by using 720Wp.

7.2 Recommendation

In this paper, electrical characteristics of the PV module, mathematical modeling of PV components and MATLAB simulation for the hourly performance evaluation of the system has been done. As a future work, the following points are recommended

- Experimental analysis of the prototype is needed to validate the theoretical modeling on the performance of the PV driven refrigerator.
- Design and performance simulation of components of the refrigerator (i.e. condenser, throttling valve, and evaporator) can be performed.
- For higher output of the PV panel, it is much better to employ a solar panel that follows tracking system to enhance the harnessing of solar irradiation for higher electricity production.
- It's much better to combine the battery and ultra-capacitors, to highly increase the system efficiency as the battery will be able to store and release energy gradually, while ultra-capacitor effectively acts as storage device with very high power density.



REFERENCES

1. Wohltre, Dieter, Meissner, “ Organic Solar cells.” Advanced Materials. Volume 3, Issue 3. Verlag GmbH & Co. KGaA, 1991.
2. Weidong Xiao, Dunford W.G. “A modified adaptive hill climbing MPPT method for photovoltaic power systems” Power Electronics Specialists Conference, IEEE, PESC 04, 2004.
3. McCann, MichelleJ. Catchpole, KylieR. Weber, Klaus J., “ A review of thin film crystalline silicon for solar cell applications. Part 1: native substrates.”, 2001
4. Milk and dairy products in human nutrition(2013), by E.Muehlhoff, A.Bennett and D.McMahon, Food and Agriculture organization of the United Nations (FAO), Rome. E-ISBN: 978-92-5-107864-8(PDF).
5. FAO.2000. Establishment of regional reference centre for milk processing and marketing: Quality control manual, edited by T.V.A. Siirtola. Rome
6. Martin John Atkins and Michael r. W. Walmsley, “ Applications of Process Integration Methodologies in Dairy and Cheese Production,” University of Waikato, New Zealand:Woodhead Publishing Limited, 2013.
7. Rajeev Kumar, Raj Kiran Prabhakar, Opportunities and challenges in Indian dairy industry supply chain: a literature review. Int J Logist Supply Chain Manag Perspect 2013;2(4):791-800.
8. Kumar Kulkarni Nisha, Usha Ganesh. Villgro case study series: promethean power systems. Villgro 2013.
9. Report by National Cooperative Development Corporation. Available:www.ncdc.in/activities_files/ColdStorageFruitsVegetables.html for Cold storage and fruits & vegetables programme. [accessed 16.01.15.]
10. Kishor H. Gedam, Rachna Gedam, Rajendra Prasad, V.K. Vijay, Value addition of traditional milk products: the study for rural entrepreneurial development, Int. J. Entrepreneursh. Bus. Environ. Perspect. 2 (3) (2013) 537-541.
11. Report from FAO, Available from: www.fao.org/ag/againfo/themes/documents/LPS/dairy/mpv/lactoperoxidase/faqanswer.html, 2013 [accessed 10.07.15.]
12. Benefits and Potential Risks of the Lactoperoxidase System of Raw Milk Preservation. Report of an FAO/WHO Technical Meeting, 2005. <http://www.fao.org/ag/dairy.html>.
13. Abebe Tesema, Markos Tibbo, Hygeinic milk processing: clean environment, Clean Utensils. Technical Bulletin No. 1 by International Center for Agricultural Research in the Dry Areas, 2009.

14. Ashwini Chothe, Sanjay Patil, D.K. Kulkarni, Unconventional wild fruits and processing in tribal area of Jawhar, Thane District, Biosci. Discov. 5 (1) (2014)19-23.
15. Eyassu Seifu, Reiner Doluschitz, Analysis of the dairy value chain: challenges and opportunities for dairy development in Dire Dawa, Eastern Ethiopia, Int. J.Agric. Policy Res. 2 (6) (2014) 224-233.
16. Auge, C. Nouveau Larousse Illustre, 7 vols. Paris, 1897-1904
17. Critof, R. E, refrigeration in developing countries-the renewable options, proc. 1st world Renewable Energy Congress, reading UK, 1990
18. Vella, G.J., Harris, L.B. , Goldsmid, H.J. A solar thermoelectric refrigerator, Solar Energy 18 (4)(1976) 355–359.
19. Fischer S., Labinov S. Not-in-kind technologies for residential and commercial unitary equipment. project report ORNL/CON-477, Oak Ridge National Laboratory, US DOE DE- AC05-C96OR22464; 2000.
20. Solangi, K.H. , Islam, M.R., Saidur, R. , Rahim, N.A. , Fayaz, H. , A review on global solar energy policy, Renewable and Sustainable Energy Reviews 15 (2011)2149–2163
21. FAO, 1983 Solar energy in small-scale milk collection and processing. Animal Production and Health Paper No. 39. Rome.
22. Hwang, Y. , Randermacher, R. , Alili, A.A., Kubo, I., Review of solar cooling technology, HVAC&R Research 14 (3) (2008) 507–528.
23. Hassan, H.Z., Mohamad, A.A. , A review on solar-powered closed physisorption cooling systems, Renewable and Sustainable Energy Reviews 16 (2012)2516–2538.
24. Srikkhirin, P., Aphornratana, S., Chungpaibulpatana, S., A review of absorption refrigeration technologies, Renewable and Sustainable Energy Reviews 5 (2001) 343–372.
25. Aed Ibrahim Owaid, Mohd Tariq, Hassan Isa, Husamsabeeh, mohannadali, “the heat losses experimentally in the evacuated tubes solar collector system in Baghdad-iraq climate,” Int. J. Res. Eng. Technol.,vol.Vol. 2, no Issue 4, pp 13-24, Apr.2014
26. Ali Naci Celik, Nasir Acikgoz, Modeling and experimental verification of the operating current of monocrystalline photovoltaic modules using four- and five-parameter models, Applied Energy, 84, 1-15, 2007 .Oliva Mah NSPRI, "Fundamentals of Photovoltaic Materials", National Solar power institute, Inc. 12/21/98.
27. Otanicar, T. , Taylor, R.A. , Phelan, P.E. , Prospects for solar cooling – an economic and environmental assessment, Solar Energy 86 (2012) 1287–1299
28. EPiA. 2014. Global Market Outlook for Photovoltaics 2014–2018. European Photovoltaic Industry Association (EPIA))

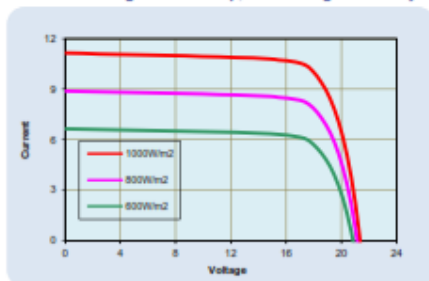
29. Hassan, H.Z. , Mohamad, A.A. , A review on solar-powered closed physisorption cooling systems, *Renewable and Sustainable Energy Reviews* 16 (2012)2516–2538.
30. Solangi, K.H., Islam, M.R. , Saidur, R. , Rahim, N.A., Fayaz, H., A review on global solar energy policy, *Renewable and Sustainable Energy Reviews* 15 (2011)2149–2163
31. Vineet Singla, and Vijay Kumar Garg: Modeling of Solar Photovoltaic Module & Effect of Insolation Variation Using MATLAB/SIMULINK. *International Journal of Advanced Engineering Technology* E-ISSN 0976-3945.
32. Marcelo Gradella Villalva, Jonas Rafael Gazoli, and Ernesto Ruppert Filho: Comprehensive Approach to Modeling and Simulation of Photovoltaic Arrays. *IEEE Transactions on power electronics*, vol.24, No.5, May 2009.
33. John A. Duffie and William A. Beckman, solar engineering of thermal processes, fourth edition. Solar Energy Laboratory University of Wisconsin-Madison,2013.
34. Gilbert M. masters: Electric Renewable and Efficient power system 1st edition, J. wiley. S.C
35. William S.Janna, handbook Engineering heat transfer second edition, pp 15-21.
36. Soteris A. Kalogirou: Solar Energy Engineering process and systems. 2nd Edition, Elsevier
37. Chaouachi, A.,Kamel,R.M., and Nagasaka,K. 2010. A novel multi-model neuro-fuzzy-based MPPT for threephase grid-connected photovoltaic system, *Solar Energy*84 (2010) 2219 – 2229
38. Ansari, F.A. , Mokhtar, A.S., Abbas K.A. and Adam, N.M. A Simple Approach for Building Cooling Load Estimation, Faculty of Engineering, UPM, Serdang, Selangor Darul Ehsan, Malaysia, *American Journal of Environmental Sciences* 1 (3): 209-212, 2005
39. ASHRAE Fundamentals Handbook (SI), Nonresidential Cooling and Heating Load Calculations, 1997
40. Elias mesfin ”Design and performance simulation of solar DC refrigerator with thermal storage system for rural dairy preservation, page 26”
41. Renewable energy products, energy conservation products, power quality product, solar PV system, solar thermal system, energy saving system
42. Otanicar, T., Taylor, R.A., Phelan, P.E., Prospects for solar cooling – an economic and environmental assessment, *Solar Energy* 86 (2012) 1287–1299

Appendix A: Electrical and Mechanical Characteristics under STC'(AKT-180-M)

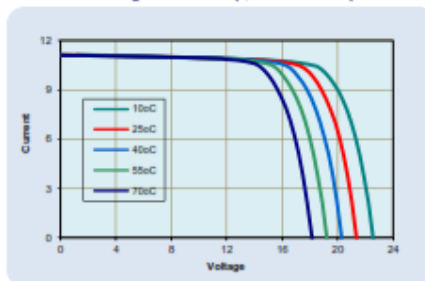
AKT-180-M

Electrical Output under Different Light Intensity and Temperature

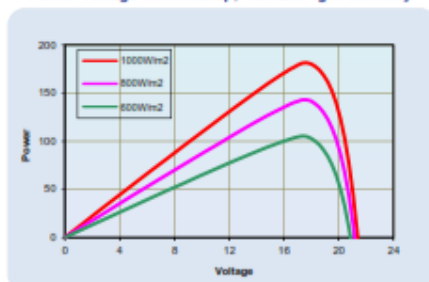
Current-Voltage Relationship, variable light intensity



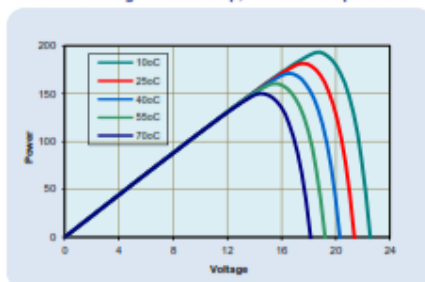
Current-Voltage Relationship, variable temperature



Power-Voltage Relationship, variable light intensity



Power-Voltage Relationship, variable temperature



Electrical Characteristics under STC¹

Open-circuit voltage (Voc)	Av 21.6V, sd 0.3
Voltage at maximum power (Vmp)	Av 17.5V, sd 0.2
Short-circuit current (Isc)	Av 11.31A, sd 0.3
Current at maximum power (Imp)	Av 10.29A, sd 0.2
Maximum power at STC (Wp)	180W ±5%
Operating temperature	-40°C to +85°C
Maximum system voltage	1000V dc
Power tolerance	±5%

¹Standard Temperature and Conditions: 25°C, AM 1.5, 1000W/m²

Applied Knowledge and Technology Ltd
 High Wycombe W: www.aksolar.co.uk
 HP15 7QE E: contact@aksolar.co.uk
 United Kingdom T: +44 (0)1494 372 301

Temperature Dependence of Isc, Voc and Wp

Nominal operating cell temperature (NOCT)	47°C ±2°C
Temperature coefficient of Wp	-0.8±0.05%/°C
Temperature coefficient of Voc	-0.06±0.002%/°C
Temperature coefficient of Isc	0.034±0.005%/°C

Mechanical Characteristics and Dimensions

Solar cells	Monocrystalline 125x125mm
No. of cells	72 (12x3+12x3)
Dimensions	1580x808x35mm
Weight	15kg
Glazing	3.2mm textured, tempered, low-iron
Frame	Anodised aluminium alloy

Appendix B: MATLAB code

Appendix B₁: Code to model the I-V, P-V electrical characteristics of the PV module for single AKT-180-M as well as for four AKT-180-M connected in series and I-V intersection of PV module and the Compressor.

```

clr all
Iscn=11.31;          %nominal short circuit current
Voc_n=21.6;          %nominal open circuit voltage for single pv module
Voc_nn=86.4;         %nominal open circuit voltage for four series pv module
KI=0.034;           %Isc current temperature cofficient
KV=-.6;             %Voc temperaute cofficeint
K=1.3806503e-23;    %Boltzman constant
q=1.60217646e-19;   %charge of an electron
a=1.2;              %value of doid constant
Tn=273+25;          %nominal tepmerature in kelvin
Gn=1000;            %nominal solar insolation
Ns=36;              %number of cells in serouse for single pv module
Nss=144;            %number of cells in serouse for four series pv module
Eg=1.12;            %Energy band gap of semiconductor
Vmmp=17.5;          %maximum voltage output of a single pv module
Vmpp=70;            %maximum voltage output of four series pv module
Immp=10.29;         %maximum current output of a pv module
Pmax=Vmmp*Immp;     %maximum power output of a single pv module
pmaxx=Vmpp*Immp;    %maximum power output of four series pv module
Vtn=N*s*K*Tn/q;     %thermal voltage of array for single pv module
Vtnn=Nss*K*Tn/q;    %thermal voltage of array for four series pv module
Rs=0;               %initialization of the iteration;
Iomn=Iscn/(exp(Voc_n/(a*Vtn))-1); %diod nominal saturation current for
single pv module
Iomnn=Iscn/(exp(Voc_nn/(a*Vtnn))-1); %diod nominal saturation current for
four seris pv module
Rp=(Vmmp+Rs*Immp)/(Iscn-Iomn*(exp((Vmmp+Rs*Immp)/(Vtn*a))-1)-Immp);
Rpp=(Vmpp+Rs*Immp)/(Iscn-Iomnn*(exp((Vmpp+Rs*Immp)/(Vtnn*a))-1)-Immp);
In=1;               %to initaite the iteration since the I(V) function is
implicit
Inn=1;              %to initaite the iteration since the I(V) function is
implicit
I=1;
format long e
for i=1:20000
    Rs=Rs+.0001;
    Ipvn=(Rp+Rs)*Iscn/Rp;
    Rp=(Vmmp+Rs*Immp)/(Ipvn-Iomn*(exp((Vmmp+Rs*Immp)/(Vtn*a))-1)-Immp);
    Rpp=(Vmpp+Rs*Immp)/(Ipvn-Iomnn*(exp((Vmpp+Rs*Immp)/(Vtnn*a))-1)-Immp);
    for j=1:500
        In=Ipvn-Iomn*(exp((Vmmp+(In*Rs))/(Vtn*a))-1)-((Vmmp+(Rs*In))/Rp);
        Inn=Ipvn-Iomnn*(exp((Vmpp+(Inn*Rs))/(Vtnn*a))-1)-((Vmpp+(Rs*Inn))/Rp);
    end
    Pn=In*Vmmp;
    pnn=Inn*Vmpp;
    error=abs(Pn-Pmax);
    error1=abs(pnn-pmaxx);
    V=0:.01:Voc_n;
    Vn=0:.01:Voc_nn;
    I=Ipvn-Iomn*(exp((V+(I*Rs))/(Vtn*a))-1)-((V+(Rs*I))/Rp);
    Ia=Ipvn-Iomn*(exp((Vn+(Inn*Rs))/(Vtnn*a))-1)-((Vn+(Rs*Inn))/Rp);
    P=V.*I;
    Pn=Vn.*Ia;
    Pmaxi=max(P);
    Pmaxii=max(Pn);
    err=abs(Pmaxi-Vmmp*In);
    
```

```

err1=abs(Pmaxii-Vmpp*Inn);
if error<.001 & err<.002;
    error1<.001 & err1<0.002;
    break
end
end
G=0;
T=Tn;
Ipvn=(Rp+Rs)*Iscn/Rp;
Ipvnl=(Rpp+Rs)*Iscn/Rpp;
for l=1:5
    G=G+200;
    Ipv=(Ipvn+KI*(T-Tn))*(G/Gn);
    Ipv1=(Ipvnl+KI*(T-Tn))*(G/Gn);
V=0:.01:Voc_n;
Vn=0:.01:Voc_nn;
for ii=1:300
    I=Ipv-Iomn*(exp((V+(I*Rs))/(Vtn*a))-1)-((V+(Rs*I))/Rp);
    Inn=Ipv1-Iomnn*(exp((Vn+(Inn*Rs))/(Vtnn*a))-1)-((Vn+(Rs*Inn))/Rpp);
end
P=V.*I;
pn=Vn.*Inn;
figure(1)
plot(V,I,'linewidth',2)
plot(Vn,Inn,'linewidth',2)
title('V-I Characterstics at 25oc')
legend('200Watt','400Watt','600Watt','800Watt','1000Watt')
xlabel('Voltage(V)')
ylabel('Current(Amp)')
grid on
hold on
axis([0 95 0 12])
axis([0 25 0 12])
figure(2)
plot(V,P,'linewidth',2)
plot(Vn,pn,'linewidth',2)
hold on
axis([0 90 0 750])
axis([0 25 0 190])
title('V-P Characterstics at 25oc')
legend('200Watt','400Watt','600Watt','800Watt','1000Watt')
grid on
xlabel('Voltage(V)')
ylabel('Power(Watt)')
end
hold off
hold off
Ta=table(V',P');

G=235;
T=273+34;
II=2;
IIn=2;
Ipv=(Ipvn+KI*(T-Tn))*(G/Gn);
Io=Iomn*(Tn/T)^3*exp(q*Eg*(1/Tn-1/T)/(a*K));
Vt=Ns*K*T/q;
Vtt=Nss*K*T/q;
V=0:1:Voc_n;
Vn=0:1:Voc_nn;
for jj=1:1000
    II=Ipv-Io*(exp((V+(II*Rs))/(Vt*a))-1)-((V+(Rs*II))/Rp);
    IIn=Ipv-Io*(exp((Vn+(IIn*Rs))/(Vtt*a))-1)-((Vn+(Rs*IIn))/Rp);
end
    
```

```
figure(3)
Ppp=V.*II;
PP=Vn.*IIIn;
plot(V,II,'linewidth',1.5)
plot(Vn,IIIn,'linewidth',1.5)
axis([0 87 0 12])
xlabel('Voltage(V)')
ylabel('Current(Amp)')
title('I-V Intersection point of PV module and Compressor')
gtext('Minimum 235Watt needed to start the Compressor')
hold on
III=89.5./V;
IIIIn=89.5./Vn;
plot(V,III,'linewidth',1.5)
plot(Vn,IIIIn,'linewidth',1.5)
hold on
axis([0 21 0 12])
axis([0 87 0 12])
grid on
```



Appendix B₂: Code to model the Total Efficiency variation of Refrigerator Compressor with Rpm

```

clear,clc
format long e
C=[-1107.663    3.94E+02    1.64E+01    -9.43E+00;
   -1.300685   -1.22E-01   -5.10E-03   -2.85E-02;
    0.000205629 2.94E-05    1.23E-06    4.16E-06;
   -4.706E-08  -2.44E-10  -1.02E-11   -7.43E-10;
   -7.62E+01   -3.82E+00  -1.59E-01   -1.22E+00;
    1.68E-01    4.17E-02    1.74E-03    2.49E-03;
   -8.43E-01    3.52E-05    1.47E-06   -1.28E-05;
    7.16E+01   -7.58E+00  -3.16E-01    1.00E+00;
   -8.93E-01    5.70E-02    2.38E-03   -1.32E-02;
    3.54E-03   -1.81E-04  -7.57E-06    5.23E-05;
   -4.13E-04   -3.80E-05  -1.58E-06   -6.92E-06;
   -4.98E-08    6.98E-09    2.91E-10   -6.89E-10;
   -1.08E-06    2.13E-07    8.89E-09   -1.17E-08;
    2.88E-06   -3.58E-08  -1.49E-09    4.62E-08;
    1.52E-02    3.82E-03    1.59E-04    2.72E-04;
    1.79E-02    1.21E-03    5.03E-05    3.51E-04;
    1.60E+00    2.21E-02    9.22E-04    2.47E-02;
    5.35E-06   -5.58E-07  -2.33E-08    7.28E-08;
    1.65E-04   -2.04E-05  -8.51E+00    1.97E-06;
    1.73E-06   -2.47E-07  -1.03E-08    1.98E-08;
   -1.23E-04    1.13E-06    4.71E-08   -1.98E-06;
   -6.05E-04   -4.79E-04  -2.00E-05   -6.54E-06;
   -8.01E-03    2.48E-04    1.04E-05   -1.21E-04];
Tc=49; %temperature of Condenser
TE=0; %temperature of Evaporator
i=0;
Eis=49200; %isentropic energy consumption of the comperssor in J/KG
for x1=1800:100:4200
    i=i+1;
    x2=(TE*9/5)+32; %conversion of Evaporator temperature into Fahrenheit
    x3=(Tc*9/5)+32; %conversion of condenser temperature into Fahrenheit

    A=C(1,:) +C(2,:)*x1+C(3,:)*x1^2+C(4,:)*x1^3+C(5,:)*x2+C(6,:)*x2^2+C(7,:)*x2^3+
    C(8,:)*x3+C(9,:)*x3^2+C(10,:)*x3^3+C(11,:)*x1*x2*x3+C(12,:)*(x1^2)*x2*x3+C(13,
    :)*x1*(x2^2)*x3+C(14,:)*x1*x2*x3^2+C(15,:)*x1*x2+C(16,:)*x1*x3+C(17,:)*x2*x3
    +C(18,:)*(x1^2)*x2+C(19,:)*x1*x2^2+C(20,:)*(x1^2)*x3+C(21,:)*x1*(x3^2)+C(22,
    :)*(x2^2)*x3+C(23,:)*x2*x3^2;
    B(i,1)=A(1)/3.42121; %performance Coefficient value of cooling capacity(watt)
    B(i,4)=A(4)/7936.6; %performance Coefficient value of mass flow rate(kg/s)
    B(i,2)=A(2); %performance Coefficient value of power consumption(watt)
    B(i,3)=A(3); %performance Coefficient value of current consumption(Amp)
    effc(i)=(B(i,4)*Eis)/B(i,2)*100;
    cop(i)=B(i,1)/B(i,2);
end

%yyaxis left
%plot(B(i,1),B(i,2),'c-', 'linewidth',2)
%xlabel('Cooling capacity');
%ylabel('Power consumption')
%title('Cooling capacity Vs Power consumption and RPM')
%grid on
%yyaxis right
QL=B(:,1);
x1=1800:100:4200;
plot(x1,effc,'c-s', 'linewidth',2)
title('RPM VS Total Efficiency of the compressor ')
gtext('Total Efficiency of compressor')
grid on
    
```

```
xlabel('RPM')  
ylabel('Total Efficiency(%)')  
B(:,4)=B(:,4)*1000;  
S=[x1' B];  
T=array2table(S);  
disp('      Rpm  QL(Watt)   Pcon(W)   current(A) mflow(g/s) ')  
format short  
disp(T)
```

© GSJ

Appendix B₃: Code to model Monthly average Solar Radiation on inclined surface, Hourly PV surface temperature, Hourly Electrical Energy output of the System, Hourly temperature of the Milk and Monthly Cop of the System.

```

clc
clear all
Te=0; % temperature of evaporator
T2s=49; % condensor temperature
Tmilk=33; % inlet milk temperature in the evaporator
Mm=50; % mass of the milk
Ast=1.039; % area of storage tank
Ae=0.078; % area of the evaporator
doe=0.01; % outer diameter of the evaporator
die=0.008; % inner diameter of the evaporator
pr1=3.919; % prandtl number for inside tube liquid
pr2=0.553; % prandtl number for inside tube vapor
rho=4.25; % density of r134a
Kvl=1.170149*10^-1; % kinematic viscosity of r134a at evaporator temperature
Kvv=2.10973*10^-3; % kinematic viscosity of r134a at evaporator temperature
mm=2.761*10^-4; % viscosity of the fluid r134a at evaporator temperature
kl=0.0947; % thermal conductivity of liquid r134a at evaporator temperature
kv=0.0121; % thermal conductivity of vapor r134a at evaporator temperature
cpm=3930; % specific heat of the milk kj/kg.K
kc=385; % thermal conductivity of copper
Veff= 0.76; % volumetric efficiency of the compressor
Vo=0.9; % overall efficiency of compressor
Vco=0.93; % overall condenser efficiency
cpr=1.34; % specific heat of r134a kj/kg.K
Vc= 9.63*10^-6; % clearance volume of the cascade compressor m3
vl=0.0692; % saturated specific volume of the refrigerant at inlet of
cascade compressor m3/kg
mr=0.008948; % refrigerant mass flow rate kg/s
hl=250.5; % enthalpy at compressor inlet kj/kg
sl=0.919; % entropy at compressor inlet kj/kg.K
h2s=431.48; % enthalpy at compressor outlet kj/kg
Apv=6.12; %collector unit area
tpv=0.0035; %Thickness of the pv module
ti=0.05; %Back insulation thickness and storage the smae thickness
eg=0.88; %Emmisisivity of the PV module
Trpv=0.1; %Transmitivity of the Pv module
hi=10; %inner heat transfer coefficient
ho=100; %outer heat transfer coefficient
ti = 0.0254; %milk tank insulation thickness
Umilk=120; %heat transfer of milk
epv=0.83; %Emmisisivity of the PV module
apv=0.9; %Absorbability of PV module
tapv=0.93; %Difference b/n Absorbativity and Transmitivity of
Module
eef=((1/epv)+(1/eg)-1)^-1; %Effective emisivity of PV and Glass
pf=0.9; %Packing Factor
ki=-0.249; %thermal conductivity of insulator
Tfp=-0.6; %Temperature cofficent of PV module
Nepv=0.155; %Nominal efficency of PV module
Trf=25; %Reference Temperature
ka=0.026; %Thermal conductivity of air
kp=1.56; %Thermal conductivity of pv
rho=0.2; %Ground refilaction
cg=1278.95; %836 Glass specific heat
Ca=1.005; %Specific heat capacity of air
cp=677; % PV specific heat
mp=15; %mass of PV
    
```

```

mcpp=mp*cp; %Mass*CP of PV module
Vw=3; %wind speed
beta=pi/18; %collector slop
phi=9.7*pi/180; %Latitude of the site
sigma=5.67e-8; %Boltzman constant
Ue=320; %heat transfer of evaporator
Tai=20; %Inital Temperature of the atmsphere
TIQsolar=0; %Intilaization of solar radiation
TElec=0;
deltt=60;
open('HSR.xlsx');
Z=xlsread(open);
for j=1:365
    data1(:, :, j)=Z(j+(23*(j-1)):j*24, :); %Data formulate for 24 hours of each
    day for all day in the year
end
for n=1:365
    decl(n)=(pi/180)*(23.45*sin((2*pi/365)*(284+n))); %Calculation of the
    declination angle )))
end
for ii=1:24
    omega(ii)=(ii-12)*pi/12; %Calculation of the hour-angle for each hour of the
    day. )))
end
for i=1:365
    Grr=data1(:, 4, i);
    Drr=data1(:, 5, i);
    Taa=data1(:, 3, i);
    qee=data1(:, 10, i);
    for j=1:24
        Gr=Grr(j);
        Dr=Drr(j);
        T=Taa(j);
        Ta=T; % Ambiente Temperature
        Tpi=T+3; % initial PV temperature
        Tsky=Ta-6; % sky temperature
        Rb=((cosd(phi-beta))*cosd(decl(i))*cosd(omega(j))+sind(decl(i))*sind(phi-
        beta))/((cosd(phi)*cosd(decl(i))*cosd(omega(j))+sind(decl(i))*sind(phi)));
        In=Rb*(Gr-Dr)+(Dr*0.5*(1+cosd(beta)))+(0.5*rho*((1-cosd(beta))*Gr));
        Ic=In*apv; % solar Energy arrived in the module and absorbed by module
        Tf=(Tai+T)/2; %Film Temperature
        Ve=2/(Tai+T); %Volume Expansion cofficent
        hc1=2.8+3*Vw; %convective heat transfer cofficent at the top of the PV
        hr1=eg*sigma*(Tpi^4-Tsky^4); %Radiation heat transfer b/n air and PV module
        a12=hc1+hr1;
        Ut=((1/(hc1+hr1)))^-1; %top heat loss
        U1=Ut+a12;
        Tpm = 30 + 0.0175.*(Ic-150) + 1.14*(Ta -25); %Initial Temperature of the PV
        Eg=Ic*tapv*pf*Nepv*((1-0.0045*(Tpi-Trf))); %Electrical Energy generation
        a12=hc1+hr1;
        Tpl=Tpi+((deltt/mcpp)*Apv*(Ic-Eg+a12*Ta^2-a12*Tpi^2));
    end
end
%Main Program
for i=1:365
    Grr=data1(:, 4, i);
    Drr=data1(:, 5, i);
    Taa=data1(:, 3, i);
    qe=data1(:, 10, i);
    for j=1:24
        Gr=Grr(j);
        Dr=Drr(j);
        T=Taa(j);
    end
end

```

```
qee=qe(j);
Ta=T;
Rb=((cosd(phi-beta))*cosd(decl(i))*cosd(omega(j))+sind(decl(i))*(sind(phi-
beta)))/(cosd(phi)*cosd(decl(i))*cosd(omega(j))+(sind(decl(i))*sind(phi)));
if Rb<0
    Rb=0.5;
end
In=Rb*(Gr-Dr)+(Dr*0.5*(1+cosd(beta)))+(0.5*rho*((1-cosd(beta))*Gr));
Ic=In*apv;
if Ic<0
    Ic=0;
end
Tpi=Tpi+((deltt/mcpp)*Apv*(Ic-Eg+a12*Ta^2-a12*Tpi^2));
TIQsolar=TIQsolar+In;
for jj=1:60
    Tf=(Tai+Ta)/2; %Film Temperature
    Ve=2/(Tai+Ta); %Volume Expansion cofficient
    Tsky=Ta-6; % sky temperature
    hcl=2.8+3*Vw; %convective heat transfer cofficient at the top of the glass
    hr1=eg*sigma*((Tpi^4-Tsky^4)); %Radiation heat transfer b/n glass and PV
    module
    Ut=((1/(hcl+hr1)))^-1; % top heat loss from the pv
    a12=hcl+hr1;
    Ul=Ut+a12; %Over all heat transfer cofficient
    Tpm =30+0.0175.*(Ic-150)+1.14*(Ta -25); %Initial Temperature of the PV module
    Tmin=33;
    TElec=TElec+Eg*deltt/3600000;
    a12=(hcl+hr1);
    V=(4*mr)/(pi*die^2); % velocity of the refrigerant inside the evaporator
    Tdif=((kl)/rhoo*cpr); % thermal diffusivity of liquid r134a
    Re=die*V*rhoo/mm; % Reynold number of the tube flow refrigerant
    prl=Kvl/Tdif; % prandtl number of liquid r134a
    Tdiff=kv/rhoo*cpr; % thermal diffusivity of vapor r134a
    prv=Kvv/Tdiff; % prandtl number of vapor r134a
    Nul=0.023*Re^0.8*prl^0.4; % Nusselt number correlation for liquid r134a
    Nuv=0.023*Re^0.8*prv^0.4; % Nusselt number correlation for vapor r134a
    hl=Nul*kl/die; % heat transfer coefficient of liquid refrigerant
    hv=Nuv*kv/die; % heat transfer coefficient of vapor refrigerant
    ue=1/(((doe/2)/((die/2)*hl))+((doe/2)/kc)*(log(doe/die))+(1/hv)); % overall
    heat transfer coeffiecent
    tstep=60;
    umilk=1/(1/hi+ti/ki+1/ho);

    %Electrical Energy generation of the PV module
    Eg=Apv*Ic*tapv*pf*Nepv*((1-0.0045*(Tpi-Trf)));
    %PV SURFACE TEMPERATURE
    Tpi=Tpi+((deltt/mcpp)*Apv*(Ic-Eg+a12*Ta^2-a12*Tpi^2));
    Tpi=Tpi;
    Qe=Ue* Ae*tstep*(Tmilk-Te); %cooling capacity of the evaporator
    %over all milk tank heat loss coefficient
    Qmloss=umilk*Ast*tstep*((Tmilk-Ta)); %heat loss from milk storage tank
    Qmilkout=Qe-Qmloss;
    if j>0 && j<14
        Tomilk=(Tmilk)-(Qmilkout*tstep/(Mm*cpm));
    end
    if Tomilk>33
        Tomilk=Tmilk;
    end
    %%% Cop of the system
    if Eg<235 % minimum PV power to start the compressor
        cop=0;
    else
```

```

        cop=(qee/(Eg*tstep*Vo));
    end
    if j<=6 && j>=12
        cop=0
    end

    Ict(i,j)=Ic;
    Tpt(i,j)=Tp1;
    copm(i,j)=cop;
    Tomilkm(i,j)=Tomilk;
    Et(i,j)=Eg;
end
end
end

rpm=[1800;2000;2100;2200;2300;2400;2500;2600;2700;2800;2900;3000;3100;3200;33
00;3400;3500;3600;3700;3800;3900;4000;4100;4200];
Tqsolar=sum(sum(TIQsolar));
Telec=sum(sum(TElec));
rr=1:24;
IclJ17=Ict(17,:);IclF16=Ict(47,:);IclM16=Ict(75,:);IclA15=Ict(105,:);...
IclM15=Ict(135,:);IclJ11=Ict(162,:);IclJul7=Ict(198,:);IclA16=Ict(228,:);...
IclS15=Ict(258,:);IclO15=Ict(288,:);IclN14=Ict(318,:);IclD10=Ict(344,:);...;
plot(rr,IclM16,'k-x',rr,IclS15,'c-x',rr,IclM15,'m-x',rr,IclA15,'g-
x',rr,IclF16,'b-x',...
rr,IclO15,'k-h',rr,IclD10,'r-x',rr,IclN14,'g-s',rr,IclJ17,'r-s',rr,IclJ11,'b-
s',...
rr,IclA16,'c-s',rr,IclJul7,'m-s','linewidth',2);
xlabel(' Time in hours','linewidth',2)
ylabel(' Solar Radiation on incliend surface(Watt)')
title('Monthly average solar radiation on incliend surface ')
legend('Jan17','Feb16','Mar16','Apr15','May15','Jun11','Jul17',.....
'Aug16','Sept15','Oct15','Nov14','Dec10')
grid on
xlim([1 24])
pause
clf
%%PVT Surface Temperature
Tpa=Tpt(17,:); Tpf=Tpt(47,:);Tpm=Tpt(75,:);
Tpap=Tpt(105,:);Tpma=Tpt(135,:);TpJ=Tpt(162,:);Tpju=Tpt(198,:);TpAu=Tpt(228,:
);Tps=Tpt(258,:);Tpo=Tpt(288,:);Tpn=Tpt(318,:);Tpd=Tpt(344,:);
plot(rr,Tpa,'k-x',rr,Tpf,'c-x',rr,Tpm,'m-x',rr,Tpap,'g-x',rr,Tpma,'b-
x',rr,TpJ,'y-x',rr,Tpd,'r-x',rr,Tpn,'g-s',rr,Tpo,'k-o',rr,Tps,'b-
s',rr,TpAu,'c-s',rr,Tpju,'m-s','linewidth',2)
grid on
legend('Jan17','Feb16','Mar16','Apr15','May15','Jun11','Jul17',.....
'Aug16','Sept15','Oct15','Nov14','Dec10')
title(' PV Surface Temperature');
xlabel('Time in hours');
ylabel('Temperature in oC');
pause
clf
%%%%%%%%%%%%%%%%%%%%%%%%%%%%%%%%%%%%%%%%%%%%%%%%%%%%%%%%%%%%%%%%%%%%%%%%
%%Electrical Energy Generation
EJ=Et(17,:);EAg=Et(228,:);EM=Et(75,:);EA=Et(105,:);EMa=Et(135,:);EN=Et(318,:
);ED=Et(344,:);EF=Et(47,:);EO=Et(288,:);ES=Et(258,:);EJu=Et(162,:);Ej=Et(198,:
);
plot(rr,EJ,'b-s',rr,EAg,'c-s',rr,EM,'k*',rr,EA,'--rs',rr,EMa,'k-x',rr,EN,'y-
s',rr,ED,'r x',rr,EF,'m-s',rr,EO,'--gs',rr,ES,'m*',rr,EJu,'r-o',rr,Ej,'c-
','linewidth',2)
grid on
legend('January','February','March','April','May','June','July','August','Sep
tember','October','November','December')
title('Electrical Energy Output of the System');

```

```

xlabel('Time in hours');
ylabel('Electrical Energy Generation in (W)');
pause
clf
% % % % % pause
% % % clf
% % % % %%% Thermal Efficiency
% % % %
TEJ=Tefi(17,:);TEF=Tefi(47,:);TEM=Tefi(75,:);TEA=Tefi(105,:);TEMa=Tefi(135,:);
TEJu=Tefi(162,:);TEj=Tefi(198,:);TEAg=Tefi(228,:);TES=Tefi(258,:);TEO=Tefi(
288,:);TEN=Tefi(318,:);TED=Tefi(344,:);
% % % % plot(jj,TEJ,'b',jj,TEF,'--
rs',jj,TEM,'c',jj,TEA,'k',jj,TEMa,'g',jj,TEJu,'y',jj,TEj,'m -x',jj,TEAg,'b-
*',jj,TES,'c-',jj,TEO,jj,TEN,jj,TED,'linewidth',2)
% % % % grid on
% % % %
legend('January','February','March','April','May','June','July','August','Sep
tember','Octowber','November','December');
% % % % title('Thermal efficiency of the system');
% % % % xlabel('Time in hours');
% % % % ylabel('Thermal Efficiency of the collector');
% % % % Pause
% % % % clf
% % % % %%% Electrical Efficiency
%EEJ=Eff111(17,:);EEF=Eff111(47,:);EEM=Eff111(75,:);EEA=Eff111(105,:);EEMa=Ef
f111(135,:);EEJu=Eff111(162,:);EEj=Eff111(198,:);EEAg=Eff111(228,:);EES=Eff11
1(258,:);EEO=Eff111(288,:);EEN=Eff111(318,:);EED=Eff111(344,:);
%plot(rr,EEJ,'b',rr,EEF,'--rs',rr,EEM,'--
gs',rr,EEA,'k',rr,EEMa,'g',rr,EEJu,'y',rr,EEj,'m -x',rr,EEAg,'b-*',rr,EES,'c-
',rr,EEO,'m*',rr,EEN,'--bs',rr,EED,'y--','linewidth',2)
%grid on
%legend('January','February','March','April','May','June','July','August','Se
pember','Octowber','November','December');
%title('Electrical Energy of the system');
%xlabel('Time in hours');
%ylabel('Electrical Energy of the collector(W)');
%pause
%clf
% % % % %%% cop of the refrigerant
copmJ17=copm(17,:);copmF16=copm(47,:);copmM16=copm(75,:);copmA15=copm(105,:);
...
copmM15=copm(135,:);copmJ11=copm(162,:);copmJu18=copm(199,:);copmA16=copm(228
,:);...
copmS15=copm(258,:);copmO15=copm(288,:);copmN14=copm(318,:);copmD10=copm(344,
:);
plot(rr,copmJ17,'k-',rr,copmF16,'g-s',rr,copmA15,'g-',rr,copmM15,'b--',...
rr,copmJ11,'k-d',rr,copmJu18,'r-*',rr,copmA16,'y-h',rr,copmS15,'c-x',...
rr,copmN14,'k-x',rr,copmD10,'m-*','linewidth',2);
xlabel(' Time in hours')
ylabel(' Cop of the refrigerator')
title('Monthly Cop of the System')
legend('Jan17','Feb16','Apr15','May15','Jun11','Jul18',.....
'Aug16','Sep15','Nov14','Decl0')
xlim([1 24])
grid on
pause
clf
% % % % %%% Milk outlet temperature hourly
TomilkA15=Tomilkm(105,:);Tomilkm15=Tomilkm(135,:);Tomilkj11=Tomilkm(162,:);To
milkJu17=Tomilkm(198,:);TomilkAug16=Tomilkm(228,:);TomilkSep15=Tomilkm(258,:)
;TomilkOct15=Tomilkm(288,:);TomilkNov15=Tomilkm(318,:);TomilkD10=Tomilkm(344,
:);
    
```

```
plot(rr,TomilkA15,'-ok',rr, Tomilkm15,'y-s',rr,Tomilkj11,'b-  
s',rr,TomilkJul7,'m-s',rr,TomilkAug16,'k-s',rr,TomilkSep15,'r-  
s',rr,TomilkOct15,'g-s',rr,TomilkNov15,'b-*',rr,TomilkD10,'c-  
*', 'linewidth',2);  
xlim([1 24])  
grid on  
xlabel('Time in hours')  
ylabel('Outlet Milk Temperature(oC)')  
title('Hourly Temperature of Milk')  
legend('April17', 'May15', 'June11', 'July17', 'Aug16', 'Sep15', 'October15', 'Nov15',  
'Dec10')
```

© GSJ

Appendix C: Performance Coefficients of CASCADE17-0244Y3 Compressor

Performance Coefficients (24V) - ARI HBP

Coefficient	Capacity (BTU/Hr)	Power (Watts)	Current (Amperes)	Mass Flow (Lbs/Hr)
C1	-1.107663E+03	3.943455E+02	1.643106E+01	-9.435642E+00
C2	-1.300685E+00	-1.223476E-01	-5.097817E-03	-2.856467E-02
C3	2.056291E-04	2.942926E-05	1.226219E-06	4.165405E-06
C4	-4.706144E-08	-2.445508E-10	-1.018962E-11	-7.435971E-10
C5	-7.624835E+01	-3.826043E+00	-1.594184E-01	-1.222140E+00
C6	1.678044E-01	4.168358E-02	1.736816E-03	2.490090E-03
C7	-8.433469E-04	3.524107E-05	1.468377E-06	-1.285188E-05
C8	7.156981E+01	-7.588050E+00	-3.161687E-01	1.008043E+00
C9	-8.933099E-01	5.706575E-02	2.377740E-03	-1.319664E-02
C10	3.539651E-03	-1.815833E-04	-7.565971E-06	5.237502E-05
C11	-4.128949E-04	-3.801532E-05	-1.583972E-06	-6.920254E-06
C12	-4.984281E-08	6.986678E-09	2.911116E-10	-6.890584E-10
C13	-1.084624E-06	2.132993E-07	8.887472E-09	-1.178531E-08
C14	2.881196E-06	-3.587806E-08	-1.494920E-09	4.619442E-08
C15	1.522813E-02	3.822661E-03	1.592776E-04	2.726404E-04
C16	1.794408E-02	1.206820E-03	5.028417E-05	3.516805E-04
C17	1.602984E+00	2.213781E-02	9.224086E-04	2.472096E-02
C18	5.350873E-06	-5.583706E-07	-2.326544E-08	7.283940E-08
C19	1.647996E-04	-2.041318E-05	-8.505493E-07	1.970873E-06
C20	1.730062E-06	-2.468870E-07	-1.028696E-08	1.989592E-08
C21	-1.230301E-04	1.131317E-06	4.713821E-08	-1.980280E-06
C22	-6.058412E-04	-4.793339E-04	-1.997224E-05	-6.546663E-06
C23	-8.010951E-03	2.484762E-04	1.035318E-05	-1.213048E-04

Performance Equation

$$Y = C_1 + C_2 X_1 + C_3 X_1^2 + C_4 X_1^3 + C_5 X_2 + C_6 X_2^2 + C_7 X_2^3 + C_8 X_3 + C_9 X_3^2 + C_{10} X_3^3 + C_{11} X_1 X_2 X_3 + C_{12} X_1^2 X_2 X_3 + C_{13} X_1 X_2^2 X_3 + C_{14} X_1 X_2 X_3^2 + C_{15} X_1 X_2^2 + C_{16} X_1 X_3 + C_{17} X_2 X_3 + C_{18} X_1^2 X_2 + C_{19} X_1 X_2^2 + C_{20} X_1^2 X_3 + C_{21} X_1 X_3^2 + C_{22} X_2^2 X_3 + C_{23} X_2 X_3^2$$

$X_1 = \text{RPM}$
 $X_2 = E_t (^{\circ}\text{F})$
 $X_3 = C_t (^{\circ}\text{F})$



(source: Masterflux)

Appendix D: Properties of Some Materials used

Appendix D₁: Thermo-physical properties

Materials	Melting point[K]	Properties at 300K			
		Density[ρ]	K[W/m.k]	Cp[J/kg.k]	$\partial \times 10^6 m^2/s$
Copper	1358	8933	385	401	117
Stainless steel	1670	7913	14.6	477	3.95
Extruded Polystyrene	-	55	24×10^{-4}	1210	-

© GSJ

Appendix E: Peak Sunshine, daily extra-terrestrial solar radiation and daily solar radiation and Hour for October Month

7.15	7.225	8.525	9.525	5.9	8.6	6.975	6.75	8.8	8.4	7
avg S	avg S									
0.37056	0.372468	0.405538	0.430977	0.338762	0.407446	0.366108	0.360385	0.412534	0.402358	0.37
0.472341	0.467775	0.388635	0.327758	0.548438	0.384069	0.482995	0.496692	0.371894	0.396245	0.46
coeff a	coeff a									
coeff b	coeff b									
0.666809	0.668931	0.696162	0.704827	0.622602	0.697182	0.661625	0.654479	0.69961	0.694328	0.66

Extra_territerial daily Solar Radiation

1	2	3	4	5	6	7	8	9	10	
8535.542	8274.713	8110.868	8190.884	8443.032	8641.275	8607.899	8372.825	8146.782	8132.406	8342
9286.063	9002.3	8824.048	8911.101	9185.419	9401.093	9364.783	9109.039	8863.12	8847.48	9076
10256.42	9943.001	9746.123	9842.271	10145.26	10383.47	10343.36	10060.89	9789.278	9772.003	1002
10820.5	10489.85	10282.14	10383.58	10703.23	10954.54	10912.23	10614.23	10327.67	10309.45	1057
10964.07	10629.03	10418.57	10521.35	10845.24	11099.89	11057.02	10755.06	10464.7	10446.24	1071
10942.99	10608.6	10398.54	10501.13	10824.39	11078.55	11035.76	10734.38	10444.58	10426.15	1069
10936.58	10602.38	10392.45	10494.97	10818.05	11072.06	11029.29	10728.09	10438.46	10420.04	1068
10897.68	10564.67	10355.49	10457.65	10779.57	11032.68	10990.07	10689.94	10401.34	10382.98	1065
10529.91	10208.13	10006.01	10104.72	10415.78	10660.35	10619.17	10329.17	10050.31	10032.58	1029
9698.438	9402.073	9215.906	9306.824	9593.324	9818.576	9780.653	9513.552	9256.713	9240.378	9479
8764.944	8497.105	8328.857	8411.024	8669.948	8873.519	8839.246	8597.854	8365.736	8350.974	85
8284.349	8031.197	7872.173	7949.835	8194.562	8386.971	8354.578	8126.421	7907.031	7893.078	809

5691.577	5535.21	5646.478	5773.156	5256.651	6024.545	5695.199	5479.834	5699.567	5646.557	5580
----------	---------	----------	----------	----------	----------	----------	----------	----------	----------	------

daily solar radiation(W/m^2)

0.666809	0.668931	0.696162	0.704827	0.622602	0.697182	0.661625	0.654479	0.69961	0.694328	0.66
----------	----------	----------	----------	----------	----------	----------	----------	---------	----------	------

Kt value(H/Ho)